A Tutorial on NB-IoT Physical Layer Design

Matthieu Kanj, Vincent Savaux, Mathieu Le Guen

A Tutorial on NB-IoT Physical Layer Design

Matthieu Kanj, Vincent Savaux, Mathieu Le Guen

***Abstract*—The Internet of things (IoT) is transforming the whole of society. It represents the next evolution of the Internet and will significantly improve the ability to gather and analyze data, as well as the ability to control devices remotely. In this respect, the usage of connected devices is continuously growing with the expansion of the applications being offered to individuals and industries. To address IoT market needs, many low-power wide-area (LPWA) technologies have been developed, some operating on licensed frequencies (e.g., narrowband-IoT [NB-IoT] and Long-Term Evolution-M [LTE-M]), and others on unlicensed frequencies (e.g., LoRa, Sigfox, etc.). In this paper, we address the Release 13 of the NB-IoT 3rd generation partnership project (3GPP) standardized LPWA technology and provide a tutorial on its physical layer (PHY) design. Specifically, we focus on the characteristics and the scheduling of downlink and uplink physical channels at the NB-IoT base station side and the user equipment (UE) side. The goal is to help readers easily understand the NB-IoT system without having to read all the 3GPP specifications or the state-of-the-art papers that generally describe the system. To this end, each presented concept is followed by examples and concrete use-cases to further aid in the reader's comprehension. Finally, we briefly describe and highlight the new features added to the NB-IoT system in Releases 14 and 15.**

***Index Terms*—Internet of things, NB-IoT, LTE, 3GPP, eNB, Protocol Stack, Physical Layer, Scheduling, Downlink and Uplink channels, LPWA.**

I. Introduction

The Internet of things (IoT) represents the concept of interaction and communication between objects from diverse environments with the purpose to collect, process and exchange data via Internet protocols or well-defined interfaces. These objects can be physical (e.g., sensors, machines, cars, products) or virtual (e.g., software applications, support systems). In other words, the IoT is the communication between smart machines over a single large-scale network.

The IoT is revolutionizing the world of telecommunication by bridging diverse technologies, enabling new applications and connecting billions of objects. It enables the generation of huge amounts of information to support intelligent decision making and remote control of diverse objects. It is a rapidly expanding phenomenon which will have a huge impact on society and the global economy. The future development of this concept will support the improvement and growth in many business sectors including manufacturing, transportation, agriculture, health, logistics, etc. The total cross-sector impact including consumer surplus for IoT applications is predicted to reach 11.1 trillion dollars per year by 2025 [1]. Moreover, it is expected that by 2022, the total number of IoT-connected devices will reach 18 billion, nearly 1.8 connections for every person in the world [2].

M. Kanj, V. Savaux, and M. Le Guen are with b<>com, 1219 avenue des Champs Blancs, 35510 Cesson-Sevigne, France (e-mail: matthieu.kanj@b-com.com; vincent.savaux@b-com.com; mathieu.leguen@b-com.com).

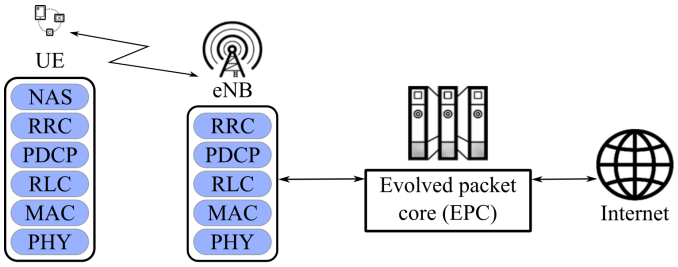

Fig. 1. General overview of the NB-IoT network including the evolved node B (eNB) and the user equipment (UE) protocol stacks: PHY, medium access control (MAC), radio link control (RLC), packet data convergence protocol (PDCP), radio resource control (RRC), non access stratum(NAS).

A. IoT Technologies and NB-IoT

Due to this anticipated IoT market growth in terms of investments, connected devices and applications, huge technological efforts have been made to meet industry needs. In recent years, many standards and communication protocols have been developed to support a wide range of applications for machine-to-machine (M2M) communication, also referred to as machine-type communication (MTC). These standards and protocols (e.g., NFC and RFID, Low-Energy Bluetooth, ZigBee, Z-Wave, Wi-Fi) were mostly dedicated to short-range applications and for well-defined usage. At the same time, new LPWA technologies were invented to address the need for wide-range communications between objects, like LoRa, LoRaWAN, Weightless SIG, Sigfox and RPMA. These technologies operate in the unlicensed spectrum and provide massive connectivity for devices but require the deployment of new infrastructures.

The MTCs enable a broad range of applications and services proposed to individuals and industries. To address the maximum number of them, cellular systems were considered as a potential candidate to provide connectivity for MTC devices. In this respect, the 3GPP introduced in June 2016[1] a new cellular technology standard called narrow-band Internet of things to provide IoT services through wide-area cellular networks. NB-IoT is based on Long-Term Evolution (LTE) and thus operates in the licensed spectrum. It is designed to take into account most of the IoT service requirements, including very good indoor coverage, support of massive numbers of connected devices, very low cost of connectivity, low power consumption, and optimized network architecture. Contrary to other IoT unlicensed technologies that require deploying new infrastructures, NB-IoT allows for easy IoT network installation with reduced cost because it reuses existing LTE infrastructures.

NB-IoT inherits from LTE most of its features as well as

[1]https://www.3gpp.org/news-events/1785-nb_iot_complete

TABLE I
LIST OF REFERENCES ON THE NB-IOT SYSTEM CITED IN THIS PAPER.

	Topics	References	Sections
General references	Generalities/Overviews on IoT & LPWA and their application domains	[1]–[10]	I
	Overviews on NB-IoT	[11]–[16]	I
	Comparison between LPWAN technologies	[10], [17]	I
	General PHY description	[18]–[24]	I & II
	Resource management & Scheduling	[25]–[27]	V
	Synchronization	[28]–[37]	III.A
	Uplink demodulation	[38]–[47]	IV.A & IV.B
	Downlink demodulation	[48]–[53]	IV.B
	Energy Saving	[54]–[57]	V.H & VI.B
	Positioning	[58]–[60]	VI.A
	Challenges & perspectives	[17], [20]–[22], [61]–[64]	I
3GPP references	Release 13	[65]–[77]	I to V
	Release 14	[78]–[85]	VI.A
	Release 15	[86]–[92]	I & VI.B

its essential channels and signals [65]. However, the complexity of these channels and signals was reduced in order to respect the low-cost and low-power constraints of NB-IoT user equipment modules. The numbers of channels and signals were reduced and they were adapted to fit the new NB-IoT frame structure [11]. The system was designed to occupy a frequency band of 180 kHz (corresponding to one resource block in the LTE system), and to handle a high number of repetitions to achieve long-range transmissions and deep indoor penetration [61]. Moreover, the protocol stack of the evolved node B (eNB) and the UE were kept the same and the complexity reduction is translated in form of reduction in capabilities/functionalities at each layer. Fig. 1, provides a general overview of the NB-IoT network and shows the different layers constituting the protocol stack of the NB-IoT eNB and the UE. Note that, the evolved packet core (EPC) is out of scope of this tutorial. Further and detailed information on the 3GPP network architecture, protocol stacks and EPC elements can be found in [77], [92].

B. State of the Art

IoT technologies have been extensively studied in recent years. Significant efforts have been made to gather information and generate a complete overview of these technologies, their protocols, architectures, application domains and future challenges [3]–[9], [63]. In the literature, the general background, development history, and standardization of the NB-IoT system have been covered in many publications. Some papers provide a general overview of the system and its features [12]–[15], including a survey on industrial actors in the NB-IoT market [16]. In [10], [17], the authors compare various LPWAN technologies in terms of technical specifications, strengths, and weaknesses with respect to their design goals and intended fields of applications. Others focus on specific functionality like power consumption [54], random access [18], [19], resource management [25], scheduling issues, and solutions for uplink or downlink physical channels [26], [27]. Many others provide surveys on NB-IoT technology to offer a complete summary on system capabilities, constraints, and challenges [20]–[22], [64]. In particular, the authors of [62] provide a detailed overview of the open issues and pending challenges related to NB-IoT. However, the literature does not include a detailed technical presentation of the system. The existing papers instead provide an overview of the entire system or a focused presentation of some NB-IoT features with dedicated performance studies. To the best of our knowledge, we are the first to present a detailed and dedicated tutorial on the physical layer of the NB-IoT system. Table I summarizes the references cited in this tutorial with the corresponding topics and provides the section(s) in which they are mentioned.

C. Contribution and Organization

In this tutorial, we aim to provide a complete and detailed presentation of the physical layer of the NB-IoT system. More specifically, we address the general operation of the eNB and UE protocol stacks, and focus on their physical layer while explaining its dependent mechanisms with other layers (e.g., the medium access control [MAC] layer and radio resource control [RRC] layer). To this end, at the PHY layer, we detail the transmission parts of the eNB and the UE that are fully described by the 3GPP specifications as well as the reception parts that are usually left to be designed by equipment manufacturers. The physical design of channels and signals for the transmitter and receiver parts is presented with precise references to the 3GPP specifications and some conventional signal processing techniques and algorithms. At the MAC layer, we address only the scheduling of the PHY layer channels and signals and provide examples aiming to improve the understanding of some difficult concepts detailed in the standard. However, in order to clearly define the dependencies between the PHY procedures and other layers, some RRC elements are considered and explained.

In this work, we address the 3GPP Release 13 of the NB-IoT standard. We aim to cover all aspects of the PHY layer through an in-depth presentation of downlink and uplink channels and an analysis of the dependencies with other layers. Moreover, we cover the newly introduced features by 3GPP in Release 14 and Release 15 to complete the overview on NB-IoT system capabilities. The goal is to allow readers to easily understand the NB-IoT standard and quickly acquire most of its features without the need to perform a deep dive into 3GPP specifications. Prior knowledge of the LTE standard is not mandatory before reading this tutorial, but it is recommended, as are basics on digital communications. Thus,

TABLE II
LIST OF ACRONYMS

3GPP	3rd generation partnership project
ACK	Acknowledgement
BPSK	Binary phase-shift keying
C-DRX	Connected discontinuous reception
CE	Coverage enhancement
CP	Cyclic prefix
CP CIoT	Control plane cellular Internet of things
CRC	Cyclic redundancy check
CRS	Cell-specific reference signal
DCI	Downlink control information
DFT	Discrete Fourier transform
DMRS	Demodulation reference signal
DRX	Discontinuous reception
eDRX	Extended discontinuous reception
EDT	Early data transmission
eNB	Evolved node B
EPS	Evolved packet system
FDD	Frequency-division duplexing
GPS	Global positioning service
GSM	Global system for mobile communications
H-SFN	Hyper-system frame number
HD-FDD	Half-duplex frequency-division duplexing
HF	Hyperframe
I-DRX	Idle discontinuous reception
IE	Information element
IMSI	International mobile subscriber identity
IoT	Internet of things
LMMSE	Linear minimum mean square error
LPWA	Low-power wide-area
LS	Least squares
LSB	Less significant bit
LTE	Long-term evolution
M2M	Machine to machine
MAC	Medium access control
MCS	Modulation and coding scheme
MIB	Master information block
ML	Maximum likelihood
MSB	Most significant bit
MTC	Machine-type communication
NACK	Negative-acknowledgement
NB-IoT	Narrowband Internet of things
NCCE	Narrowband control channel element
NPBCH	Narrowband physical broadcast channel
NPDCCH	Narrowband physical downlink control channel
NPDSCH	Narrowband physical downlink shared channel
NPRACH	Narrowband physical random access channel
NPRS	Narrowband positionning reference signal
NPSS	Narrowband primary synchronization signal
NPUSCH	Narrowband physical uplink shared channel
NRS	Narrowband reference signal
NSSS	Narrowband secondary synchronization signal
NWUS	Narrowband wake up signal
OFDM	Orthogonal frequency-division multiplexing
OFDMA	Orthogonal frequency-division multiple access
OTDOA	Observed time difference of arrival
PAPR	Peak-to-average power ratio
PF	Paging frame
PH	Paging hyperframe
PHY	Physical
PO	Paging occasion
PRB	Physical resource block
PSM	Power saving mode
PTW	Paging time window
QPSK	Quadrature phase-shift keying
RA-RNTI	Random access-radio network temporary identifier
RACH	Random access channel
RAI	Release assistance indication
RAPID	Random access preamble identifier
RAR	Random access response
RE	Resource element
RLC	Radio link control
RRC	Radio resource control
RSRP	Reference signal receive power
RU	Resource unit
SC-FDMA	Single carrier-frequency division multiple access
SC-MCCH	Single cell multicast control channel
SC-MTCH	Single cell multicast traffic channel
SC-PTM	Single cell point to multipoint
SF	Subframe
SFN	System frame number
SIB	System information block
TA	Timing advance
TAU	Tracking area update
TBS	Transport block size
TDD	Time-division duplexing
ToA	Time of arrival
UE	User equipment
UM	Unacknowledged mode
UP CIoT	User plane cellular Internet of things
ZC	Zadoff-Chu

this work is directed towards readers who aim to improve their knowledge and skills related to NB-IoT, from undergraduate and postgraduate students to engineers and academics. This work can be read in its entirety, or readers can focus on specific topics (e.g., NB-IoT receiver, scheduling, improvements in Release 14, etc.).

The remaining sections of this paper are organized as follows. Section II presents an overview of the general characteristics of the NB-IoT system, including its operation and transmission modes, as well as its frame structure. Section III provides a description of the PHY layer of the NB-IoT system, including the transmitter design of the eNB and UE. The transmission chains of downlink and uplink channels and signals are then presented with a focus on their mapping processes. In Section IV, we complete the PHY layer description by addressing the receiver design for both the NB-IoT eNB and UE. Section V presents the scheduling process for the downlink and uplink channels and signals at the MAC layer. In Section VI, we present the new features introduced to the NB-IoT standard in the 3GPP Releases 14 and 15, and describe in detail the features related to PHY layer aspects. Finally, the conclusion is presented in Section VII.

II. SYSTEM OVERVIEW

The NB-IoT system was conceived based on an extensive reuse of the LTE system. This design allows for rapid and flexible deployment over the legacy LTE cellular network infrastructures, while ensuring the coexistence of the two technologies. In fact, the NB-IoT system reuses the modulation schemes for downlink and uplink transmissions, namely the orthogonal frequency-division multiple access (OFDMA) and the single carrier-frequency division multiple access (SC-FDMA), respectively. A detailed comparison of these two multicarrier modulation schemes is provided in [23]. The NB-IoT downlink transmissions occupy only 12 subcarriers of 15 kHz each, corresponding in LTE to one physical resource block (PRB) of 180 kHz bandwidth. Similar to the downlink, a bandwidth of 180 kHz is allocated for the uplink transmissions. Moreover, the same framing structure is utilized from the LTE with differences in the mapping of channels and signals. The set of bands defined by the 3GPP in which NB-IoT can be operated are listed in Table 5.6.1-1 of [66]. These bands are basically LTE bands, which can now be used for NB-IoT communications.

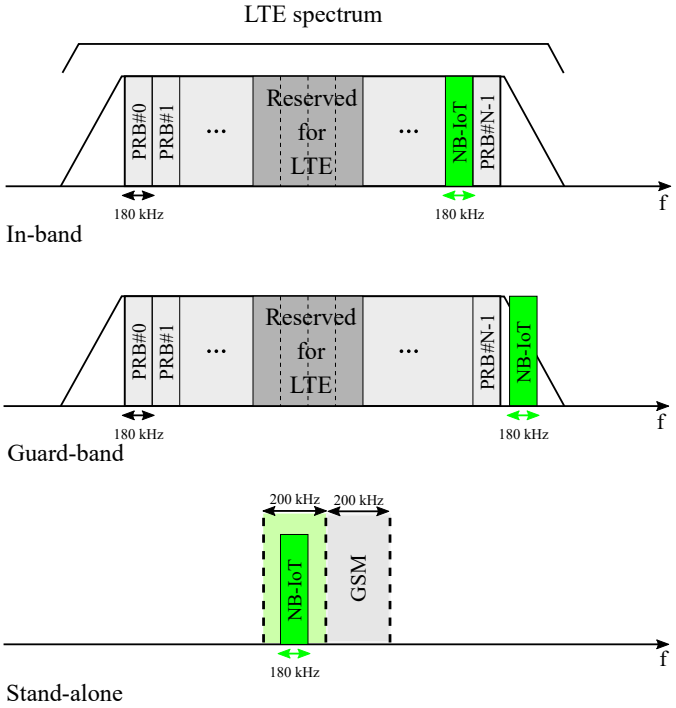

Fig. 2. Three possible operation modes of NB-IoT: the PRB of 180 kHz bandwidth can be transmitted in the LTE band (in-band mode), at the edge of the LTE band (guard-band mode), or in the liberated GSM channels (stand-alone mode).

In the following subsections, we present how NB-IoT will coexist with LTE and how it will be integrated into the existing networks. We also provide the main specificities of the NB-IoT system compared to the LTE system.

A. Operation Modes

The NB-IoT air interface was optimized to ensure the coexistence with LTE carriers while maintaining the performance of the LTE system. In this context, three operation modes were defined by 3GPP for NB-IoT [67]:

- In-band mode: the NB-IoT signal occupies one PRB from the LTE bandwidth.
- Guard-band mode: the NB-IoT signal occupies one PRB from the unused guard band PRBs of LTE bandwidth.
- Stand-alone mode: the NB-IoT signal is intended to occupy the liberated spectrum of the global system for mobile communications (GSM) system. In this case, the NB-IoT signal still occupies 180 kHz from the 200 kHz GSM carrier, with 10 kHz of band-guard on both sides of the spectrum.

These operation modes are summarized in Fig. 2. In this figure, the PRBs are indexed from 0 to N-1, where N depends on the LTE bandwidth (up to N=100 in 20 MHz bandwidth). The in-band operation mode is the most privileged mode due to the benefits in terms of cost savings and ease of integration over the legacy LTE networks. However, in this mode the NB-IoT anchor carrier[2] can take only a predefined set of possible PRBs as shown in Table III. These possible PRB indexes are related to the used LTE bandwidth and can be found using 3GPP Table 16.8-1 defined in [68]. The six middle PRBs of the LTE system are always forbidden for NB-IoT to avoid conflicts between NB-IoT transmissions and some essential LTE channels and signals, such as the physical broadcast channel and the synchronization signals. For the guard-band mode, any PRB can be used for NB-IoT transmissions. In this tutorial, we focus only on the in-band operation mode as it is the most privileged mode due to the previously mentioned benefits. However, we provide the necessary information to deduce the operation methods of the other modes.

In fact, for all the aforementioned operation modes, it is possible to deploy several NB-IoT anchor carriers in the same network cell. At the same time, the 3GPP also proposed to use what are called non-anchor[3] carriers to increase the capacity of NB-IoT cells. This feature is further presented in Section VI-A1 of this tutorial.

B. Transmission Mode

The NB-IoT system was first conceived to operate in a frequency-division duplexing (FDD)-based mode in the 3GPP Release 13 [66]. This means that downlink and uplink transmissions are performed in completely separated frequency bands. In other words, the eNB and the UE will transmit in one frequency band and receive in another. However, due to the constraints of the NB-IoT UE modules in terms of low power, low complexity, and battery life, the system at the UE side operates in a type B half-duplex FDD (HD-FDD) mode [69]. This means that the UE can either transmit or receive, but cannot do both at the same time. Moreover, a guard time interval is inserted between transmissions. This type of transmission mode was chosen for the UE due to the low processing capacity of its hardware. In contrast, the eNB operates in full duplex FDD mode where it can simultaneously transmit and receive (exactly as in LTE FDD mode). Recently in 3GPP Release 15, it became possible to operate NB-IoT in time-division duplexing (TDD) mode. This new feature is further addressed in Section VI.

An illustration of the type B HD-FDD transmission mode is provided in Fig. 3. It can be seen that a frequency gap called "duplex spacing" always exists between the downlink and uplink bandwidth (only for the FDD band). The value of this duplex spacing depends on the used LTE band from the set of bands defined by 3GPP in [66]. In this figure, we illustrate the transmissions from the NB-IoT UE point of view. We assume that the UE receives first a downlink signal from the eNB, then replies after a guard time, and finally attends for next downlink transmission after another guard time. In NB-IoT, the guard time between transmissions is configurable. However, there is a minimum guard time to to be maintained between the different uplink and downlink transmissions. This is further presented in Section V-I.

[2]This is the carrier over which the initial connection setup can be performed by the UE (i.e., cell selection, getting master/system information blocks and random access procedure).

[3]This is a carrier to be used for only data exchange (i.e., NPSS, NSSS and master/system information blocks are not transmitted over such a carrier).

TABLE III
LIST OF LTE PRB INDEXES THAT CAN BE USED BY NB-IOT FOR IN-BAND OPERATION MODE

LTE system bandwidth	3 MHz	5 MHz	10 MHz	15 MHz	20 MHz
LTE PRB indices for NB-IoT	2, 12	2, 7, 17, 22	4, 9, 14, 19, 30, 35, 40, 45	2, 7, 12, 17, 22, 27, 32, 42, 47, 52, 57, 62, 67, 72	4, 9, 14, 19, 24, 29, 34, 39, 44, 55, 60, 65, 70, 75, 80, 85, 90, 95

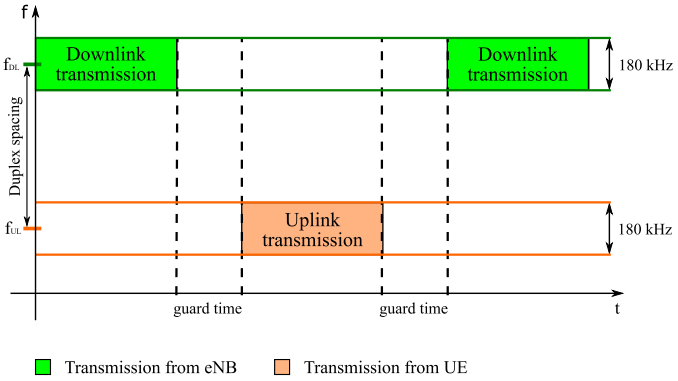

Fig. 3. Illustration of type B Half Duplex Frequency-Division Duplexing (HD-FDD): downlink and uplink transmissions are separated in both frequency and time.

C. NB-IoT Framing System

The NB-IoT system follows the same framing principle of LTE, where the downlink and uplink transmissions are organized into radio frames with a duration of 10 ms each. The same radio frame structure as that of LTE is retained, but with some differences in terms of channels and signals mapping. Each frame is composed of 10 subframes (SFs), where each subframe has a duration of 1 ms and is composed of two time slots with a duration of 0.5 ms each. The indexing of radio frames is done using the "system frame number (SFN)".

Fig. 4 shows the framing system of the NB-IoT standard. It can be seen that the SFN index has a maximum value of 1023 to account for 1024 frames ($= 1024 \times 10$ ms $= 10.24$ s). Moreover, in NB-IoT, the concept of hyper frame was introduced to count the SFN periods (i.e., to count the periods of 1024 frames). Therefore, the term "hyper-SFN (H-SFN)" is used to represent the index of SFN periods which have a maximum value of 1023. This means that the H-SFN counter returns to zero after a duration of 1024 SFN periods which corresponds to 1024×10.24 s $\approx$ 2 h 54 min 46 s.

1) Physical Signal Composition: At the signal level, one NB-IoT downlink subframe is constituted from 12×14 resource elements (REs), where 12 and 14 correspond to the number of subcarriers and to orthogonal frequency-division multiplexing (OFDM) symbols of the subframe, respectively. Fig. 4 shows the format of downlink subframes, where k stands for the subcarrier index and l for the OFDM symbol index. In the LTE system, two cyclic prefix (CP) formats can be used for OFDM symbols: normal and extended. The extended format reduces the number of OFDM symbols per slot to six. In NB-IoT, the extended CP is not allowed and thus each slot is strictly composed of seven OFDM symbols. In the same way as in LTE, the CP of the first OFDM symbol of each slot lasts 5.2 μs, whereas each CP of the other six symbols lasts 4.7 μs. Moreover, the only possible subcarrier spacing in downlink is 15 kHz.

In uplink, a similar timing diagram as that for downlink is used, except that there are two possible subcarrier spacing formats: 15 kHz and 3.75 kHz. If the 15 kHz spacing is used for uplink transmissions, the system framing will be the same as the one in downlink (i.e., one frame = 10 ms = 10 SFs). However, if the 3.75 kHz spacing is used, the radio frame format and the representation of the resource elements will change. Fig. 5 shows the impact on the resource grid when using the 3.75 kHz spacing. In fact, the use of such spacing over a 180 kHz bandwidth will provide 48 subcarriers rather than 12 compared to the case of 15 kHz spacing.

Accordingly, the slot duration is four times longer with 3.75 kHz spacing, which results in a slot length of 2 ms. This implies that a radio frame in uplink will be composed of only five slots of 2 ms each. The slot in such a configuration is still composed of seven symbols, but the same CP duration is used for each symbol. The time duration of each CP and symbol is 8.33 μs and 266.67 μs, respectively. However, to reach the 2 ms duration for each slot, a guard time of 75 μs that is left blank after the 7^{th} symbol. Thus, it can be verified that $7 \times (266.67 + 8.33) + 75$=2000 μs = 2 ms. Moreover, in uplink, the SFN and H-SFN counters still apply as they do in downlink.

2) Transmission Options in Downlink and Uplink: In NB-IoT, two transmission options are possible: single-tone and multi-tone. For downlink transmissions, the multi-tone option is the only possible one in which the 12 available subcarriers are used. In contrast, the uplink transmissions can be done using both options, but they depend on the used subcarrier spacing. In this respect, if the 3.75 kHz spacing is used, only the single-tone option is possible (i.e., one subcarrier is used). In contrast, in the case of 15 kHz spacing, the two options can be performed through four possible transmission configurations: one, three, six or 12 subcarriers. In addition to these transmission options, another concept for uplink transmissions was introduced in the 3GPP specifications [65]. It defines the "resource unit (RU)", which represents the smallest unit that can be transmitted in uplink regardless of the subcarrrier spacing being used and depends only on the transmission option (i.e., single-tone or multi-tone). Table IV summarizes the slots number, the resource elements number, the symbols number, and the duration of one RU according to the chosen transmission option.

For the single-tone transmissions using 15 kHz or 3.75 kHz spacing, one RU will have exactly the same number of REs (112 REs). However, as presented earlier in this section, when

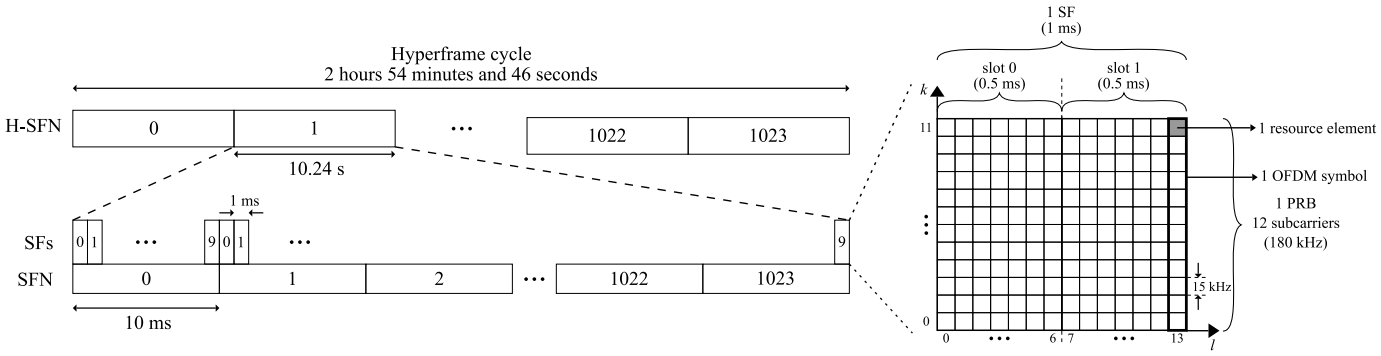

Fig. 4. NB-IoT framing system in downlink.

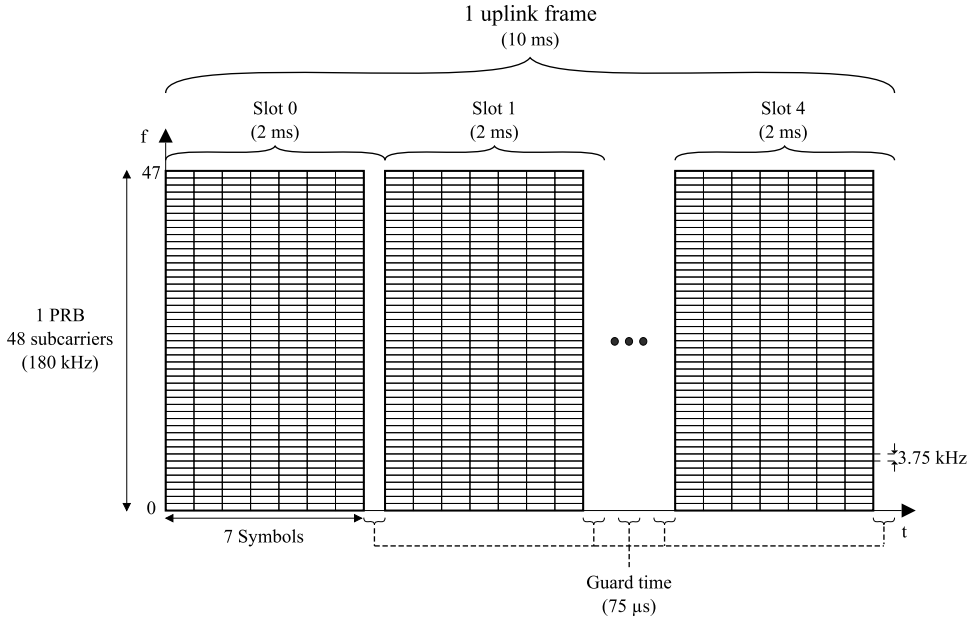

Fig. 5. NB-IoT framing system in uplink with 3.75 kHz subcarrier spacing. One frame consists in five slots of 2 ms each.

the 3.75 kHz spacing is used, the slot duration will be four times longer than the slot of 15 kHz spacing. Therefore, the RU will last 8 ms with 15 kHz spacing and 32 ms with 3.75 kHz spacing. For multi-tone transmissions, one RU will have 168 REs for any configuration (i.e., three, six or 12 subcarriers). In such cases, the duration of the RU will be shorter when a higher number of subcarriers is used since a greater number of REs can be transmitted within a shorter duration. It is important to note that, when uplink transmissions contain control information (i.e., acknowledgement (ACK) or negative-acknowledgement (NACK)), the RU is defined as one subcarrier and four slots. In this case, the RU lasts 2 ms and 8 ms with 15 kHz and 3.75 kHz subcarrier spacing, respectively. The ACK/NACK information is always transmitted with the single-tone option as is further explained in Section III-B2.

TABLE IV
TRANSMISSION OPTIONS IN UPLINK.

Subcarrier spacing	Subcarriers number	Slots number	Resource elements number	SC-FDMA symbols number	RU duration
3.75 kHz	1	16	112	112	32 ms
15 kHz	1	16	112	112	8 ms
	3	8	168	56	4 ms
	6	4	168	28	2 ms
	12	2	168	14	1 ms

III. PHY LAYER: TRANSMITTER DESIGN AT ENB AND UE

In this section, we focus on the transmission part of the PHY layer of the NB-IoT system. We cover all the channels and signals that are used for downlink and uplink transmissions and provide an illustration of the transmission chain at the eNB and UE side. Table V shows the list of channels and signals used in the NB-IoT system for downlink and uplink transmissions. For clarity, this section is organized in two parts: the first part is dedicated to the downlink channels and signals, and the second part is dedicated to the uplink channels and signals.

A. Downlink Channels and Signals

As previously stated, the PHY layer of the NB-IoT system is inherited from LTE. Many PHY blocks constituting the channels and signals were adapted to fit the constraints

TABLE V
CHANNELS AND SIGNALS OF THE NB-IOT SYSTEM.

	Type	Name	Role and usage
Downlink	Signals	NPSS	Time & frequency synchronization
		NSSS	Transportation of cell ID
		NRS	Channel estimation
		NPRS (R14)	Positionning
	Channels	NPBCH	Transmission of MIB
		NPDCCH	Transmission of control/scheduling
		NPDSCH	Transmission of data
Uplink	Signals	DMRS	Channel estimation
	Channels	NPUSCH	Transmission of data/control
		NPRACH	Transmission of preambles

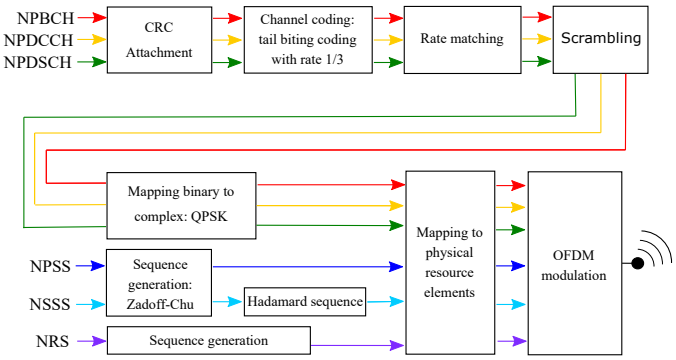

Fig. 6. Overall transmission chain of the NB-IoT eNB (Release 13).

and requirements of the NB-IoT system (e.g., adaptation of blocks like channel coding, modulation, mapping, etc.). Fig. 6 presents the overall transmission chain of the eNB transmitter part. All these channels and signals are mapped over a radio frame of duration 10 ms. Fig. 7 illustrates the NB-IoT radio frame for the three possible operation modes presented in Section II-A.

For in-band operation mode, it can be seen that the first three OFDM symbols in each subframe are avoided since they may be occupied by the LTE control channel. Indeed, the LTE control channel may occupy up to three OFDM symbols of each subframe. Therefore, in general, the NB-IoT signal avoids these symbols, except if the LTE control channel was configured to occupy less than three symbols. Moreover, the REs dedicated to LTE cell-specific reference signal (CRS) are always avoided by the NB-IoT signal.

In contrast, for stand-alone and guard-band operation modes, the NB-IoT signal can occupy all the OFDM symbols of a subframe since the NB-IoT band in such modes is completely separated from the LTE band. However, the mapping of some channels and signals (e.g., NPBCH, NPSS and NSSS) remains unchanged as in in-band operation mode due to the constraints related to the synchronization procedure at the UE side (this is further explained in the following paragraphs).

It is important to note that no more than two antenna ports can be used for the eNB transmitter [65]. Moreover, the quadrature phase-shift keying (QPSK) is the only modulation format that can be used for NB-IoT downlink transmissions. In the following subsections, we present the specific characteristics of each channel and signal.

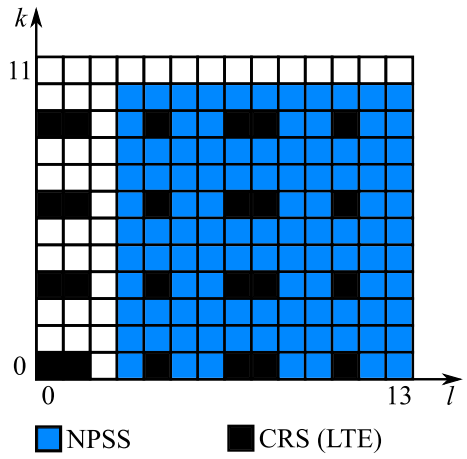

Fig. 8. Mapping of NPSS with one antenna port for NB-IoT and four antenna ports for LTE.

1) Narrowband Primary Synchronization Signal (NPSS): The NPSS is the first essential signal transmitted by the eNB. It is based on a Zadoff-Chu (ZC) sequence [28], [29] that has a very good correlation property. This signal is used by the UE to perform time and frequency synchronization. In other words, it allows the UE to find the beginning of the NB-IoT frame and remove the frequency offset due to its low-cost oscillator.

The NPSS is always transmitted in the 6^{th} subframe (i.e., subframe #5) of each frame as shown in Fig. 7. The mapping to resource elements is done from subcarrier $k = 0$ to $k = 10$, and from symbol $l = 3$ to $l = 13$. However, the NPSS REs that coincide with LTE CRS are not transmitted, as depicted in Fig. 8.

According to Section 10.2.7 of [65], the ZC sequence denoted $c_{l,k}$, is expressed as follows:

$$c_{l,k} = a_l e^{-\frac{\pi u k(k+1)}{11}}, \quad (1)$$

where $l = 3, 4, .., 13$ is the index of OFDM symbols within the subframe, $k = 0, 1, .., 10$ is the index of the subcarriers, $\{a_3, a_4, .., a_{13}\} = \{1, 1, 1, 1, -1, -1, 1, 1, 1, -1, 1\}$, and $u = 5$ is the ZC root sequence index.

In the literature, several time and frequency synchronization methods [30]–[32] have been proposed for NB-IoT UE modules. These methods are further discussed in Subsection IV-B1.

2) Narrowband Secondary Synchronization Signal (NSSS): The NSSS is the second essential signal transmitted by the eNB. It only carries the cell identity (cell ID) information and it is transmitted in the 10^{th} subframe (i.e., subframe #9) of each even frame as shown in Fig. 7. The NSSS is based on the ZC sequence of 132 elements multiplied by a Hadamard sequence. The 132 elements correspond to 11 OFDM symbols multiplied by 12 subcarriers. According to Section 10.2.7.2 of [65], the sequence d_n of length N with $n = 0, .., 131$, that contains the cell ID information is defined as follows:

$$d_n = b_q(m) e^{-2j\pi\theta_f n} e^{-j\frac{\pi u n'(n'+1)}{131}}, \quad (2)$$

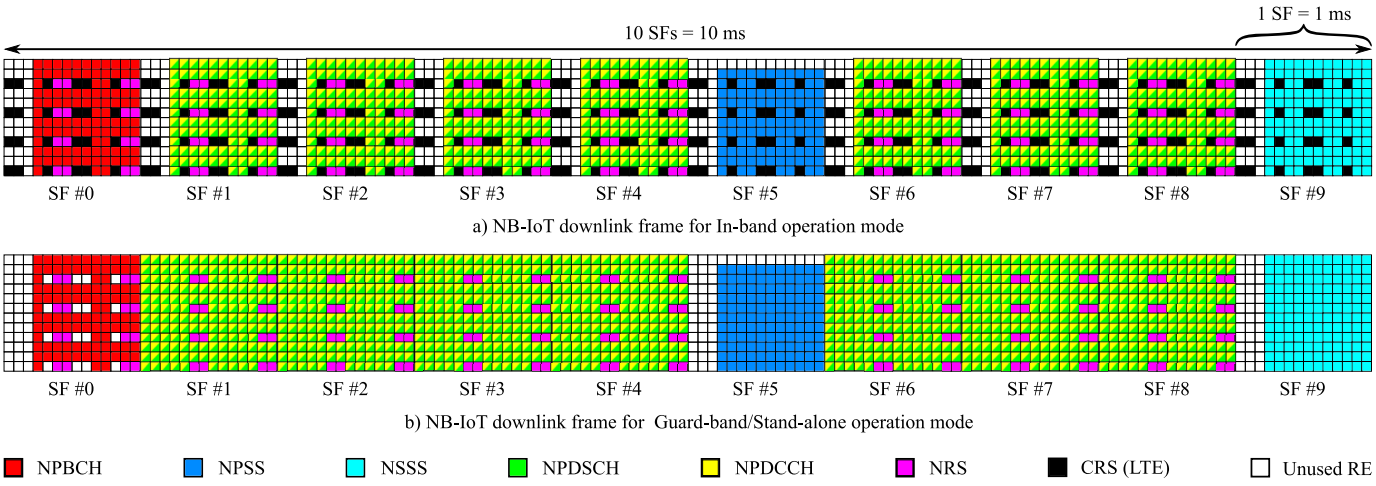

Fig. 7. NB-IoT downlink frame for in-band, guard-band and stand-alone operation modes.

where θ_f is expressed as:

$$\theta_f = \left[\frac{33}{132} \times \left(\frac{n_f}{2}\right)\right] \mod 4 = \left[\frac{1}{4} \times \left(\frac{n_f}{2}\right)\right] \mod 4, \tag{3}$$

where n_f is the frame index, which is always an even number (since NSSS is transmitted in even frames). The other parameters of (2) are expressed as:

$$\begin{aligned} n' &= n \mod 131 \\ m &= n \mod 128 \\ u &= (N_{ID}^{Ncell} \mod 126) + 3 \\ q &= \left\lfloor \frac{N_{ID}^{Ncell}}{126} \right\rfloor, \end{aligned}$$

with N_{ID}^{Ncell} is the cell ID. The last element of the ZC sequence is $\{b_q(m)\}$, which is one of the four Hadamard sequences defined in Table 10.2.7.2.1-1 of [65], where $b_q(m) \in \{-1, 1\}$.

The d_n elements of NSSS occupy the 12 subcarriers of the NB-IoT PRB in increasing order from $k = 0$ to $k = 11$ and are mapped from the 4^{th} to the 14^{th} OFDM symbol (i.e., from $l = 3$ to $l = 13$), as shown in Fig. 9. Thus, the first NSSS sample d_0 is mapped on the RE position $(k = 0, l = 3)$ and d_{131} is mapped on the position $(k = 11, l = 13)$. Note that, similar to NPSS, the REs that are occupied by LTE CRS are avoided during the mapping of d_n elements.

In NB-IoT, as in LTE, the cell ID can take any value between 0 and 503. However, in LTE the cell ID information is shared between the primary synchronization signal (PSS) and the secondary synchronization signal (SSS). Moreover, for in-band operation mode, the NB-IoT eNB can be configured to have the same or different cell ID as that of LTE. The impact of this configuration is discussed in the following Section III-A3.

3) Narrowband Reference Signal (NRS): The NRS, usually called "pilot", is dedicated to channel estimation in the frequency domain. It is always transmitted in all subframes except those dedicated to NPSS and NSSS. The NRS is

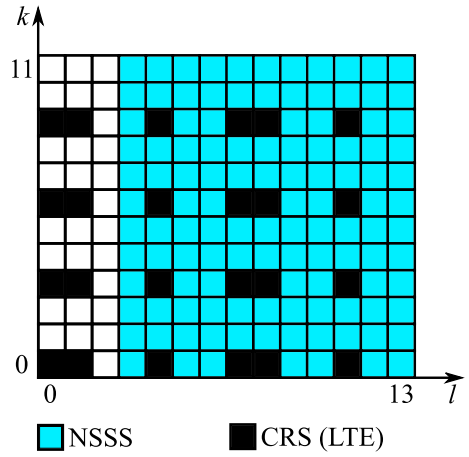

Fig. 9. Mapping of NSSS with one antenna port for NB-IoT, four antenna ports for LTE, and $N_{ID}^{Ncell} = 0$ for both systems.

mapped over the 6^{th}, 7^{th}, 13^{th}, and 14^{th} OFDM symbols of each subframe as illustrated in Fig. 10. The frequency position of NRS REs depends on the value of the cell ID (N_{ID}^{Ncell}) as described in [65]. In addition, depending on the number of antenna ports used by the NB-IoT eNB, more or less REs are occupied by the NRS. Fig. 10 shows the two possible configurations and the disposition of the NRS over the frequency axis.

It can be seen that, in the case of one antenna port, two pilots are multiplexed per OFDM symbol and they are always separated by six subcarriers [65]. For the case of two antenna ports, the same principle is applied, and another two pilots are multiplexed per OFDM symbol with a separation of six subcarriers as shown in Fig. 10. Moreover, for in-band operation mode, the NB-IoT and LTE pilots are aligned over the frequency axis only in the case where the value of the cell ID is the same for both systems.

The NRS is composed of QPSK-like complex elements with values $\frac{1}{\sqrt{2}}(\pm 1 \pm j)$. They are generated by the same pseudo-random sequence as in LTE, called the "gold sequence" (further details are provided in Section 7.2 of [65]), and their

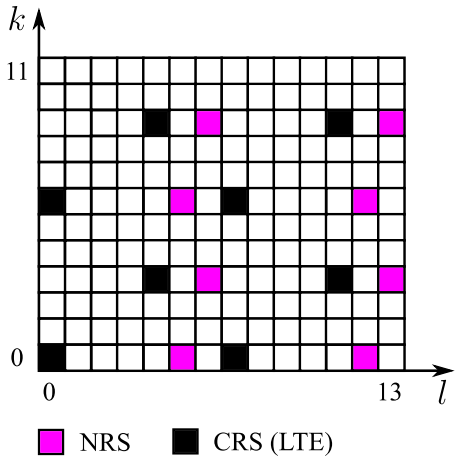

(a) Mapping of the NRS with one antenna port for NB-IoT and one antenna port for LTE.

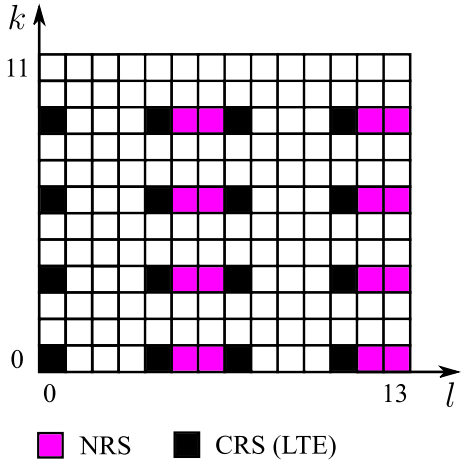

(b) Mapping of the NRS with two antenna ports for NB-IoT and two antenna ports for LTE.

Fig. 10. Mapping of the NRS over one subframe with $N_{ID}^{Ncell} = 0$ for both systems.

values are generated like the CRS of LTE. In NB-IoT, the positions of the REs dedicated to the NRS are very important, since the mapping process of all downlink channels should avoid them.

4) Narrowband Physical Broadcast Channel (NPBCH): The NPBCH is the first essential channel for the NB-IoT UE modules as it is the first to be decoded. It is always transmitted in subframe #0 of each frame and carries the narrowband master information block (MIB-NB). The latter contains the essential information required by UE modules to receive further essential system information (i.e., SIB1-NB which is described in Section V-A). The MIB-NB contains 34 bits of data and 16 bits of cyclic redundancy check (CRC). These 50 bits are encoded using tail-biting convolutional coding, then interleaved, rate-matched, scrambled and finally mapped to REs as shown in Fig. 6. The details of this encoding process are presented in Section V-A.

The mapping of NPBCH over subframe #0 for in-band operation mode is depicted in Fig. 11. It can be seen that the first three OFDM symbols and the REs dedicated to the

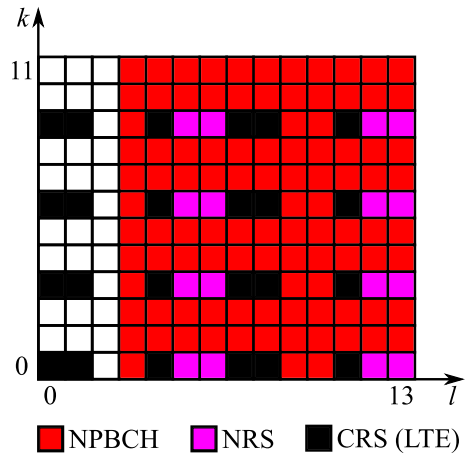

Fig. 11. Mapping of NPBCH with two antenna ports for NB-IoT, four antenna ports for LTE, and $N_{ID}^{Ncell} = 0$ for both systems.

pilots of LTE and NB-IoT systems are avoided (i.e., LTE CRS and NRS). This leads to only 100 REs per subframe that can be used for the transmission of NPBCH symbols. It is important to note that, regardless of the NB-IoT operation mode, the mapping of NPBCH is always done as if there are four antenna ports for LTE and two antenna ports for NB-IoT. Indeed, the UE module is completely blind before acquiring the MIB-NB (i.e., it does not know the operation mode of NB-IoT eNB, the symbols number of the LTE control channel, or the number of LTE and NB-IoT antennas ports). Therefore, the first three OFDM symbols are never used to avoid any possible conflicts with the LTE control channel. Moreover, since the UE a priori supposes a maximum usage of antenna ports (i.e., four antennas for LTE and two for NB-IoT), all the REs dedicated to the pilots of LTE and NB-IoT are thus avoided. During the acquisition of the MIB-NB, the UE has already decoded the cell ID (N_{ID}^{Ncell}) from NSSS, and thus, can find the frequency positions of the NB-IoT pilots to be avoided.

To demonstrate the importance of the broadcast channel, we present the content of the MIB-NB and the usage of each parameter [74]:

- *systemFrameNumber-MSB-r13*: Four bits indicating the most significant bits (MSBs) of the SFN
- *hyperSFN-LSB-r13*: Two bits indicating the two less significant bits (LSBs) of the H-SFN
- *schedulingInfoSIB1-r13*: Four bits for the SIB1-NB scheduling and size
- *systemInfoValueTag-r13*: Five bits indicating the system information value tag
- *ab-Enabled-r13*: One bit indicating whether access class barring is applied or not
- *operationModeInfo-r13*: Seven bits indicating the operation mode of NB-IoT
- *spare*: Eleven spare bits for future extensions

The first two parameters hold part of the information for the SFN and H-SFN. The UE gets the rest of the information after decoding the "narrowband system information block type 1 (SIB1-NB)" (presented in Section V-B). The third parameter

"*schedulingInfoSIB1-r13*" is used by the UE to get the location in the time of the SIB1-NB. The "*systemInfoValueTag-r13*" parameter is used to indicate to the UE that a modification occurred in the content of the system information blocks. The "*ab-Enabled-r13*" parameter is beyond the scope of this tutorial, however, it is used to indicate if the access barring feature is activated. Finally, the last parameter, "*operationModeInfo-r13*", is used to indicate the operation modes of the NB-IoT eNB. At the same time, it indicates in the case of the in-band operation mode, if the NB-IoT eNB is using the same or different cell ID as that of LTE.

It is important to recall that, for downlink transmissions, only QPSK modulation is used and thus only two bits can be mapped per RE. Therefore, the maximum number of bits that can be transmitted over subframe #0 is limited to 200 bits since only 100 REs are available. Moreover, the UE is able to find the number of used antenna ports for NB-IoT and LTE only when the MIB-NB is decoded.

From Release 13.5, the 3GPP defined an additional scrambling block for the NPBCH to make the channel more tolerant to interference. The goal is to reduce the interference related to neighbor cells. This scrambling is applied to all complex QPSK elements of each transmitted NPBCH subframe. The new scrambling method consists of applying additional phase shifting $e^{j\phi}$ to all NPBCH REs, where $\phi \in \{-\frac{\pi}{2}, 0, \frac{\pi}{2}, \pi\}$. The scrambling sequence of the new block only depends on the cell ID and the frame index and is initialized at the beginning of each radio frame.

5) Narrowband Physical Downlink Shared Channel (NPDSCH): The NPDSCH is dedicated to data transmissions. It is used to transmit system information blocks and the data for users. This channel can be mapped over any downlink subframe except the subframes allocated to NPBCH, NPSS and NSSS (i.e., subframe #0, subframe #5 and subframe #9 if used by the NSSS).

The mapping of the NPDSCH is done according to a parameter called $l_{DataStart}$ [65] that determines the starting OFDM symbol as shown in Fig. 12. The $l_{DataStart}$ can take several values depending on the high layer parameter *eutraControlRegionSize* (transmitted in SIB1-NB [74]). For the case of in-band operation mode, this parameter can take three possible values (1, 2 or 3) depending on the length of LTE control region. For the other modes, it always takes 0 as a value.

In Fig. 12, we set the value of $l_{DataStart}$ to 3, since we assumed an in-band operation mode with *eutraControlRegionSize* that equals to 3. The mapping of REs is done in the same way as for all other channels and signals, from $k = 0$ to $k = 11$ and from $l = l_{DataStart}$ to $l = 13$. However, all REs dedicated to NRS and LTE CRS are avoided, considering one antenna port for NB-IoT and one antenna port for LTE. Besides, the number of available REs is identified in advance at the rate-matching block level.

The only particularity of NPDSCH occurs when it is used to transmit the SIB1-NB. In this case, the $l_{DataStart}$ parameter will be set to 3 for the in-band operation mode and to 0 otherwise. In fact, the *eutraControlRegionSize* parameter is transmitted in the SIB1-NB and thus it is impossible for any

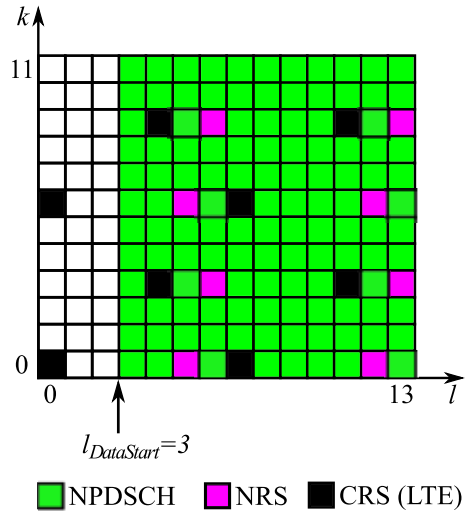

Fig. 12. Mapping of NPDSCH with a single antenna port for LTE and NB-IoT, and a $N_{ID}^{Ncell} = 0$ for both systems.

TABLE VI
LIST OF DCI FORMATS.

DCI format	Size in bits	Content and usage
N0	23	UL resource grant
N1	23	NPDSCH resource scheduling RACH procedure initiated by NPDCCH order
N2	15	Paging and direct indication

UE to get this value before decoding SIB1-NB. For this reason, for the case of in-band operation mode, the first three OFDM symbols are always left blank when transmitting MIB-NB and SIB1-NB.

6) Narrowband Physical Downlink Control Channel (NPDCCH): As in LTE, a control channel is needed to prepare the phase of data transmission. In NB-IoT, the NPDCCH is dedicated to the transmission of control information from the network towards the UEs. In this respect, the eNB can transmit different types of control information, including the following:

- Downlink resource scheduling
- Data acknowledgement (i.e., acknowledgement for uplink transmission)
- Uplink resource grant (i.e., uplink resource scheduling)
- Paging and direct indication

The control information is carried in a logical block called "downlink control information (DCI)". In NB-IoT, three types of DCI formats are defined: N0, N1 and N2 (see section 6.4.3 of [75]). The choice between the different formats depends on the kind of data to be further exchanged between the eNB and the UEs. Table VI shows the list of DCI formats with the size, content, and usage of each one. The list of parameters composing each DCI format can be found in Section 6.4.3 of [75].

Exactly like the NPDSCH, the NPDCCH can be allocated to any available downlink subframe except the subframes allocated to NPBCH, NPSS and NSSS. Also, the mapping process is exactly the same as that of NPDSCH, but with a different starting OFDM symbol index "$l_{NPDCCHStart}$".

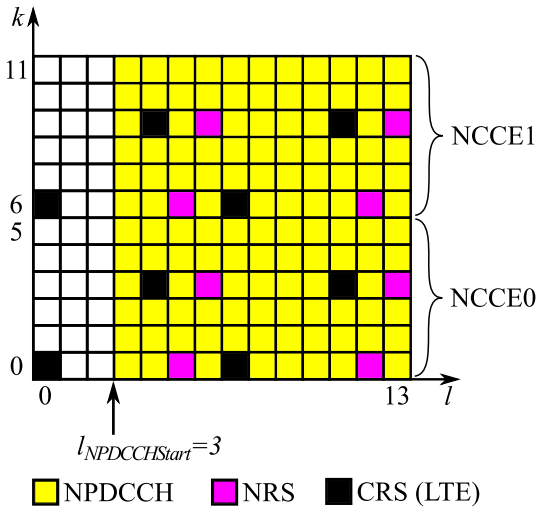

Fig. 13. Mapping of the NPDCCH with a single antenna port for LTE and NB-IoT, and a $N_{ID}^{Ncell} = 0$ for both systems.

For in-band operation mode, this index takes three possible values (1, 2 or 3) depending on the LTE control region size (*eutraControlRegionSize*), and equals 0 in the other modes.

The basic physical block unit of the NPDCCH channel is called the "narrowband control channel element (NCCE)". The transmission of the NPDCCH can be done through one or two NCCEs (NCCE0 & NCCE1), where each NCCE corresponds to six consecutive subcarriers within one subframe. Fig. 13 shows the frequency mapping of the two NCCEs over a NPDCCH subframe.

Two NPDCCH formats are supported in NB-IoT: format 0 and format 1. These formats indicate the number of used NCCEs during the transmission of the DCI, where format 0 uses one NCCE and format 1 uses both NCCEs. The use of format 0 or format 1 depends on the search space over which the NPDCCH is transmitted. The principle of search space will be further detailed in Section V-H.

In case of format 0, one NCCE is used (NCCE0 or NCCE1) and thus the mapping to REs will be either on the lower six subcarriers or on the upper six subcarriers, as shown in Fig. 13. The NCCE0 occupies subcarriers $k = 0$ to $k = 5$ and the NCCE1 occupies subcarriers $k = 6$ to $k = 11$. In the case of format 1, the two NCCEs are used. The mapping of REs is done exactly like for NPDSCH, from $k = 0$ to $k = 11$ and from $l = l_{NPDCCHStart}$ to $l = 13$. However, for both formats, all REs dedicated to NRS and LTE CRS are also avoided as in NPDSCH.

B. Uplink Channels and Signals

As for downlink, NB-IoT uplink channels and signals also inherit most of the characteristics of LTE uplink channels and signals, but they are optimized to respect the constraints of NB-IoT UE modules. In this respect, the SC-FDMA technique is used for uplink transmissions. Moreover, most of the blocks of the LTE UE transmission chain were kept unchanged, but the possible configurations to be used were reduced (e.g., sets of used modulation formats).

The main differences with LTE appear at two levels: the random access channel level and the data/control channel level. At the random access level, a new waveform was designed for the NB-IoT preamble. However, at the data/control channel level, the data and control information were grouped into a single channel rather than having a dedicated channel for each kind of information as in LTE. The details of these differences are discussed in the following subsections.

1) Narrowband Physical Random Access Channel (NPRACH): The NPRACH is dedicated to the transmission of the NB-IoT preamble which is the first transmitted signal by the UE towards the eNB in order to request access to the network. Each preamble is composed of four groups of symbols as illustrated in Fig. 14. Each group of symbols is a set of five symbols with one CP. These symbols form a pure sinusoid of amplitude β and have a frequency f_i with $i \in \{0, 1, 2, 3\}$ (f_i is the frequency used for each sinusoid as shown in Fig. 14). Moreover, the subcarrier spacing used for the transmission of NPRACH is equal to 3.75 kHz. This leads to 48 possible subcarriers that can be used to transmit a preamble over the 180 kHz bandwidth of the NB-IoT system.

Two NPRACH formats are defined for NB-IoT in Release 13: format 0 with a CP duration of 66.7 μs, and format 1 with a CP duration of 266.7 μs. However, the symbol duration for the two formats is the same and equals 266.7 μs. This consequently leads to a preamble duration of 5.6 ms for format 0 and 6.4 ms for format 1. It is noteworthy that, format 1 with longer CP facilitates the detection of the preamble by the eNB, since it inherently carries more energy than the format 0.

In order to reduce the probability of collision between the preambles transmitted from different UEs in a cell, the mechanism of frequency hopping is used. Therefore, as shown in Fig. 14, to transmit one preamble, four frequencies are required. These frequencies f_i (in kHz) are pseudo-randomly chosen according to the formula given in Section 10.1.6 of [65]:

$$f_i = (n_{sc}^{RA}(i) + Kk_0 + \frac{1}{2}) \times 3.75, \quad (4)$$

where $n_{sc}^{RA}(i) \in \{0, 1, .., 47\}$ is the pseudo-random subcarrier index, K and k_0 are two parameters defined in [65] and $K \times k_0$ always equals -24 which leads to $f_i = (n_{sc}^{RA}(i) - 23.5) \times 3.75$ kHz.

To understand how this frequency hopping is done, we consider here only one preamble transmission. Therefore, we assume that the four frequencies required for the first preamble transmission are $\{f_0, f_1, f_2, f_3\}$ as illustrated in Fig. 14. As indicated in [65], the frequency hopping is performed in strictly 12 consecutive subcarriers within a set of N_{sc}^{NPRACH} subcarriers (N_{sc}^{NPRACH} are chosen from the 48 available subcarriers). The N_{sc}^{NPRACH} parameter and the process to identify these 12 subcarriers is further explained in Section V-E.

Based on these inputs, the mechanism of frequency hopping consists of computing $n_{sc}^{RA}(i)$ in order to find each f_i. In [65], $n_{sc}^{RA}(i)$ has the following formula "$n_{sc}^{RA}(i) = n_{start} + \tilde{n}_{sc}^{RA}(i)$", where n_{start} and $\tilde{n}_{sc}^{RA}(i)$ are computed using the following steps:

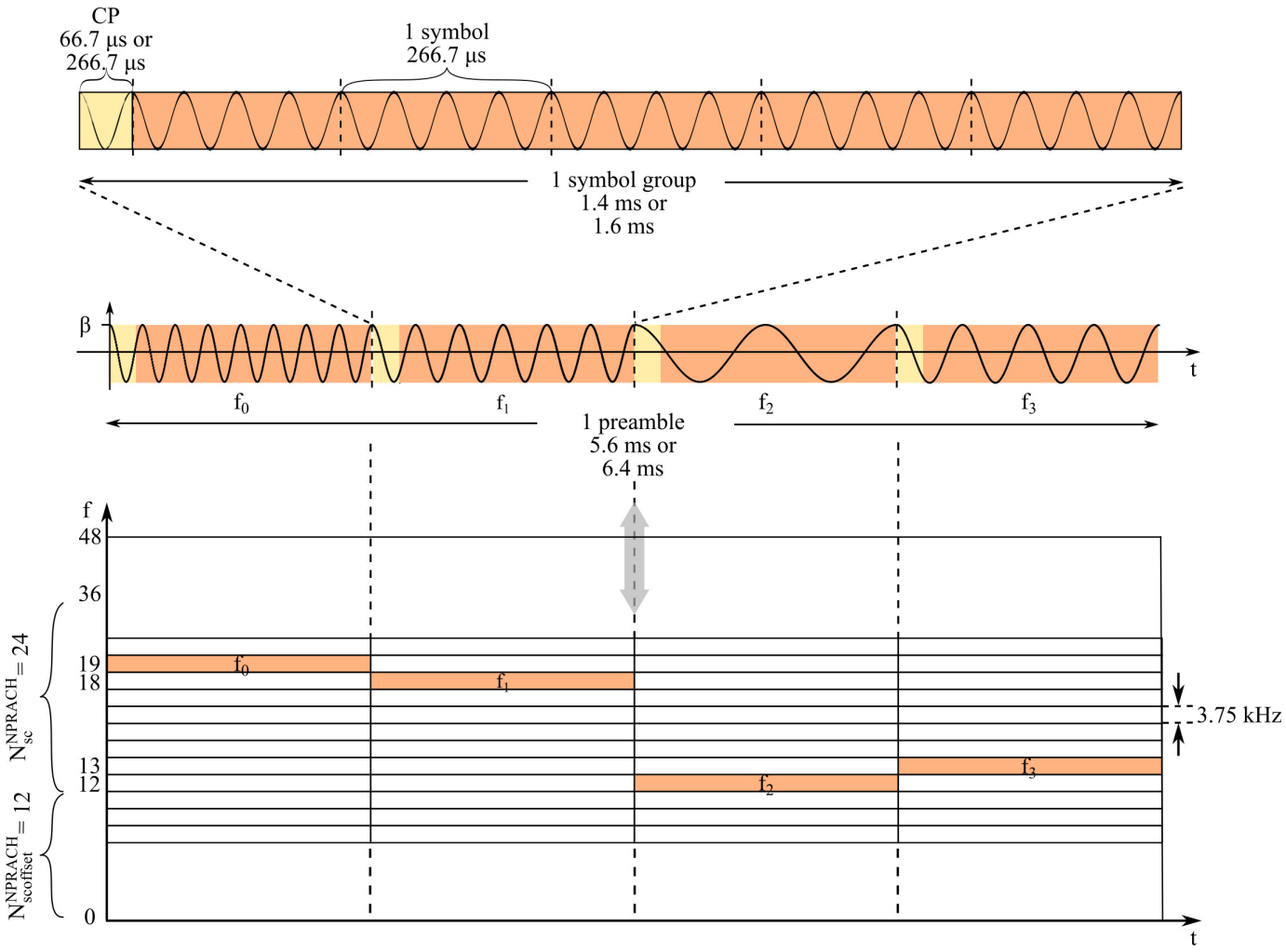

Fig. 14. Time and frequency representation of one NPRACH preamble where $N_{scoffset}^{NPRACH} = 12$, $N_{sc}^{NPRACH} = 24$, and $n_{init} = 7$.

1) The first subcarrier index $n_{sc}^{RA}(0)$ is selected randomly by the UE according to the following formula (see Section 10.1.6 of [65]):

$$n_{sc}^{RA}(0) = n_{start} + \underbrace{(n_{init} \mod 12)}_{\tilde{n}_{sc}^{RA}(0)}, \tag{5}$$

where n_{init} parameter is the part of the formula which is randomly chosen by the UE in $\{0, 1, .., N_{sc}^{NPRACH} - 1\}$. The other parameter n_{start} corresponds to the lowest subcarrier index of the selected 12 consecutive subcarriers over which the preamble transmission is performed, such that $n_{start} = N_{scoffset}^{NPRACH} + 12 \times \lfloor \frac{n_{init}}{12} \rfloor$. Note that, the value of $N_{scoffset}^{NPRACH}$ parameter is transmitted by the eNB through the system information blocks (as is further explained in Section V-E).

2) Once the value of $n_{sc}^{RA}(0)$ is found through (5), the computation of the following subcarrier indexes is performed using the formula "$n_{sc}^{RA}(i) = n_{start} + \tilde{n}_{sc}^{RA}(i)$" for $i \in \{1, 2, 3\}$ (i is hereby limited to three since we consider only one preamble transmission). In general, the values of $\tilde{n}_{sc}^{RA}(i)$ follow a deterministic sequence that allows the computation of any further value for $n_{sc}^{RA}(i)$. The extensive expression of the deterministic hopping sequence is provided in Section 10.1.6 of [65]. To summarize, the $\tilde{n}_{sc}^{RA}(i)$ values, for any $i \geq 1$ are constrained by the following rule:

$$\tilde{n}_{sc}^{RA}(i) = \begin{cases} \tilde{n}_{sc}^{RA}(i-1) + 1, \text{ if } (i \bmod 4) \in \{1, 3\}, \\ \qquad \text{and } \tilde{n}_{sc}^{RA}(i-1) \bmod 2 = 0 \\ \tilde{n}_{sc}^{RA}(i-1) - 1, \text{ if } (i \bmod 4) \in \{1, 3\}, \\ \qquad \text{and } \tilde{n}_{sc}^{RA}(i-1) \bmod 2 = 1 \\ \tilde{n}_{sc}^{RA}(i-1) + 6, \text{ if } i \bmod 4 = 2, \\ \qquad \text{and } \tilde{n}_{sc}^{RA}(i-1) < 6 \\ \tilde{n}_{sc}^{RA}(i-1) - 6, \text{ if } i \bmod 4 = 2, \\ \qquad \text{and } \tilde{n}_{sc}^{RA}(i-1) \geq 6 \\ (\tilde{n}_{sc}^{RA}(0) + f(\frac{i}{4})) \bmod 12, \\ \qquad \text{if } i \bmod 4 = 0 \text{ and } i > 0 \end{cases}, \tag{6}$$

where f is a deterministic function that is defined in Section 10.1.6 of [65].

In order to illustrate the pseudo-random NPRACH frequency hopping mechanism, we consider the example of Fig. 14. We assume that the set of 12 consecutive subcarriers

TABLE VII
CONFIGURATION PARAMETERS FOR NPUSCH FORMATS 1 AND 2.

Format	1			2	
Δ_f (kHz)	3.75	15		3.75	15
N_{sc}	1		3, 6, 12	1	
Mapping b2c	$\frac{\pi}{2}$-BPSK, $\frac{\pi}{4}$-QPSK		QPSK	$\frac{\pi}{2}$-BPSK	
Pre-coding	No		DFT	No	
Modulation	Single carrier		SC-FDMA	Single carrier	
Coding	Turbo-code 1/3			Repetition	
Pilot position #	4	3		0,1,2	2,3,4
CP length (μs)	8.33	5.21 (1st symb.) 4.69 (other symb.)		8.33	

dedicated to the transmission of the preamble are located between index number 12 and 23 (i.e., $N_{scoffset}^{NPRACH} = 12$ and $N_{sc}^{NPRACH} = 24$). Moreover, we assume that the random parameter n_{init} chosen by the UE equals 7, hence $\tilde{n}_{sc}^{RA}(0) = 7$. Thus, we can deduce that $n_{start} = 12$ and $n_{sc}^{RA}(0) = 19$.

Furthermore, using the above assumptions and the aforementioned deterministic hopping sequence, we can find the other subcarriers indexes. Using $n_{sc}^{RA}(0) = 19$, we get the following indexes: $n_{sc}^{RA}(1) = n_{sc}^{RA}(0) - 1 = 18$, $n_{sc}^{RA}(2) = n_{sc}^{RA}(1) - 6 = 12$, and $n_{sc}^{RA}(3) = n_{sc}^{RA}(2) + 1 = 13$. The frequency hopping mechanism is the same within all preamble repetitions, and the frequency hopping procedure between two repetitions (i.e., when $i \mod 4 = 0$) is defined through the deterministic function f of Section 10.1.6 in [65].

In summary, the only random element of the NPRACH frequency hopping mechanism is the choice of $n_{sc}^{RA}(0)$ index by the UE, even if the whole process seems to be random in [65]. Therefore, if two NB-IoT UEs in a cell select the same $n_{sc}^{RA}(0)$ index, the other indexes of their preambles will have exactly the same values. Thus, in such case, a collision happens between the two preambles. More details on preamble scheduling, repetitions and possible configurations are provided in Section V-E.

2) Narrowband Physical Uplink Shared Channel (NPUSCH): The NPUSCH is dedicated to the transmission of data and control information from the UE side. In this respect, two formats were defined: format 1 for data and format 2 for control information (i.e., ACK/NACK). However, in order to adapt the signal robustness to the severity of the propagation environment, different configurations for uplink transmissions are possible. These transmission configurations are summarized in Table VII, showing the parameters to be used for format 1 and 2. Note that Δ_f and N_{sc} stand for the subcarrier spacing and the number of subcarriers, respectively.

To clearly understand how uplink transmissions are done, an overview of the NPUSCH transmission chain, which includes several sequential binary and physical processes, is provided in Fig. 15. One can notice that the uplink transmission chain contains many blocks that are similar to the PHY blocks of downlink channels. Therefore, we only focus on the blocks that are specific to NPUSCH.

It can be seen on Fig. 15 that NPUSCH format 1 and format 2 share only a few processes. In NPUSCH format 1, the payload + CRC are encoded with a turbo-encoder with rate 1/3. Then, after a dedicated rate matching block, a channel interleaving is applied to strengthen the encoded bits

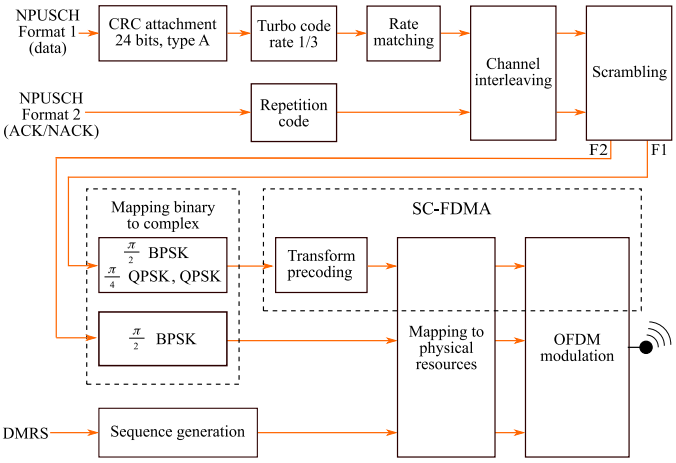

Fig. 15. Overall transmission chain of the NB-IoT UE (Release 13).

from errors induced by the propagation channel. These binary processes are described in Sections 6.3 and 5.2 of [75]. After scrambling, the binary to complex (b2c) conversion is limited to three modulation formats: $\frac{\pi}{2}$-BPSK, $\frac{\pi}{4}$-QPSK and QPSK. The $\frac{\pi}{2}$-BPSK and $\frac{\pi}{4}$-QPSK formats are used for single-tone transmissions, whereas the QPSK format is used for multi-tone transmissions. These modulation formats used by the UE modules allow for a reduction in the peak-to-average power ratio (PAPR) which reduces the power consumption.

Finally, a SC-FDMA modulation technique is used which is similar to that of OFDM, but with a difference at the complex elements level that are pre-coded with a discrete Fourier transform (DFT) matrix (i.e., in transform pre-coding block) of size $N_{sc} \in \{3, 6, 12\}$ before being mapped to REs. The benefit of SC-FDMA is to mainly reduce the PAPR which helps reducing the power consumption in UE devices. Additional information on PAPR impacts on multi-tone systems with a low number of subcarriers can be found in [24].

In NPUSCH format 2, a repetition code is used instead of turbo coding. It consists of repeating the ACK/NACK bit (1 for ACK, 0 for NACK) 16 times. Then, a channel interleaving and a scrambling are applied in order to add randomness to the transmitted binary message. The resulting bits are then mapped to a complex using only $\frac{\pi}{2}$-BPSK format and transmitted over a RU of four slots. The mapping of complex elements to physical resources for both formats is performed according to a "frequency-first" rule for any chosen configuration (i.e., all the available N_{sc} consecutive subcarriers of a given symbol are mapped from lowest to highest frequency before moving to the next non-pilot symbol). The pilots are presented in the following subsection.

Different subsets of N_{sc} subcarriers can be used for uplink transmissions with 15 kHz of subcarrier spacing, but their indexes can only take a specific set of values as defined in Table 16.5.1.1-1 of [83]. These indexes are denoted by n_{sc} and are reported as follows:

- If $N_{sc} = 1$, $n_{sc} \in \{0, 1, .., 11\}$
- If $N_{sc} = 3$, $n_{sc} \in \{\{0, 1, 2\}, \{3, 4, 5\}, \{6, 7, 8\}, \{9, 10, 11\}\}$
- If $N_{sc} = 6$, $n_{sc} \in \{\{0, 1, 2, 3, 4, 5\}, \{6, 7, 8, 9, 10, 11\}\}$

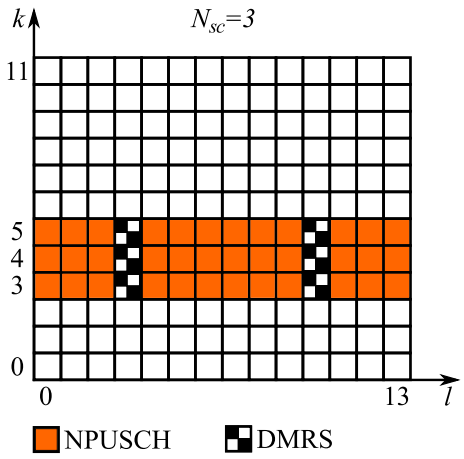

Fig. 16. Mapping of DMRS considering NPUSCH format 1 with $\Delta_f = 15$ kHz, $N_{sc} = 3$, and $n_{sc} = \{3, 4, 5\}$.

- If $N_{sc} = 12$, $n_{sc} = \{\{0, 1, 2, 3, 4, 5, 6, 7, 8, 9, 10, 11\}\}$
- In the case of $\Delta_f = 3.75$ kHz, $n_{sc} \in \{0, 1, .., 47\}$

It is noteworthy that the subcarrier spacing and the number of subcarriers are the differentiating parameters of uplink transmissions. In fact, depending on the position of the UE in the cell (i.e., in what coverage condition), a specific configuration should be used to achieve a successful transmission. For example, if the UE is in the basement of a building, the eNB will ask the UE to transmit using format 1, with $\Delta_f = 3.75$ kHz and $\frac{\pi}{2}$-BPSK, because it is more resistant to high frequency fading. However, if the UE is in line of sight with good coverage condition, the eNB can ask the UE to transmit with, for example, 12 subcarriers using QPSK modulation to achieve a higher data rate. Moreover, the NPUSCH transmissions can be repeated many times to improve the reception of the uplink messages at the eNB side. In Release 13, NPUSCH transmissions can be repeated up to 128 times.

3) Demodulation Reference Signal (DMRS): The DMRS, also called the "uplink pilot", is dedicated to channel estimation in the frequency domain for uplink transmissions. Unlike the NRS in downlink, DMRS elements are not multiplexed within a symbol, but are instead allocated over the N_{sc} subcarriers of an entire symbol (one or three symbols per slot can be used for uplink pilots). These pilot symbols are also called "midambles". The position of the midambles within the slot depends on the NPUSCH configuration, as provided in Table VII. Moreover, as shown in Fig. 15, these midambles are not precoded by a DFT matrix, allowing for simple channel estimation at the receiver side of the eNB (as in the OFDM system).

An example of DMRS mapping to physical resources is illustrated in Fig. 16, where a NPUSCH format 1 transmission is considered with $\Delta_f = 15$ kHz, $N_{sc} = 3$, and $n_{sc} = \{3, 4, 5\}$. The mapping of the REs dedicated to DMRS is done exactly like the mapping for NPUSCH, i.e., from lowest to highest frequency before moving to the next pilot symbol. In this configuration, there is only one symbol per slot used for uplink pilots.

The values of the DMRS sequence depend on the NPUSCH configuration, as described in Section 10.1.4.1 of [65]. Therefore, in the case of single-tone transmission ($N_{sc} = 1$), the midambles are obtained from a base sequence denoted by $\bar{r}_u(n)$, and defined by:

$$\bar{r}_u(n) = \frac{1}{\sqrt{2}}(1 + j)(1 - 2c(n))w(n \mod 16), \quad (7)$$

where $n = 0, 1, .., N_{seq} - 1$ and N_{seq} is the size of the base sequence. $c(n) \in \{0, 1\}$ is generated with a pseudo-random gold sequence, and $w(n)$ is a Hadamard sequence of length 16 defined in Table 10.1.4.1.1-1 of [65]. For the case of $N_{sc} = 1$, the size of the sequence N_{seq} corresponds exactly to the number of slots to be transmitted for a given NPUSCH message (including all the repetitions of the message). The $w(n)$ values are chosen as a function of the values of u parameter (where $u = N_{ID}^{Ncell} \mod 16$), as shown in Table 10.1.4.1.1-1 of [65]. However, this is valid only for the case of NPUSCH format 2 and when the group hopping (described in Section 10.1.4.1.3 of [65]) is deactivated for NPUSCH format 1. For the case of format 1 with group hopping enabled, the u parameter follows another expression described in Section 10.1.4.1.3 of [65].

To summarize, from the base sequence in (7), the reference signal sequence (DMRS sequence) denoted by $r(n)$ is defined as follows: in the case of NPUSCH format 1, $r(n) = \bar{r}_u(n)$, i.e., each pilot value is defined from a unique base sequence value. In the case of NPUSCH format 2, $r(3n + m) = \bar{r}_u(n)\bar{w}(m)$ with $m = 0, 1, 2$ and $\bar{w}(m)$ corresponds to a phase rotation defined in Table 5.5.2.2.1-2 of [65]. This means that the three pilots in a given slot are defined from the same base sequence value.

For example, if a NPUSCH format 2 message (ACK/NACK) is transmitted with only two repetitions, since an ACK/NACK transmission occupies 4 uplink slots, thus $N_{seq} = 8$, and the pilot sequence $r(n)$ will have a length of 24.

For multi-tone transmissions ($N_{sc} > 1$), the base sequence is defined as in Section 10.1.4.1 of [65]:

$$r_u(n) = e^{j\alpha n} e^{j\frac{\pi}{4}\phi(n)}, \quad (8)$$

where $n = 0, 1, .., N_{sc} - 1$. This base sequence generates the values of each pilot symbol carried over the used N_{sc} subcarriers in a given slot. The α parameter called "cyclic shift" is defined in Table 10.1.4.1.2-3 of [65] for N_{sc} = 3 or 6, and $\alpha = 0$ for $N_{sc} = 12$.

The other parameter $\phi(n)$ is given by three Tables 10.1.4.1.2-1, 10.1.4.1.2-2, and 5.5.1.2-1 of [65] for N_{sc}=3, 6, and 12, respectively. However, the values of $\phi(n)$ also depend on the u parameter. If the group hopping is enabled, the u values are found as described in Section 10.1.4.1.3 of [65]. If the group hopping is disabled, the u values can be found through high layer parameters defined by the eNB as indicated in Section 10.1.4.1.2 of [65]. If these high layer parameters were not present, u will be equal to "$N_{ID}^{Ncell} \mod 12$", "$N_{ID}^{Ncell} \mod 14$" and "$N_{ID}^{Ncell} \mod 30$" for N_{sc}=3, 6, and 12, respectively.

Similar to LTE, the group hopping may be enabled/disabled in NB-IoT for NPUSCH format 1. The aim of group hopping is to provide diversity for pilot values by pseudo-randomly changing the value of u parameter from one slot to another (the sequences $w(n)$ and $\phi(n)$ are configured by u). This allows preventing two neighboring cells from sharing the same pilot sequence.

IV. PHY Layer: Receiver Design at eNB and UE

We recall that the design of the transmitter for the UE and the eNB is always specified by the 3GPP, and that the receiver design is left to the manufacturers. Therefore, in this section, we describe a basic receiver design for both UE and eNB, and discuss the possible improvements or alternative implementations that can be applied.

A. Receiver Design at eNB

Any designed receiver at the eNB side should be able to handle the reception of the two uplink channels: NPRACH and NPUSCH.

1) Reception of NPRACH: As previously described in Section III-B1, the UE transmits preambles through the NPRACH to trigger the connection with the eNB. The detection of such preambles is essential in order to identify any UE trying to join the network. However, since the preamble is a pure complex sine wave that does not carry any usefulbinary information, the eNB should deduce several essential parameters and include them in its response according to the 3GPP specifications. Fig. 18 provides an overview of the reception blocks used after the detection of a preamble at the eNB.

It can be seen in Fig. 18 that after detecting a preamble, the eNB estimates first the frequency offset θf between the expected preamble and the received one. This frequency offset is illustrated in Fig. 17 (an example of a frequency offset estimator for NB-IoT can be found in [38]). In the second step, the eNB estimates the delay δt between the expected time of arrival and the actual one. This delay is due to the signal propagation time between the eNB and the UE. It is equal to $\delta t = 2\frac{D}{c}$, where D is the distance between the eNB and the UE, and c is the speed of light. Note that the factor 2 is to account for signal round-trip propagation delay. The parameter δt, also called timing advance (TA), is always transmitted to the UE so it can trigger any further transmission with a time advance of δt. In this way, the UE becomes temporally synchronized with the eNB. The concept of TA is detailed and illustrated in [39]. Note that TA values can be large in NB-IoT, as the cell range D can be greater than 10 km, whereas it is less than a few kilometers in LTE. Such long ranges can be achieved due to the repetitions mechanism, allowing for up to 164 dB of tolerated maximum coupling loss in NB-IoT (20 dB greater than in LTE). More details about downlink and uplink achievable performance are provided in Tables VI and VII in [62], as well as in [61].

In addition to the estimation of frequency and time offsets, the eNB should deduce the first subcarrier index of the received preamble. This subcarrier index $n_{sc}^{RA}(0)$ also called random access preamble identifier (RAPID) [84] corresponds to the first group of symbols constituting the preamble as presented in Section III-B1. Finally, the eNB computes an identifier called random access-radio network temporary identifier (RA-RNTI) to identify the UE. This RA-RNTI is computed using the following formula: RA-RNTI = $1 + SFN/4$, where SFN corresponds to the frame index in which the preamble was received.

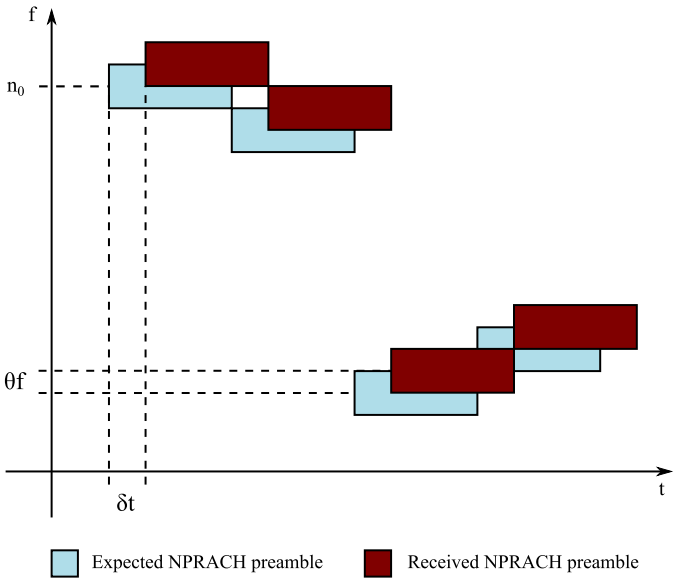

Fig. 17. Example of frequency/time offset between the received NPRACH preamble and the expected one.

2) Decoding Chain of NPUSCH: The reception chain of the NPUSCH is generally symmetric with the transmission chain at the UE side, as depicted in Fig. 15. In fact, the binary processes are exactly symmetric (i.e., descrambling, channel deinterleaving, etc.). However, additional blocks are required to overcome the disruptions due to the propagation channel and the possible radio frequency impairments [38]. These blocks perform what is commonly known as channel estimation and equalization, and are essential to the receiver chain to ensure better decoding of the received information.

In the literature, many channel estimation and equalization techniques for SC-FDMA were proposed as in [40]–[42] for both single and multiple antenna(s) systems. However, in NB-IoT, the pilots of NPUSCH (i.e., DMRS) are transmitted in specific symbols without undergoing a transform precoding. Therefore, similar estimation and equalization techniques can be used as those used for OFDM. In [43]–[46], an overview of channel estimation and equalization techniques in the OFDM system is provided. These techniques can be adapted to the NB-IoT system as proposed in [47].

An illustration of the estimation and equalization process for NPUSCH is given in Fig. 18. For single-tone transmissions, the process is even easier; it only requires the estimation and equalization of the phase of the channel because of the constant modulus of the constellation. Furthermore, it is possible (even recommended) to "softly" combine the different estimations of the phase of the channel through the successively received pilots (e.g., in NPUSCH format 2 where three

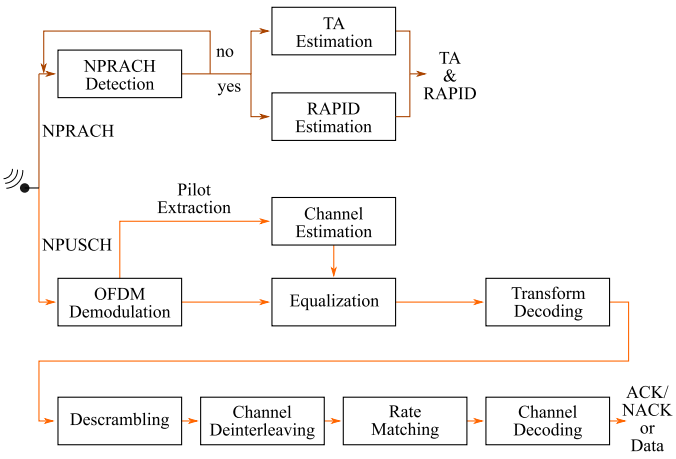

Fig. 18. Simplified representation of the receiver chain for the NB-IoT eNB (Release 13).

pilots per slot are transmitted).

B. Receiver Design at the UE

The receiver design at the UE side should include the reverse processes executed at the transmitter side of the eNB. This concerns all downlink channels (i.e., NPBCH, NPDCCH and NPDSCH); however, the downlink signals (i.e., NPSS and NSSS) require different dedicated processing blocks since they are used by the UE to achieve synchronization with the eNB. In the following paragraphs, we address separately the reception blocks used for downlink channels and signals.

1) Receiver Chain of NPSS and NSSS: The synchronization process is the first task the UE undertakes when it is switched on. It consists of a physical synchronization in both time and frequency using the NPSS. As presented in [30], there are two main techniques to perform the time-frequency synchronization. The first technique is based on cross-correlation, and the second one is based on auto-correlation. The cross-correlation technique is optimal in the maximum likelihood (ML) sense, but requires a known sequence at the receiver side and is computationally expensive. In contrast, the auto-correlation is sub-optimal, but can be performed blindly (such as in OFDM systems where the CP can be used for synchronization in time and frequency through cross-correlation [33]).

In NB-IoT, the synchronization can be performed with a cross-correlation between the received signal and the known sequence of NPSS. In practice, it is preferable to perform an auto-correlation followed by an cross-correlation, such as suggested in [30]–[32]. The first step of these synchronization methods is called "coarse synchronization", which is computationally simple and allows a complexity reduction of the second step, called "refined synchronization".

Once synchronized in time and frequency with the eNB, the UE estimates the cell ID transmitted through the NSSS. The receiver chain of NSSS should simply include a processing block that is capable of estimating the cell ID. In the literature, only a few papers address the cell ID estimation [34]–[37]. In [34], the exhaustive ML search of the 504 possible cell ID values leads to a complexity of 266 K complex multiplications. This value has been divided by four and 16 in [35], [36] by taking into account that, among others, the Hadamard sequence $b_q(m)$ in (2) is only composed of elements of value ± 1, which only involves changes of signs. In [37], the ML estimator of cell ID is rewritten using a DFT, reducing the complexity compared to the cross-correlation used in [34]–[36].

It is important to note that the success of time and frequency synchronization improves the performance of the cell ID estimation. Moreover, the success of the cell ID estimation step is verified upon decoding of the NPBCH. In addition, the UE cannot further decode any channel if NPSS and NSSS decoding was not successfully performed.

2) Receiver Chain of NPBCH, NPDCCH, and NPDSCH: The receiver chain of downlink channels at the UE side can be conceived through the symmetric processes (i.e., decoding, channel deinterleaving, etc.) of the those used at the transmitter of the eNB illustrated in Fig. 6. However, channel estimation and equalization blocks are also required and thus should be inserted between the OFDM demodulation and the demapping block (similarly to Fig. 18 for NPUSCH). In NB-IoT, the channel estimation procedure can be carried out as in LTE [48]–[51], but with a limitation to one PRB.

The pilots of downlink channels are sparse in time and frequency over the PRB as presented in Section III-A3. Thus, after the extraction of these pilots, the frequency response is estimated according to their time-frequency positions. This can be done using a least squares (LS) estimator. Then, an interpolation is required to obtain the channel estimation over the whole time-frequency grid.

Among the numerous interpolation techniques, we can mention here the 2-D and 2×1-D linear minimum mean square error (LMMSE) interpolation [46], [52], the Kalman interpolation [51], or the polynomial interpolations [50]. Note that in practice, the polynomial interpolations are usually implemented in devices due to their low computational cost, even if they generate interpolation errors [53] that slightly reduce performance.

V. MAC Layer: Scheduling of Channels and Signals

In NB-IoT, the MAC layer performs several tasks: scheduling of all channels and signals, handling the time/frequency resource allocation (at the eNB side), multiplexing/demultiplexing data blocks of higher/lower layers, mapping between logical channels and transport channels, managing UEs priority (at the eNB side), etc. In this tutorial, we focus only on the scheduling of channels and signals in order to complete the understanding of the PHY layer.

Before being able to exchange data with the network, the NB-IoT UE has to acquire a set of essential information like the MIB-NB, SIB1-NB, SIB2-NB and other SIBs-NB (if indicated). Therefore, in this section, we present first the scheduling of these essential information blocks and then address the scheduling of PHY layer channels and signals. Finally, we present the set of guard times defined by 3GPP between all PHY channels of the NB-IoT system.

A. MIB-NB Scheduling

As previously presented in Section III-A4, the NPBCH is always transmitted in subframe #0 and has a periodicity of 640 ms (i.e., 64 frames). It carries the MIB-NB and follows a fixed scheduling in which the encoding process of the MIB-NB is triggered every 64 frames. Fig. 19 illustrates the scheduling pattern of the encoded MIB-NB over one NPBCH period.

It can be seen that this process transforms the 50 bits of the MIB-NB into 1600 bits at the output of the scrambling block. These 1600 bits are then sliced into eight self-decodable blocks of 200 bits each (since only 100 REs are available in SF #0). Each block is transmitted eight times in eight consecutive frames leading to 64 frames to entirely transmit the 1600 bits [74].

It is important to recall that, the MIB-NB carries the two essential parameters: *systemFrameNumber-MSB-r13* and *hyperSFN-LSB-r13*. In this respect, triggering the encoding process of the MIB-NB after each of the 64 frames allows updating the values of these parameters, and thus ensuring the synchronization of NB-IoT UEs in terms of SFN and H-SFN.

B. Scheduling of SIB1-NB

The *SystemInformationBlockType1-NB* (SIB1-NB) is the second important information block to be decoded by the UE after the MIB-NB. It carries additional information on the NB-IoT cell in addition to scheduling information to further receive other system information blocks (i.e., other SIBs-NB). Of course, some of the SIB1-NB parameters are similar to those transmitted in the SIB1 of LTE [74]. However, the remaining parameters are different and specific to NB-IoT (e.g., *hyperSFN-MSB-r13*, *eutraControlRegionSize-r13*, *nrs-CRS-PowerOffset-r13*, etc.).

In NB-IoT, the transmission of SIB1-NB is scheduled in eight frames within 16 contiguous frames as described in Section 5.2.1.2a of [74]. In other words, the transmission of SIB1-NB is done in every one over two frames within 16 consecutive frames (i.e., SIB1-NB requires 16 frames to be fully transmitted). These physical transmissions occur only in subframe #4 of each radio frame. The SIB1-NB has a periodicity of 256 frames in which equally spaced repetitions are performed.

The scheduling pattern of SIB1-NB over one period of 256 frames is deduced from two parameters: "*schedulingInfoSIB1-r13*" (MIB-NB parameter) previously presented in Section III-A4, and cell ID parameter (acquired through NSSS). The "*schedulingInfoSIB1-r13*" parameter allows determination of the transport block size (TBS) and the repetition number of SIB1-NB (within a period of 256 frames) using the 3GPP Tables 16.4.1.5.2-1 and 16.4.1.3-3, respectively, in [68]. In contrast, the cell ID allows obtaining the starting radio frame in each SIB1-NB period as presented in Table 16.4.1.3-4 in [68] (i.e., the frame offset to apply at the beginning of SIB1-NB period).

Different repetition patterns (e.g., 4, 8 and 16) and frame offsets (e.g., 0, 1, 16, 48) are possible as indicated in [68]. Fig. 20 shows an example of scheduling for SIB1-NB over one period (i.e., 256 frames). In this example, the value of *schedulingInfoSIB1-r13* is set to 10 and the value of cell ID is set to 3. Thus, using 3GPP tables, we get eight equally spaced repetitions for SIB1-NB over one period of 256 frames and a radio frame offset of 16 frames. It is important to note that SIB1-NB encoding is triggered at the beginning of each SIB1-NB period which allows updating of the SIB1-NB parameter "*hyperSFN-MSB-r13*" (used by the UE to deduce the H-SFN). Moreover, the encoding result of SIB1-NB is always composed of eight blocks and the scrambling sequence shall be (re)initialized for each SIB1-NB repetition.

1) Mapping Process of SIB1-NB: The SIB1-NB is physically transmitted over the NPDSCH. However, its mapping process is slightly different and depends on the NB-IoT operation mode. As previously mentioned in Section III-A5, the mapping process of the NPDSCH is related to the parameter $l_{DataStart}$ that represents the index of the first OFDM symbol of the mapping zone. For SIB1-NB, this parameter is set to 3 for the in-band operation mode and to 0 for the other operation modes. Thus, for in-band mode, the first 3 OFDM symbols are always avoided when transmitting SIB1-NB since the information on the LTE control region size (*eutraControlRegionSize-r13*) is not yet acquired by the UE (it is included in SIB1-NB).

Similar to NPBCH, the SIB1-NB mapping avoids the first three OFDM symbols, but the number of available REs could be different. In the case of NPBCH mapping, we recall that all the REs dedicated to NRS and CRS signals were avoided assuming two antenna ports for NB-IoT and four antenna ports for LTE. In the case of SIB1-NB mapping, the unused REs by antenna ports are thus used to allocated SIB1-NB data (i.e., if less than two and four antenna ports are used by NB-IoT and LTE, respectively). This is justified since the UE at this stage already has the information on the number of used antenna ports (through the decoded MIB-NB).

C. Scheduling of Other SIBs-NB

As in LTE, the narrowband system information blocks (SIBs-NB) are used to diffuse information on the NB-IoT cell. They are regularly transmitted based on a predefined scheduling pattern. In NB-IoT, the information on the number of transmitted SIBs-NB and their scheduling information are carried by SIB1-NB. However, more or less system information blocks are transmitted depending on the type of functionality required within the network. In the 3GPP Release 13, the list of narrowband system information blocks that can be transmitted by an NB-IoT cell is: SIB2-NB, SIB3-NB, SIB4-NB, SIB5-NB, SIB14-NB and SIB16-NB. Some of these blocks are mandatory like SIB2-NB and the others are optional depending on the application.

The scheduling pattern of the SIBs-NB is a very important element since it impacts the used spectral resources as well as the power consumption of the UE battery (i.e., battery consumption related to SIBs-NB decoding). Therefore, the list of diffused SIBs-NB and their dedicated scheduling configuration should be chosen such that the occupied resources are optimized. In the following subsections, we provide the essential information required to understand the scheduling

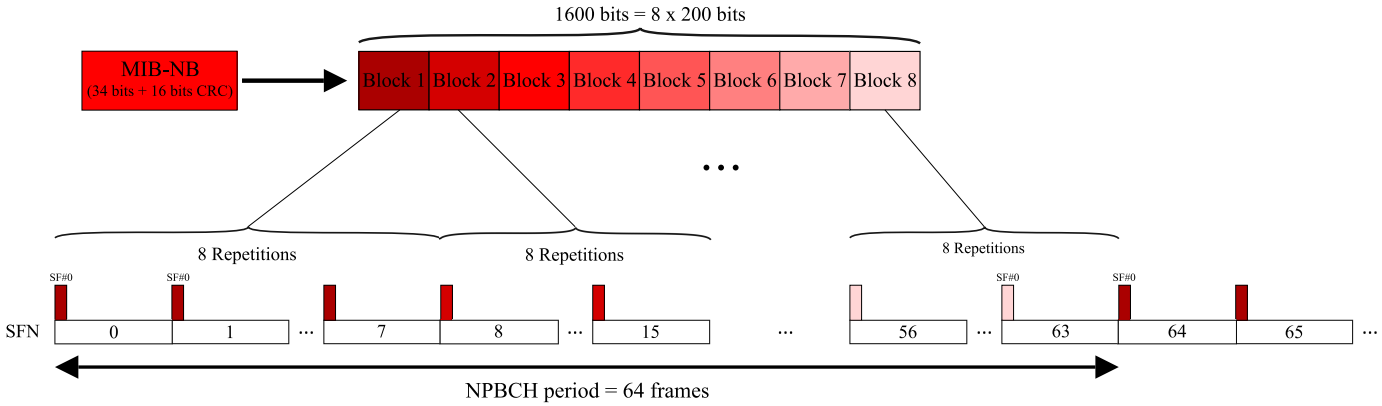

Fig. 19. Scheduling of MIB-NB over one NPBCH period of 64 frames.

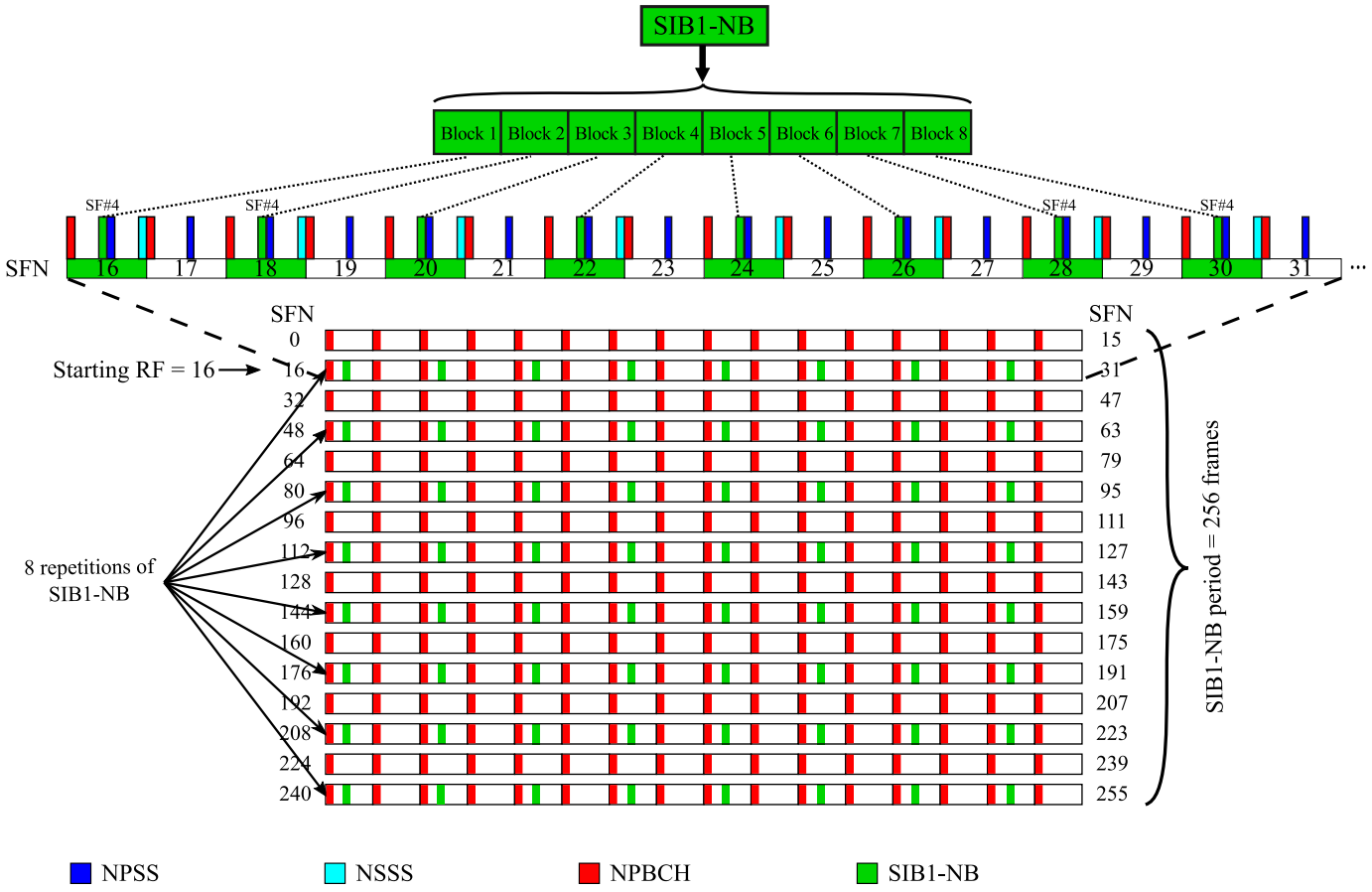

Fig. 20. Example of SIB1-NB scheduling over one SIB1-NB period of 256 frames with *schedulingInfoSIB1-r13*=10 and $N_{ID}^{Ncell} = 3$.

process for all SIBs-NB. Scheduling strategies for SIBs-NB that may help increase the capacity of the network are beyond the scope of this tutorial.

1) Scheduling Information of SIBs-NB: The scheduling information of SIBs-NB is included in SIB1-NB. This information is comprised of three parameters: *schedulingInfoList-r13*, *si-WindowLength-r13* and *si-RadioFrameOffset-r13*. These parameters hold the necessary information required by the UEs modules to decode any transmitted SIB-NB. In NB-IoT, the SIBs-NB are transmitted in what it is called a "system information message (SI-message)". Thus, depending on the requirements of the NB-IoT cell, one or several SI-messages can be transmitted. Each SI-message can hold one or several SIBs-NB in turns.

The parameter *schedulingInfoList-r13* carries the scheduling information of the list of SI-messages to be transmitted. The *schedulingInfoList-r13* is an "information element (IE)" holding a list of other IEs called "*SchedulingInfo-NB-r13*". Each of these IEs (i.e., *SchedulingInfo-NB-r13*) carries the dedicated scheduling information for one SI-message.

The IE *SchedulingInfo-NB-r13* carries the following parameters: *si-Periodicity-r13*, *si-RepetitionPattern-r13*, *si-TB-r13*,

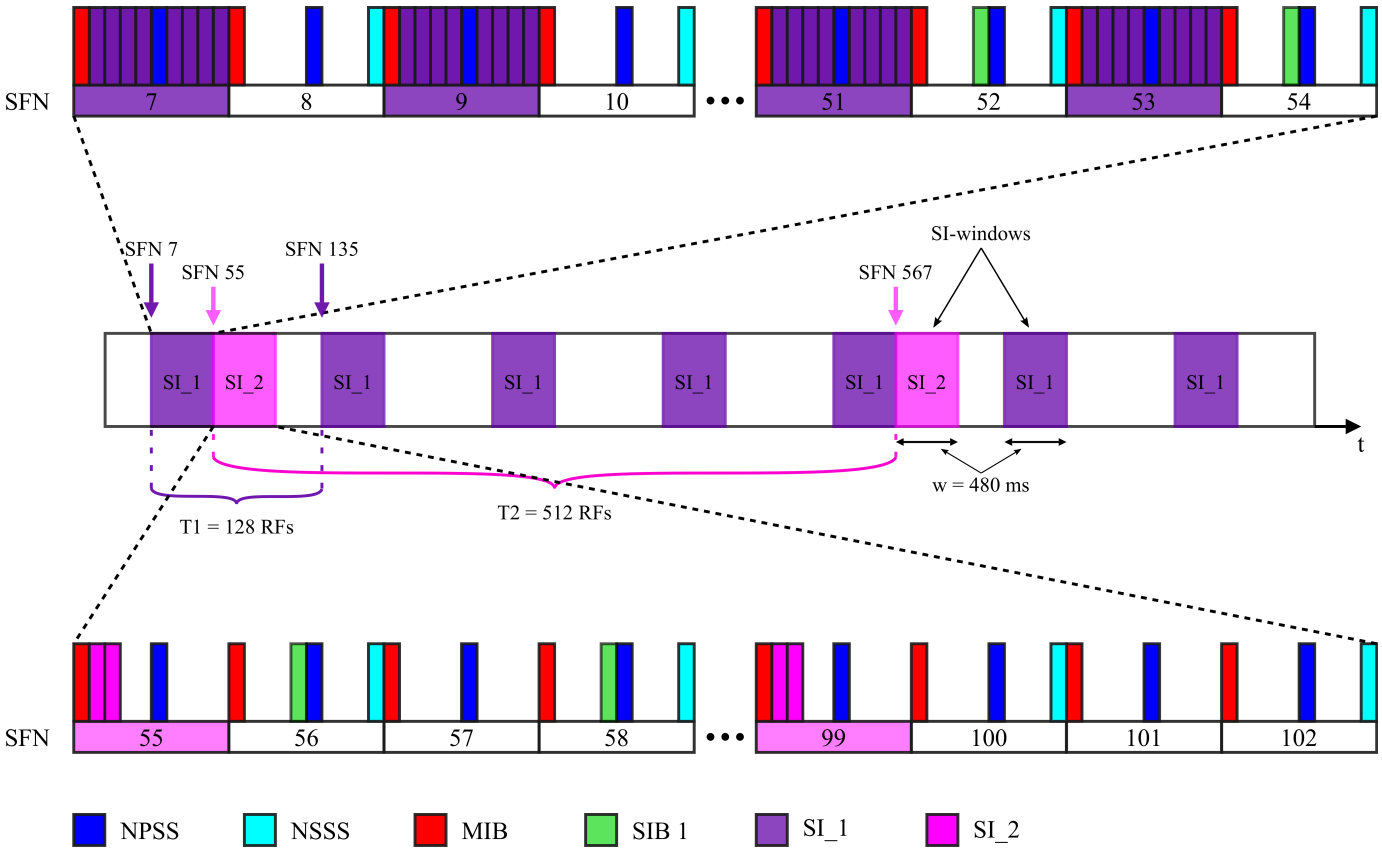

Fig. 21. Example of scheduling for two SI-messages with *si-WindowLength-r13* = 480 ms and *si-RadioFrameOffset-r13* = 7 frames and for SI_1: *si-Periodicity-r13* = 128 frames, *si-RepetitionPattern-r13* = Every2ndRF, *si-TB-r13* = 680 bits and *sib-MappingInfo-r13* = Type3-NB-r13 ; & for SI_2: *si-Periodicity-r13* = 512 frames, *si-RepetitionPattern-r13* = Every4thRF, *si-TB-r13* = 56 bits and *sib-MappingInfo-r13* = Type4-NB-r13.

sib-MappingInfo-r13. The first three parameters represent the periodicity, the repetition pattern, and the transport block size that are applied for the SI-message. The last parameter is dedicated to list the SIBs-NB that are carried by the SI-message. For example, if *sib-MappingInfo-r13* contains the two elements *sibType3-NB-r13* and *sibType4-NB-r13*, thus the SI-message holds the two SIBs-NB: SIB3-NB and SIB4-NB. It is important to note that there is no mapping information for SIB2-NB since it is always transmitted in the first SI-message listed in the IE *schedulingInfoList-r13*.

Finally, the last two parameters carried by SIB1-NB (*si-WindowLength-r13* and *si-RadioFrameOffset-r13*) are common to all SI-messages. They define the transmission window length and the radio frame offset to be applied for all SI-messages. The impact of these two parameters on the scheduling pattern is presented in an example in the following subsection.

2) Physical Transmission Pattern of SIBs-NB: The system information blocks other than SIB1-NB are transmitted in time domain windows called "SI-windows" that are periodically occurring in time. These SI-windows do not overlap in time, and each SI-window is dedicated to one SI-message. The size of SI-windows is common to all SI-messages as previously described in Subsection V-C1. The information on the size and periodicity of SI-windows is indicated in *si-WindowLength-r13* and *si-Periodicity-r13*, respectively.

Two physical transmission schemes are possible for any SI message within an SI-window. The SI-message can be transmitted over two or eight consecutive NB-IoT downlink subframes depending on the TBS value indicated for each SI-message. If the TBS value is less than or equal to 120 bits, the SI-message is transmitted over 2 SFs. If the TBS is greater than 120 bits, the SI-message is transmitted over 8 SFs.

To find the starting frame of the SI-message, the 3GPP specifications defined the following formula (see Section 5.2.3a of [74]):

$$(H - SFN \times 1024 + SFN) \bmod T = \left\lfloor \frac{x}{10} \right\rfloor + Offset, \quad (9)$$

with $x = (n-1) \times w$, where n is the index of the SI-message within the list to be transmitted (i.e, within *schedulingInfoList-r13*) and w is the window length in milliseconds of the SI-message(s) (i.e., *si-WindowLength-r13*). In this respect, the transmission of the SI-message begins in subframe #0 of the SFN that respects the formula, where T is the periodicity of the SI-message and $Offset$ is the *si-RadioFrameOffset-r13* parameter that is common to all SI-messages.

To easily understand the scheduling process of the SIBs-NB, an example of scheduling for two SI-messages is illustrated in Fig. 21. In this example, the values of the scheduling parameters common to the two SI-messages are as follows: *si-WindowLength-r13* = 480 ms and *si-RadioFrameOffset-r13*

= 7 frames. Moreover, we assume the same configuration considered in Section V-B for SIB1-NB (*schedulingInfoSIB1-r13* equals 10 and the cell ID equals 3).

The specific parameters to each SI-message are as follows: for the first SI-message (SI_1), the *si-Periodicity-r13* = 128 radio frames, *si-RepetitionPattern-r13* = Every2ndRF, *si-TB-r13* = 680 bits and *sib-MappingInfo-r13* = Type3-NB-r13 (Type2-NB-r13 is implicitly included in the first SI-message). For the second SI-message (SI_2), the *si-Periodicity-r13* = 512 radio frames, *si-RepetitionPattern-r13* = Every4thRF, *si-TB-r13* = 56 bits and *sib-MappingInfo-r13* = Type4-NB-r13.

It can be seen in Fig. 21 that, using (9), the starting radio frame of SI_1 and SI_2 is the SFN number 7 and SFN number 55, respectively. Moreover, the second transmission for SI_1 and SI_2 occurs in SFN #135 and SFN #567, respectively, which is consistent with the chosen periodicity for each SI-message. However, the number of subframes used for the transmission of SI_1 and SI_2 is different since a different TBS size is used for each SI-message. It is noteworthy that the transmission process of SI-messages always avoids the subframes that are dedicated to NPBCH, NPSS, NSSS and SIB1-NB. Therefore, if the number of available SFs in the frame dedicated to the SI-message is not sufficient, the remaining SFs are transmitted in the next available SFs of the following frames.

The SI-messages are transmitted through the NPDSCH like SIB1-NB. However, the mapping is different since at this stage, the NB-IoT UE module already has all the necessary information related to the antenna number, cell ID, and control region size of LTE. Therefore, the mapping process of SI-messages follows exactly the mapping process of the NPDSCH (explained earlier in Subsection III-A5).

Finally, to decode the SI-message, the NB-IoT UE simply acquires one SI-message transmission within an SI-window. However, if the UE is in poor coverage condition, it may need to accumulate the SI-message across multiple transmissions or even across multiple SI windows. It is important to note that in NB-IoT, the SystemInformationBlockType2-NB (SIB2-NB) holds the radio resources configuration common for all UEs. This configuration is very essential for the UEs since it sets several transmission parameters related to the PHY channels (especially for NPRACH transmissions addressed hereafter in Section V-E).

D. Scheduling of NPSS, NSSS, NRS and DMRS

The scheduling of downlink and uplink signals is very straightforward. In downlink, the NPSS is always transmitted in subframe #5 (see Section 10.2.7.1.2 in [65]). Its content never changes and thus there is no specific requirement for the scheduling of such a signal. The NSSS is transmitted in every subframe #9 of an even frame number (i.e., $n_f \mod 2 = 0$) (see Section 10.2.7.2.2 in [65]). However, as presented in Section III-A2, the content of NSSS depends on the value of cell ID and on the radio frame index (n_f). Therefore, the MAC layer of the eNB generates the content of NSSS each time before triggering the transmission at the PHY layer. Finally, the NRS signal is always transmitted over all subframes except

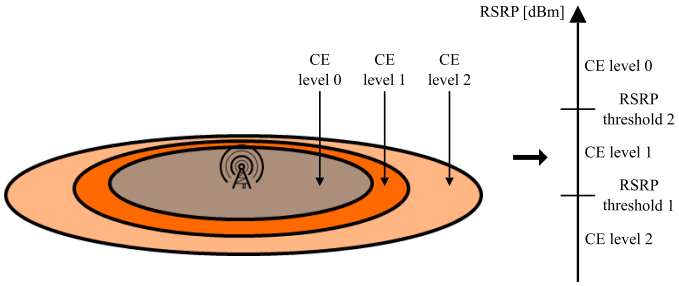

Fig. 22. Relation between the CE levels and the RSRP thresholds in a NB-IoT cell.

those used by NPSS and NSSS. The frequency/time positions of NRS REs are always the same. However, the content is generated in each slot according to a pseudo-random sequence presented in Section 10.2.6.1 of [65], and depends on the slot and OFDM symbol indexes.

In uplink, the DMRS is transmitted only in the NPUSCH subframes. The content of DMRS depends on the cell ID, slot index, and the configuration of the NPUSCH transmission, as presented in Section III-B3.

E. Scheduling of NPRACH

As in LTE, the coverage zone of the eNB is divided into several zones called ”coverage enhancement levels (CE levels)” to address the different radio conditions. These zones are defined by the eNB through power thresholds according to the requirements of the network. These thresholds are based on the values of what is called the ”reference signal receive power (RSRP)”. The value of the RSRP is computed in the NB-IoT UE devices by averaging the received power over the REs carrying the NRS within the considered NB-IoT bandwidth [70].

1) CE Level Selection and NPRACH Configuration: In NB-IoT, two RSRP thresholds can be defined per cell; thus, there are at most three CE levels. Fig. 22 shows the relation between the CE levels and the RSRP thresholds of a NB-IoT cell. Every UE in the NB-IoT cell computes its RSRP level and then, depending on the obtained value, selects the corresponding CE level according to the defined RSRP thresholds.

As previously described in Section V-C2, most of the essential information about the NB-IoT cell are transmitted in SIB2-NB. This includes the information on the RSRP thresholds and the parameters of NPRACH scheduling. In fact, there are three scheduling configurations for NPRACH in case three CE levels were considered for the cell (i.e., in case RSRP thresholds are included in SIB2-NB). This means that each UE applies a different configuration for NPRACH transmissions according to its CE level (e.g., different number of repetitions, frequency location, etc.). If the RSRP thresholds were not defined (i.e., not transmitted in SIB2-NB), there will be only one CE level for all UEs and thus one configuration for NPRACH.

2) NPRACH Scheduling Parameters: For each CE level, the following scheduling parameters of NPRACH are transmitted in SIB2-NB [74]:

- *nprach-Periodicity-r13* (N_{period}^{NPRACH})
- *nprach-StartTime-r13* (N_{start}^{NPRACH})
- *nprach-NumSubcarriers-r13* (N_{sc}^{NPRACH})
- *nprach-SubcarrierOffset-r13* ($N_{scoffset}^{NPRACH}$)
- *numRepetitionsPerPreambleAttempt-r13* (N_{rep}^{NPRACH})
- *maxNumPreambleAttemptCE-r13* ($N_{att\_max}^{NPRACH}$)
- *nprach-SubcarrierMSG3-RangeStart-r13* (N_{MSG3}^{NPRACH}),

where N_{period}^{NPRACH} is the periodicity of the preamble transmissions and N_{start}^{NPRACH} is the starting time within the NPRACH period. The N_{sc}^{NPRACH} is the number of selected subcarriers over which the UE can perform its preamble transmission and $N_{scoffset}^{NPRACH}$ is the starting subcarrier index of the N_{sc}^{NPRACH} selected. The N_{rep}^{NPRACH} is the number of preamble repetitions during one attempt (i.e., within one NPRACH period), and $N_{att\_max}^{NPRACH}$ is the maximum number of preamble transmission attempts that can be made in the corresponding CE level. The last parameter is further explained in this section.

As previously described in Section III-B1, the UE will select 12 subcarriers from N_{sc}^{NPRACH} to perform its preamble transmission ($N_{sc}^{NPRACH} \leqslant 48$). The indexes of the N_{sc}^{NPRACH} consecutive subcarriers are found using $N_{scoffset}^{NPRACH}$, which indicates the starting subcarrier index of the N_{sc}^{NPRACH} subcarriers configured for the CE level.

The UE uses the N_{period}^{NPRACH} parameter to obtain the periodicity of NPRACH occasions. The time and frequency zone occupied by one preamble attempt is called an "NPRACH occasion". This periodicity can take values like 40 ms, 80 ms, etc. As defined by 3GPP in Section 10.1.6 of [65], the starting time of preamble transmission is found by first determining the starting frame within a period using the following:

$$n_f \mod \left(\frac{N_{period}^{NPRACH}}{10}\right) = 0, \tag{10}$$

then, adding a delay of $N_{start}^{NPRACH} \times (30720 \times T_s)$, where $30720 \times T_s$ equals 1ms. This provides the frame and subframe indexes in which the transmission of the preamble begins. The transmission will last $t_{preamble} \times N_{rep}^{NPRACH}$, where $t_{preamble}$ is the preamble length (5.6 ms or 6.4 ms depending on the used preamble format).

Once the UE transmits a preamble with the corresponding repetitions, it waits for a specific time defined by what is called "random access response window (RAR window)". During this time window, the UE waits for an expected response from the eNB. However, if the UE doesn't receive a response during this time window, it continues with another preamble transmission attempt. This process continues until the $N_{att\_max}^{NPRACH}$ attempts are reached. However, the process stops once a response is received from the eNB.

In general, the NPRACH occasions of different CE levels should not overlap in frequency and time domain. In order to avoid such a scenario, the NPRACH parameters dedicated to each CE level can take different values while respecting several constraints defined by 3GPP. For example, the N_{rep}^{NPRACH} parameter should be different in each CE level and the values should be in increasing order, i.e., the N_{rep}^{NPRACH} of CE2 is bigger than the one for CE1 and CE0 ($N_{rep}^{NPRACH,CE2} \geqslant N_{rep}^{NPRACH,CE1} \geqslant N_{rep}^{NPRACH,CE0}$). In contrast, the N_{start}^{NPRACH} value can be the same for the 3 CE levels, however, the chosen subcarriers for each CE level should be different to avoid overlapping in frequency domain.

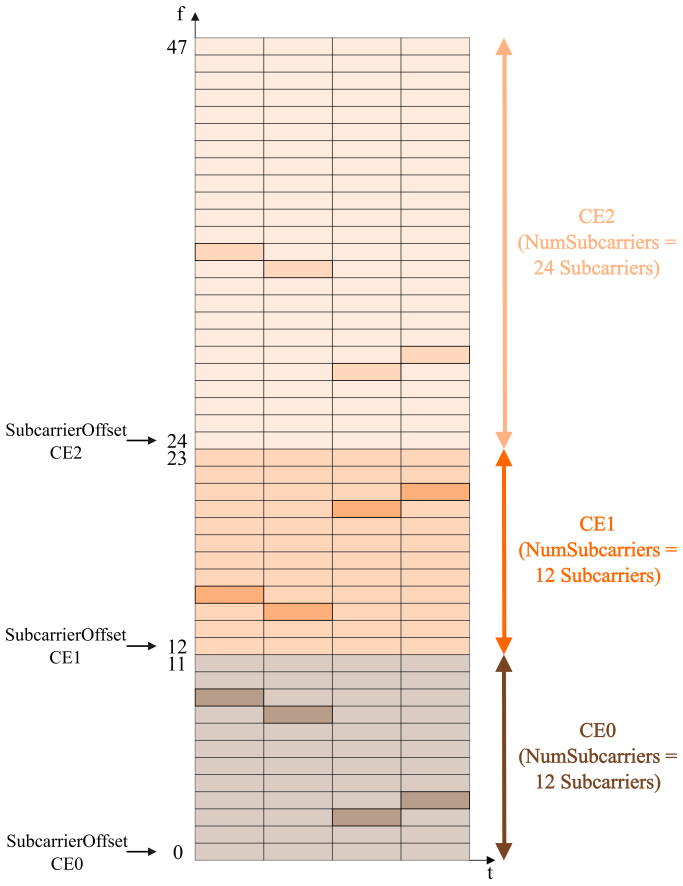

Fig. 23. Example of 3 CE levels mapping over NPRACH frequency resources with SubcarrierOffset CE0 = 0, SubcarrierOffset CE1 = 12, SubcarrierOffset CE2 = 24 & NumSubcarriers CE0 = 12, NumSubcarriers CE1 = 12, NumSubcarriers CE2 = 24.

3) Example of NPRACH Scheduling: To better understand the scheduling of NPRACH transmission occasions, we consider an example of three CE levels with different NPRACH configurations as illustrated in Table VIII. From Table VIII, we show in Fig. 23 how NPRACH frequency resources are shared between the three CE levels. We also plotted one preamble transmission in each CE level to show how the frequency mapping may occur for the different preambles. In this example, the three CE levels were separated in frequency to avoid any kind of frequency overlapping, but leveraging a time domain overlapping (as shown in Fig. 24). This example can be inverted, by having a configuration that overlaps in the frequency domain but does not overlap in the time domain.

In addition, the number of repetitions per attempt in Table VIII (i.e., N_{rep}^{NPRACH}) was set in an increasing order to improve the detection of the farthest UEs through the higher preamble energy that can be accumulated from long repetitions. Furthermore, we can see that N_{sc}^{NPRACH} parameter is set to 24 for CE2 and to 12 for the other CE levels. This configuration provides more subcarriers for the UEs that are far from the eNB and thus reduces the probability of having

TABLE VIII
EXAMPLE OF NPRACH SCHEDULING PARAMETERS FOR CE LEVELS 0, 1 AND 2.

Parameters	CE level 0	CE level 1	CE level 2
CP length	66.7 μs	66.7 μs	66.7 μs
N_{period}^{NPRACH}	80 ms	160 ms	640 ms
N_{start}^{NPRACH}	32 ms	32 ms	32 ms
$N_{att\_max}^{NPRACH}$	3	5	6
N_{rep}^{NPRACH}	2	8	64
N_{sc}^{NPRACH}	12	12	24
$N_{scoffset}^{NPRACH}$	0	12	24

preamble collisions. This can be inversely applied to the UEs in CE0 or CE1, but it depends on the requirements of the network operator. In this tutorial, we will not address the possibilities of MAC configurations for NPRACH resources because that is beyond the scope of this work.

To complete our example of Table VIII, we show in Fig. 24, the time and frequency illustration of a preamble transmission in the three CE levels. In this figure, we assume that there are three UEs each belonging to a different CE level (UE1 $\in$ CE0, UE2 $\in$ CE1 and UE3 $\in$ CE2), and suppose that they wake up at SFN #39 and trigger the attachment procedure. It can be seen that the starting frame of the NPRACH occasion in each CE level will be different since the value of N_{period}^{NPRACH} is different (due to (10)). In this example, the NPRACH occasions for the three CE levels begin in SFN #40, SFN #48 and SFN #64. However, the preamble transmission in each CE level is 32 ms after the beginning of the NPRACH occasion and the durations of the preamble attempts are not the same since different values were set to N_{rep}^{NPRACH}. Finally, we can notice the 3, 5 and 6 preamble attempts in CE0, CE1, and CE2, respectively (only one attempt was illustrated for CE2 due to the lack of space).

4) Support of Multi-Tone Transmission for Message 3: In an NB-IoT cell, some UEs can perform the two possible transmission techniques in uplink (single-tone and multi-tone) while others will support only the single-tone transmission technique. However, at the beginning of the random access procedure, the eNB does not know in advance if the UE supports the multi-tone transmission. This information is usually gained in further exchanges with the eNB. Thus, in order to allow early multi-tone transmissions for message 3 (i.e., third message exchanged during the random access channel (RACH) procedure), the 3GPP specifications defined a method to indicate such an option.

This method consists of dividing the NPRACH resources dedicated to each CE level into two sets of subcarriers. The first set will be used by the UEs that support only single-tone transmission and the second set will be used by UEs that support multi-tone transmission. These sets are computed through the previously mentioned NPRACH parameter "nprach-SubcarrierMSG3-RangeStart-r13 (N_{MSG3}^{NPRACH})".

To understand how the method works, we consider one

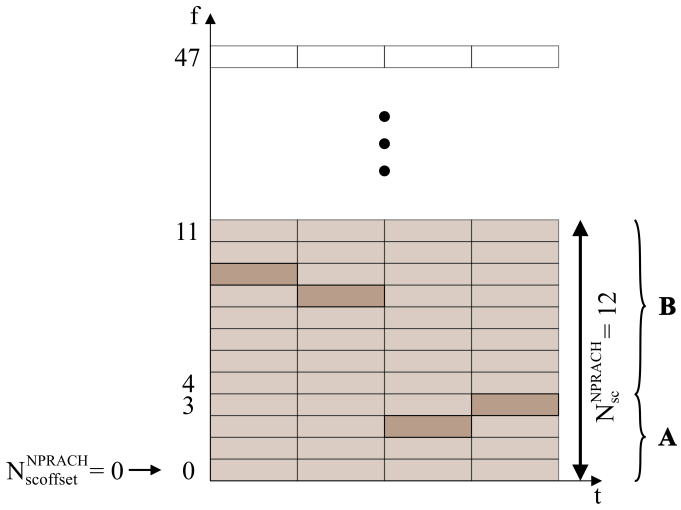

Fig. 25. Example of multi-tone frequency allocation over NPRACH resources of one CE level (N_{sc}^{NPRACH} = 12, $N_{scoffset}^{NPRACH}$ = 0, and N_{MSG3}^{NPRACH} = oneThird).

CE level in Fig. 25 and suppose that there are only 12 subcarriers that can be used to perform a preamble transmission (i.e., $N_{sc}^{NPRACH} = 12$). These subcarriers are divided into two sets, A and B. The UE that can to perform multi-tone transmission will select a starting subcarrier index from the set A; otherwise, it will select an index from the set B. In 3GPP specifications, the parameter "nprach-SubcarrierMSG3-RangeStart-r13" can have the following values $N_{MSG3}^{NPRACH} \in \{zero, oneThird, twoThird, one\}$. In this example, we suppose that $N_{MSG3}^{NPRACH} = oneThird$, thus the two sets of subcarriers A and B are defined as follows: $A = [0, 1, ..., (N_{MSG3}^{NPRACH} \times N_{sc}^{NPRACH}) - 1]$ and $B = [N_{MSG3}^{NPRACH} \times N_{sc}^{NPRACH}, ..., N_{sc}^{NPRACH} - 1]$. After replacing the parameters with their values, we get: $A = [0, 1, 2, 3]$ and $B = [4, 5, 6, 7, 8, 9, 10, 11]$.

F. Scheduling of NPUSCH

As previously presented in Section V-E2, the NPRACH transmissions have their own dedicated time/frequency zones over which the UE can perform its preamble transmission. The same principle is applied for NPUSCH, where the uplink data or control (i.e., ACK/NACK) can be transmitted only in the time/frequency zones outside those used for NPRACH transmissions.

In NB-IoT, the NPUSCH transmissions are scheduled by the downlink control channel (i.e., NPDCCH) through DCI format N0 or N1 depending on the type of NPUSCH content to be transmitted (e.g., data or control information). If the UE has uplink data to transmit, the eNB will send a DCI format N0 to schedule the NPUSCH transmission. In the other case, when the UE has control information to transmit, the eNB will send the scheduling information in the DCI format N1. This happens when the eNB sends a NPDSCH message and wants feedback about the successful/unsuccessful reception of the message by the UE.

1) Scheduling of NPUSCH Carrying Data:

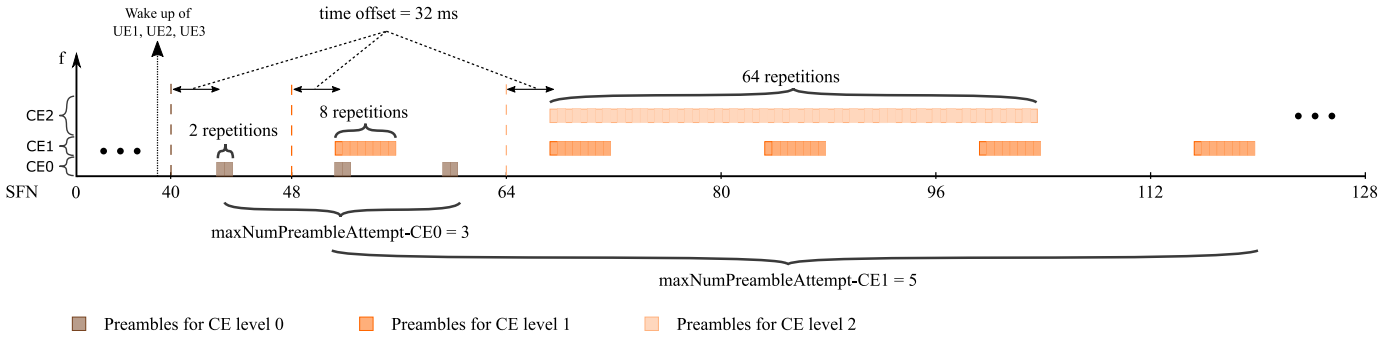

Fig. 24. Example of preamble transmissions in 3 CE levels using the parameters of Table VIII (i.e., CP length = 66.7 μs and for CE level 0: N_{period}^{NPRACH} = 80 ms, N_{start}^{NPRACH} = 32 ms, $N_{att\_max}^{NPRACH}$ = 3, N_{rep}^{NPRACH} = 2, N_{sc}^{NPRACH} = 12, $N_{scoffset}^{NPRACH}$ = 0 ; & for CE level 1: N_{period}^{NPRACH} = 160 ms, N_{start}^{NPRACH} = 32 ms, $N_{att\_max}^{NPRACH}$ = 5, N_{rep}^{NPRACH} = 8, N_{sc}^{NPRACH} = 12, $N_{scoffset}^{NPRACH}$ = 12 ; & for CE level 2: N_{period}^{NPRACH} = 640 ms, N_{start}^{NPRACH} = 32 ms, $N_{att\_max}^{NPRACH}$ = 6, N_{rep}^{NPRACH} = 64, N_{sc}^{NPRACH} = 24, $N_{scoffset}^{NPRACH}$ = 24).

a) NPUSCH Scheduling Parameters in DCI Format N0: In DCI format N0, there are six scheduling parameters that are related to NPUSCH transmission:

- *scheduling delay (I_{Delay})*
- *subcarrier indication (I_{sc})*
- *resource assignment (I_{RU})*
- *repetition number (I_{Rep})*
- *modulation and coding scheme (I_{MCS})*
- *redundancy version (rv_{DCI}).*

The sets of possible values for I_{Delay}, I_{sc}, I_{RU}, I_{Rep} and I_{MCS} are defined in Tables 16.5.1-1, 16.5.1.1-1, 16.5.1.1-2, 16.5.1.1-3, 16.5.1.2-1/16.5.1.2-2 of [68], respectively. The parameter I_{sc} allows to obtain the index(es) of the subcarrier(s) (n_{sc}) used in the uplink transmission. If 15 kHz is used as the subcarrier spacing, n_{sc} indexes are determined by Table 16.5.1-1 of [68]. If 3.75 kHz is used, then $n_{sc} = I_{sc}$. The I_{Delay} gives the delay k_0 to apply between the last subframe of the transmitted DCI N0 and the start subframe of the upcoming NPUSCH transmission.

On the other hand, I_{RU} and I_{Rep} indicate the number of resource units and the repetition number (N_{rep}) of the NPUSCH message, respectively. The I_{MCS} allows to obtain two other parameters, the first is the modulation order (Q_m) and the second one is the TBS. Finally, the rv_{DCI} is the redundancy version parameter used by the rate matching block which has only two possible values: 0 or 1.

According to all these parameters, the transmission of the NPUSCH message will start in subframe $n + 1 + k_0$ with n is the subframe in which the NPDCCH transmission carrying DCI format N0 ends. Since $k_0 \geq 8$ ms as defined in Table 16.5.1-1 of [68], the NPUSCH transmission can start at earliest in the 9^{th} subframe after the end of DCI reception. Moreover, the total number of NPUSCH slots to be transmitted is given by $N = N_{Rep} \times N_{RU} \times N_{slots}^{UL}$, with N_{slots}^{UL} is the number of slots per RU given in Table IV of Section II-C. Therefore, the duration of NPUSCH transmission (i.e., the number N of NPUSCH slots) depends on the subcarriers number n_{sc} and on the subcarrier spacing Δ_f. For instance, if the subcarriers number n_{sc} is set to 1, and there is N slots to be transmitted, the NPUSCH duration is four times longer with $\Delta_f = 3.75$ kHz in comparison to the transmission with $\Delta_f = 15$ kHz.

In Release 13, the maximum TBS for NPUSCH transmission is 1000 bits and the maximum delay k_0 that can be set is 64 ms. The maximum number of RUs (N_{RU}) and repetitions (N_{Rep}) are 10 and 128, respectively. Thus, according to the duration of the RUs given in Table IV, the maximum duration that can be achieved for a NPUSCH transmission is $10 \times 128 \times 32$ ms $= 40.96$s.

b) Repetition Process for NPUSCH Carrying Data: The repetition process for NPUSCH scheduled by DCI format N0 depends on whether the transmission technique is single-tone or multi-tone. In the case of single-tone transmission (i.e., $N_{sc} = 1$), using a subcarrier spacing of $\Delta_f = 3.75$ kHz or $\Delta_f = 15$ kHz, the repetition process is the same. Thus, if $N_{RU} \times N_{slots}^{UL}$ slots of NPUSCH data are to be transmitted and repeated N_{Rep} times, the process is carried out as follows: $N_{RU} \times N_{slots}^{UL}$ slots of data are first transmitted, then another $N_{RU} \times N_{slots}^{UL}$ slots are transmitted and so on up to the N_{Rep} repetitions. During this process, each repetition is scrambled by a different sequence, and the rate matching block is parametrized by a different redundancy version value (i.e., rv_{idx}). Note that, $rv_{idx} = 2 \mod (rv_{DCI} + j, 2)$, where j is the index of the current repetition. The value of rv_{idx} thus alternates between "0" and "2", and changes at each repetition.

In the case of multi-tone transmission (which is only possible when $N_{sc} > 1$ and $\Delta_f = 15$ kHz), the scheduling of the repetitions for $N_{RU} \times N_{slots}^{UL}$ slots of data is done as follows: the first two slots among the $N_{RU} \times N_{slots}^{UL}$ slots are transmitted and then repeated $L = \min(\lceil \frac{N_{Rep}}{2} \rceil, 4)$ times. Then, the following two slots from the remaining $N_{RU} \times N_{slots}^{UL} - 2$ slots are transmitted and repeated L times. The process continues until $L \times N_{RU} \times N_{slots}^{UL}$ slots are transmitted. Finally, this repetition pattern is repeated until it reaches N_{Rep} for all the $N_{RU} \times N_{slots}^{UL}$ slots. In addition, the scrambling process is (re)initialized every $2L$ slots, whereas the parameter rv_{idx} changes every block of $L \times N_{RU} \times N_{slots}^{UL}$ slots. Note that the parameter L in [68] is the same as $M_{identical}^{NPUSCH}$ defined in [65], so we use L for clarity.

c) Examples of Scheduling of NPUSCH Carrying Data: Fig. 26, illustrates an example of NPUSCH transmissions using single-tone and multi-tone techniques to better explain this repetition pattern. Fig. 26-(a) shows the repetition pattern

for a single-tone NPUSCH transmission. It is assumed that the useful data to be transmitted occupy one RU ($N_{RU} = 1$) and should be repeated twice ($N_{Rep} = 2$). According to Table IV, there are $N_{RU} = N_{slots}^{UL} = 16$ slots since $N_{sc} = 1$ (the 16 slots are denoted with letters from "a" to "p"). Therefore, the total number of slots to be transmitted after considering the repetitions is $N = 16 \times N_{Rep} = 32$ slots. It can be observed that, the $N_{RU} \times N_{slots}^{UL}$ (here 16 slots) are sequentially transmitted and then repeated. The (re)initialization of the scrambling sequence always coincides with the change of the rv_{idx} value.

Fig. 26-(b) shows the repetition pattern for a multi-tone NPUSCH transmission using 12 subcarriers ($N_{sc} = 12$). It is assumed that useful data to be transmitted occupy 2 RUs ($N_{RU} = 2$) and should be repeated eight times ($N_{Rep} = 8$). Moreover, according to Table IV, one RU equals two slots when $N_{sc} = 12$ (i.e., $N_{RU} = N_{slots}^{UL} = 2$). Therefore, there will be $N_{slots}^{UL} \times N_{RU} = 4$ different slots to be transmitted (denoted by "a", "b", "c", and "d" on Fig. 26-(b)). In this respect, the repetition process will be as follows: the first two slots "a" and "b" are transmitted and repeated three other times. Then, the same process is applied for slots "c" and "d". The transmission of four repetitions of "a" and "b" starts again up to the requested repetitions number ($N_{Rep} = 8$). The same process is applied for slots "c" and "d". It can be seen that the scrambling sequence is (re)initialized every $L = 4$ groups of two slots (i.e., every eight slots), whereas the parameter rv_{idx} changes every $L \times N_{RU} \times N_{slots}^{UL} = 16$ slots.

d) NPUSCH Transmission During NPRACH Occasions: By default, the NPUSCH transmissions are performed continuously and over contiguous uplink slots. However, an exception applies when there are a high number of repetitions. More specifically, an exception occurs after a transmission time of 256 ms, where a transmission gap of 40 ms is introduced before continuing the transmission. This gap is necessary to allow the UE to receive downlink channels and signals and thus avoid losing synchronization with the eNB.

However, as previously mentioned in this section, the NPUSCH transmission should avoid all NPRACH occasions. Therefore, the NPUSCH transmission is postponed every time it coincides with a NPRACH occasion. If the portion of a postponement due to a NPRACH occasion coincides with the gap of 40 ms, it is then counted as a part of the gap.

2) Scheduling of NPUSCH Carrying ACK/NACK:

a) Scheduling Parameters in the DCI Format N1: The NPUSCH carrying ACK/NACK is scheduled by the DCI format N1 through the parameter "*HARQ-ACK resource*" (here denoted by I_{AN}). The UE should start the transmission of the NPUSCH-carrying ACK/NACK indication in subframe $(n + k_0 + 1)$ after receiving a NPDSCH message that ends in subframe n. The delay k_0 is indicated by I_{AN} in Tables 16.4.2-1 and 16.4.2-2 of [68] for $\Delta_f = 3.75$ kHz and $\Delta_f = 15$ kHz, respectively. In both cases, the total number of transmitted slots is always 16. The scrambling sequence is initialized at the beginning of the transmission and reinitialized after each repetition. The repetitions are scheduled in the same way as for single-carrier NPUSCH carrying data, as illustrated in Fig. 26-(a).

It is important to note that the parameter rv_{idx} is not used for the NPUSCH-carrying ACK/NACK. It is simply a repetition code ("1" for ACK and "0" for NACK) that is used instead as previously presented in Section III-B2. The repetition number of the NPUSCH-carrying ACK/NACK is set by the SIB2-NB parameter "*ack-NACK-NumRepetitions*".

G. Scheduling of NPDSCH

In NB-IoT, since the NPDSCH scheduling is always handled by a DCI, the NPDSCH transmission (not carrying SIBs-NB) only occurs after a NPDCCH transmission. Therefore, the UE has to first decode the received DCI in order to obtain the scheduling of NPDSCH data. However, a NPDSCH message can hold two kinds of data: system information data (i.e., SIB1-NB and other SIBs-NB) or user data (e.g., random access messages and other data).

In the case where the NPDSCH is holding SIB1-NB data, there is no need for NPDCCH information in advance. The UE directly acquires the scheduling of SIB1-NB from the MIB-NB, as previously described in Section V-B. In the same way, the UE acquires from SIB1-NB the scheduling of the other SIBs-NB and thus can obtain their dedicated subframes, as previously detailed in Section V-C. In the case of data user, the scheduling of the NPDSCH requires a DCI transmission towards the UE. Thus, as described in Section 6.4.3 of [75], a DCI of type N1 is used to carry the scheduling information of NPDSCH data.

1) Scheduling Parameters of NPDSCH in DCI: The DCI of type N1 has four scheduling parameters that are related to NPDSCH transmission:

- *scheduling delay (I_{delay})*
- *resource assignment (I_{SF})*
- *modulation and coding scheme (I_{MCS})*
- *repetition number (I_{Rep}).*

The values of these parameters are chosen from Tables 16.4.1-1, 16.4.1.3-1, 16.4.1.5.1-1 and 16.4.1.3-2 of [68]. The MAC of the eNB sets the values of these parameters as a function of NPDSCH message length, propagation channel condition, and spectrum resource availability. The eNB can set a delay between the end of the transmission of the DCI and the beginning of the NPDSCH transmission (using I_{delay} to find k_0 subframes using Tables 16.4.1-1 of [68]). This delay is added after a predefined guard-time interval that is equal to four subframes (the list of guard-time intervals are addressed further in Section V-I). This means that if the NPDCCH transmission ends in subframe n, the transmission of the NPDSCH starts in subframe $n + 5 + k_0$.

The I_{SF} is used with Table 16.4.1.3-1 in [68] to obtain the number of subframes (N_{SF}) constituting the NPDSCH message. Then, using the other parameter I_{MCS} ($I_{MCS} = I_{TBS}$ as defined in [68]) and Table 16.4.1.5.1-1 of [68], the transport block size can be found. The TBS is a particularly important element that is used in the transmission/reception chain to correctly encode/decode the data message. Finally, using I_{Rep} parameter and Table 16.4.1.3-2 in [68], the UE can obtain the number of repetitions N_{Rep} of the NPDSCH transmission.

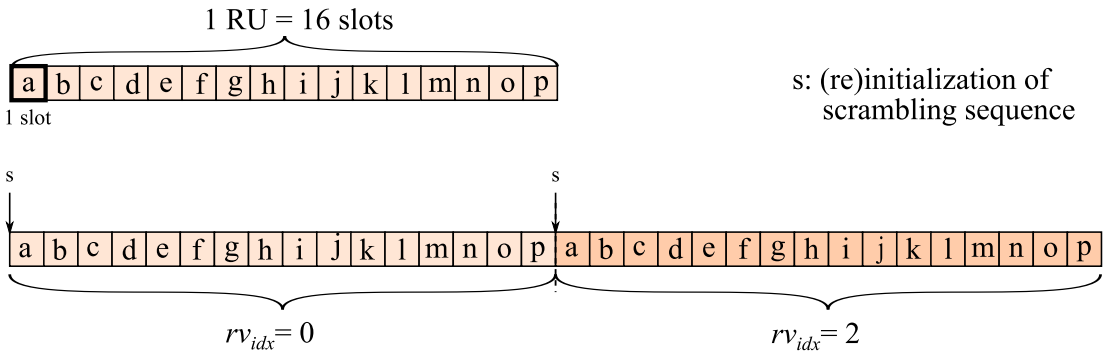

(a) Single-tone transmission with $N_{RU} = 1$, $N_{Rep} = 2$, and $rv_{DCI} = 0$.

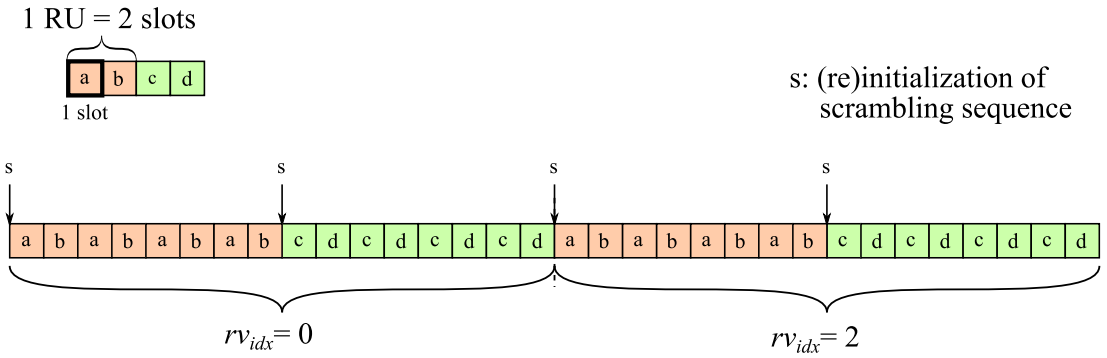

(b) Multi-tone transmission with $N_{sc} = 12$, $N_{RU} = 2$, $N_{Rep} = 8$, $rv_{DCI} = 0$.

Fig. 26. Example of uplink data transmission over NPUSCH with repetitions, considering both (a) single-tone and (b) multi-tone configurations.

In Release 13, the maximum number of subframes (N_{SF}) that can be used for one NPDSCH message is 10 SFs. The maximum size of a transport block is 680 bits and the maximum delay that can be inserted is 1024 ms. Moreover, a NPDSCH transmission can be repeated up to 2048 times. Such a high number of repetitions allows the eNB to reach the NB-IoT UEs that are in very poor coverage conditions.

2) Repetition Process of NPDSCH and Transmission Gaps:

a) Repetitions in NPDSCH: The repetition process for the NPDSCH consists in simply repeating the message N times. In other words, the generated N_{SF} subframes are repeated in $N_{SF} \times N_{Rep}$ consecutive subframes. The total transmission time is then equal to $N_{SF} \times N_{Rep}$ ms. The mapping of these subframes can only be performed in downlink subframes that do not contain NPBCH, NPSS, NSSS or SI messages. However, the physical transmission follows a repetition process that consists of repeating $\min(N_{Rep}, 4)$ times each subframe of the NPDSCH message before continuing the transmission of the next subframe.

To better understand this process, we consider an example of a NPDSCH message of six subframes that is transmitted according to two different repetition patterns. Fig. 27 shows an illustration of two repetition scenarios. In the first scenario, the NPDSCH message is repeated two times ($R = 2$). Thus, according to the repetition rule, each subframe will be repeated twice. In the second scenario, since we have eight repetitions, each subframe will be repeated four times, and then the process is repeated for the other four repetitions.

In fact, the repetition process of the NPDSCH is related to its scrambling process where the scrambling function is triggered with a different initialization parameter at the beginning of each $\min(N_{Rep}, 4)$ subframe(s) to be transmitted. Fig. 27 shows in which subframes the scrambling of the NPDSCH is triggered and (re)initialized for the two considered repetition scenarios.

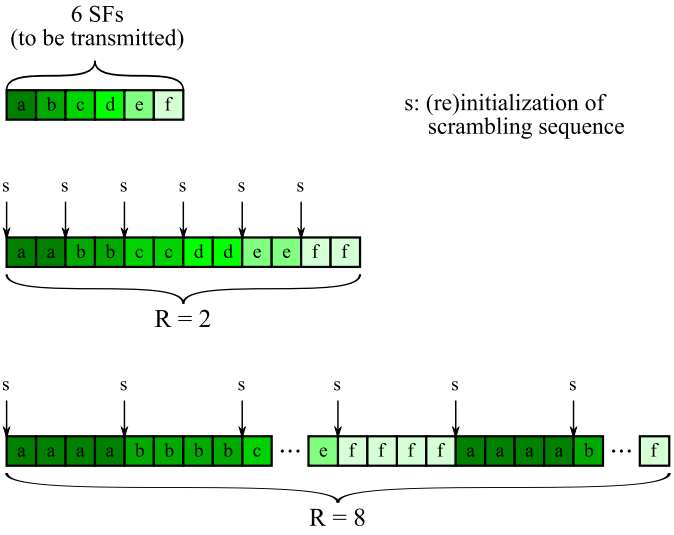

Fig. 27. Example of downlink transmission over the NPDSCH with repetitions, considering two configurations: R = 2 and R = 8.

b) Transmission Gaps: As the NPDSCH can perform up to 2048 repetitions, a NPDSCH transmission can thus occupy a high number of consecutive downlink subframes

and consequently prevents the eNB from communicating with other UEs for a long period of time. In this respect, the 3GPP defined what are called "transmission gaps". These gaps allow postponing the NPDSCH transmission for a time interval during which the eNB can communicate with other UEs. This concerns only NPDSCH data that do not carry MIB-NB, SIB1-NB, or other SIBs-NB.

The transmission gaps are computed through three parameters defined in Section 10.2.3.4 of [65]. These three parameters are: $N_{gap,period}$, $N_{gap,coeff}$, and $N_{gap,duration}$. The first parameter is the periodicity of the gaps with possible values $N_{gap,period} \in \{64$ ms, 128 ms, 256 ms, 512 ms$\}$. The second parameter is a fractional number with values $N_{gap,coeff} \in \{$oneEighth, oneFourth, threeEighth, oneHalf$\}$. The last parameter is the length of the gaps in ms and has the following expression: $N_{gap,duration} = N_{gap,period} \times N_{gap,coeff}$. The $N_{gap,period}$ and $N_{gap,coeff}$ are named "*dl-GapPeriodicity-r13*" and "*dl-GapDurationCoeff-r13*", respectively, in the higher layer (i.e., RRC layer). In Release 13, these two parameters are defined in an IE of the *RRCConnectionSetup-NB-r13* message.

Another essential parameter $N_{gap,threshold}$ is transmitted along with these two parameters. It is used to check if the gaps are authorized for NPDSCH transmissions and takes the following values $N_{gap,threshold} \in \{32, 64, 128, 256\}$. This can be determined through the constraint $R_{max} < N_{gap,threshold}$ where R_{max} is the maximum repetition number fixed by the eNB for the NPDCCH (the R_{max} parameter is further described in Table X).

In summary, the transmission gaps are only authorized during the RRC connected mode [74] of the UE, since gap parameters are transmitted in *RRCConnectionSetup-NB-r13* message. Moreover, the transmission gaps are only authorized if the constraint $R_{max} < N_{gap,threshold}$ is not respected (i.e., the repetition number of NPDSCH is higher than the $N_{gap,threshold}$).

To find the starting frame and subframe indexes of the transmission gaps, the eNB applies the following formula (found in Section 10.2.3.4 in [65]):

$$(10n_f + \left\lfloor \frac{n_s}{2} \right\rfloor) \mod N_{gap,period} = 0, \qquad (11)$$

where $n_f \in \{0, 1, .., 1024\}$ is the frame index and $n_s \in \{0, 1, ..., 19\}$ is the slot index.

In Fig. 28, we provide a simplified example of NPDSCH transmission with 128 repetitions that is assumed bigger than the fixed threshold $N_{gap,threshold} = 64$. In this example, we suppose that the UE has already received a DCI of type N1 which ends in subframe #1 of SFN #0 and that the corresponding NPDSCH transmission begins in subframe #6 of SFN #0 (considering a minimum guard time between the NPDCCH and the NPDSCH of 4 ms). We suppose also that $N_{gap,period} = 64$ and $N_{gap,coeff} = oneFourth$. It can be seen that three transmission gaps with $N_{gap,duration} = N_{gap,period} \times N_{gap,coeff} = 64 \times \frac{1}{4} = 16$ subframes are introduced. The starting subframes of these transmission gaps are computed using (11), leading to SF #4 of SFN #6, SF #8 of SFN #12 and SF #2 of SFN #19 for the first, second and third transmission gap, respectively. In this example, the transmission of the 128 NPDSCH subframes ends in subframe #4 of SFN #22.

TABLE IX
RELATION BETWEEN SEARCH SPACES, NPDCCH FORMATS AND DCI TYPES.

Search space types	NPDCCH formats	DCI types
Type1 common	format 1	N2
Type2 common	format 1	N0 & N1
UE-specific	format 0 & 1	N0 & N1

H. Scheduling of NPDCCH

In NB-IoT, the eNB considers all downlink subframes as available for the transmission of the NPDSCH and the NPDCCH, except subframes used by NPBCH, NPSS, NSSS, SIB1-NB, and other SIBs-NB. However, according to 3GPP specifications, the NPDCCH transmissions can only be made in specific time intervals, called "search spaces". These search spaces are defined by 3GPP in Section 16.6 of [68] and are described in this section.

In 3GPP Release 13, three search spaces were defined for the NB-IoT system: Type1 common search space, Type2 common search space and UE-specific search space. Depending on the type of control information to be transmitted, the eNB uses one of these search spaces. Moreover, for each search space there are dedicated NPDCCH formats and specific types of DCI that can be used. Table IX summarizes the list of formats and DCIs that can be used for each search space.

It can be seen in Table IX that the Type1 common search space is dedicated to the transmission of paging information (since only DCI type N2 is used). Moreover, only the NPDCCH format 1 is considered for this search space and thus two NCCEs are used to transmit the DCI type N2. This search space is addressed in Section V-H2 since its scheduling is different from the other search spaces.

1) Scheduling of Type2 Common and UE-specific Search Spaces: The Type2 common search space and the UE-specific search space are used for the transmission of control information related to random access messages and user data, respectively. The Type2 common search space only uses the NPDCCH format 1 (i.e., both NCCEs are used to transmit the DCIs). In contrast, the UE-specific search space can use the format 0 and the format 1. However, each search space has its own set of dedicated high layer parameters (i.e., RRC layer parameters) that allows determination of its time zones.

In order to find the starting subframes $k0$ of these time zones (for the Type2 common and UE-specific search spaces), the UE should apply this formula (found in Section 16.6 in [68]):

$$(10n_f + \left\lfloor \frac{n_s}{2} \right\rfloor) \mod T = \lfloor \alpha_{offset} \times T \rfloor, \qquad (12)$$

where n_f is the frame index, $n_s \in \{0, 1, ..., 19\}$ is the slot index and $T = R_{max} \times G$ represents the periodicity of these time zones. The high layer parameters R_{max}, α_{offset} and G are specific to the considered search space. It is important to note that the values of these parameters are related not only

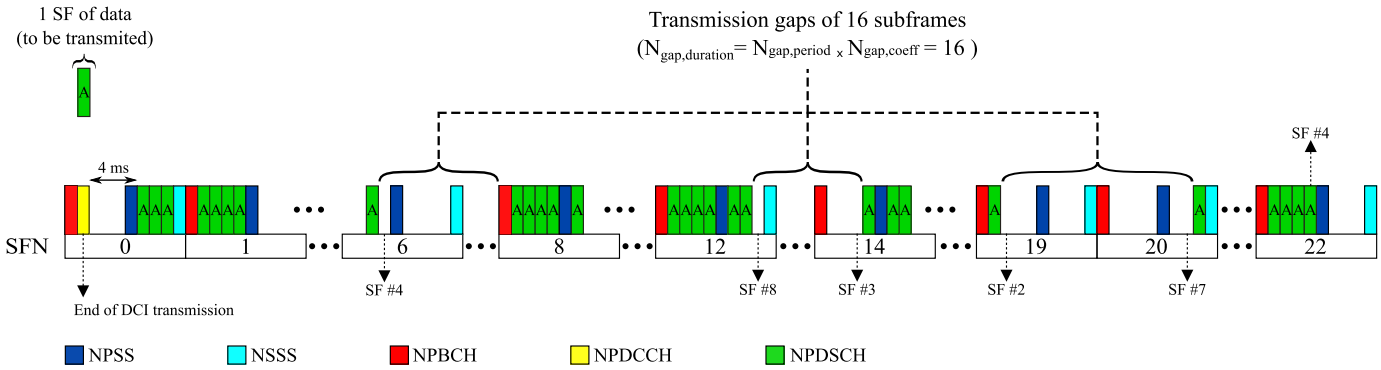

Fig. 28. Scheduling of NPDSCH not carrying SIBs-NB with transmission gaps (example with NPDSCH repetitions = 128, $N_{gap,threshold} = 64$, $N_{gap,period} = 64$ and $N_{gap,coeff} = oneFourth$).

TABLE X
HIGH LAYER PARAMETERS FOR THE TYPE2 COMMON AND UE-SPECIFIC SEARCH SPACES.

Parameter	Type2 common	UE-specific
R_{max}	npdcch-NumRepetitions-RA-r13	npdcch-NumRepetitions
α_{offset}	npdcch-Offset-RA-r13	npdcch-Offset-USS-r13
G	npdcch-StartSF-CSS-RA-r13	npdcch-StartSF-USS-r13

to the type of search space but also to the CE level of the UE. Table X presents the list of these parameters as named in the 3GPP specifications for the Type2 common and UE-specific search spaces [74].

a) Transmission process of NPDCCH: From the beginning of the search space, the NPDCCH transmission can start in subframe $k = k_b$, where b is the b^{th} subframe from k_0 that respects $b = u \times R$ with $u = 0, 1, .., \frac{R_{max}}{R} - 1$ (as defined in [68]). The parameter R represents the repetition number of the transmitted DCI. In other words, the NPDCCH transmission can be scheduled in one of the possible NPDCCH candidates having a starting subframe in $k = k_b$.

However, since the NB-IoT UE does not know in advance in which candidate the DCI will be transmitted, it should thus monitor the entire search space. To this end, the UE applies what is called blind decoding over all the candidates constituting the search space. Note that the value of R is decided by the eNB according to a resource assignment algorithm implemented in the MAC layer. The R parameter is always transmitted in the DCI and its value is set by the field "DCI subframe repetition number" [75].

From the previous formula (12), we can deduce that, once the NPDCCH candidate is selected by the eNB, the NPDCCH transmission is triggered over R consecutive subframes. The length of the search space is R_{max} subframes (without counting the unavailable subframes). According to 3GPP specifications, the NPDCCH transmission absolutely occurs in the computed time zone and avoids downlink subframes that are occupied by NPSS, NSSS, NPBCH and SIBs-NB. It is important to note that, one DCI transmission always occupies one subframe due to the small amount of control information constituting any type of DCI (at most 23 bits).

b) Example of NPDCCH Transmission: To better understand NPDCCH scheduling, we consider an example of DCI transmission in a Type2 common search space. We suppose that the eNB has random access data to send for a specific UE (in such case, a DCI of type N1 is used) and that the values of RRC parameters are: $R_{max} = 32$, $\alpha_{offset} = oneFourth$ and $G = 2$. In this example, we assume that R parameter was set to 8 by the eNB MAC layer. Fig. 29 illustrates this example and shows the location of the first search space with its possible NPDCCH candidates.

It can be observed that the periodicity of the search spaces is $T = R_{max} \times G = 32 \times 2 = 64$ ms, which means that there is one search space within every 64 consecutive subframes. In addition, four NPDCCH candidates are possible since $\frac{R_{max}}{R} = \frac{32}{8} = 4$. Thus, using (12), the starting subframe $k = k_b$ for each NPDCCH candidate can be deduced. In this example, k_0 is in subframe #6 of SFN #1, k_8 is in subframe #6 of SFN #2, k_{16} is in subframe #7 of SFN #3 and k_{24} is in subframe #7 of SFN #4. Moreover, the distance between two consecutive NPDCCH candidates (e.g., k_0 and k_8) is not exactly eight subframes since the NPDCCH transmission should avoid all subframes occupied by NPSS, NSSS, NPBCH, SIB1-NB and other SIBs-NB.

According to (12), the search space begins after an offset of $\alpha_{offset} \times T = \frac{1}{4} \times 64 = 16$ subframes from the beginning of the NPDCCH period. This offset is applied for any NPDCCH period. This can be seen in Fig. 29 where the next possible NPDCCH period begins in subframe #4 of SFN #6 (i.e., just after the end of the first period). However, the next search space occurs after adding the offset, and thus, in subframe #1 of SFN #8 (since subframe #0 is occupied by the NPBCH). The search space time zone lasts until R_{max} NPDCCH subframes are counted. The transmission of any DCI occurs in one of the NPDCCH candidates (e.g., it starts at k_8 and will be repeated R-1 times $(8 - 1 = 7)$), and thus ends at subframe #6 of SFN #3.

c) Repetition Process of the NPDCCH and Transmission Gaps: The repetition process of the NPDCCH is straightforward compared with the other channels. The encoded DCI is repeated $R - 1$ times over a set of consecutive subframes. However, the transmission of these NPDCCH subframes follows a scrambling process in which the scrambling function is

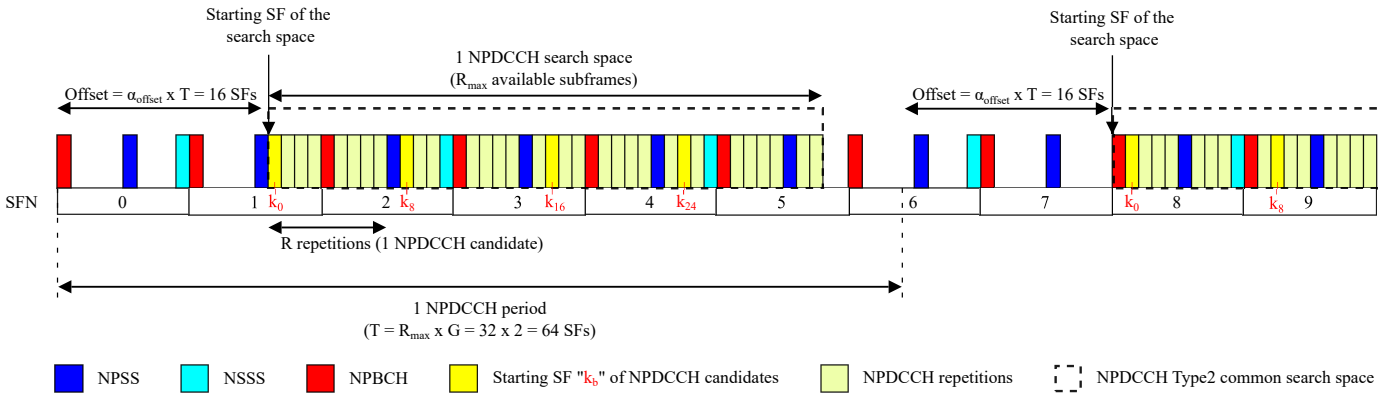

Fig. 29. Example of Type2 common search space scheduling, with $R_{max} = 32$, $\alpha_{offset} = oneFourth$, $G = 2$ and $R = 8$.

triggered and initialized every four transmitted subframes. This occurs only when R is bigger than four. Moreover, similarly to the NPDSCH, a set of transmission gaps can be configured for long NPDCCH transmissions. These transmission gaps for the NPDCCH are computed exactly as for the NPDSCH and are authorized only when the number of repetitions is bigger than the configured threshold $N_{gap,threshold}$.

2) Scheduling of Type1 Common Search Space & Discontinuous Reception: The NB-IoT UE modules have two possible "Radio Resource Control (RRC)" states [74]: RRC connected and RRC idle. The UE enters the RRC connected state when it has to perform data exchange with the network. In this state, the UE consumes higher power. In the RRC idle state, the UE has no more data to exchange with the network, and thus switches off most of its electronic components in order to reduce power consumption and save the energy of its battery.

In both RRC states, the UE can apply what is called "discontinuous reception (DRX)" mode. During this mode, the UE switches its receiver off to save energy and only wakes up to monitor some NPDCCH transmission occasions. The goal of this mode is to always make any NB-IoT UE modules within a cell reachable by the network and at the same time save the energy of their batteries.

To better explain the DRX concept, we show in Fig. 30 how the two DRX modes operate during the two RRC states at the UE side. The first mode is called "connected DRX (C-DRX)" and the second is called "Idle DRX (I-DRX)". In both modes, the UE wakes up for a short time to monitor a set of specific NPDCCH occasions and then sleeps the rest of the time.

In the following, we present these two modes with their relation to the NPDCCH search spaces. We then complete the presentation by briefly addressing other power saving features of NB-IoT that are related to the Type1 common search space.

a) C-DRX and I-DRX Concepts: In order to reach the UE during DRX mode, the eNB uses a dedicated search space according to the RRC state of the UE. For the C-DRX mode, the UE is reachable using the UE-specific search space. For the I-DRX mode, however, the UE is reachable using the Type1 common search space. To get the on/off phases in each DRX mode (i.e., C-DRX or I-DRX), the UE relies on several high layer parameters (described further in this section).

The C-DRX mode allows performing discontinuous reception when the UE has no more data to exchange with the network. This allows the UE to reduce its power consumption during connected mode and, if required, quickly resume communication with the eNB. As shown in Fig. 30, the UE enters the C-DRX mode when the "drx-InactivityTimer" expires (this occurs when no more data is exchanged). After that, the UE enters the I-DRX mode in two cases: when the C-DRX phase expires or when the UE receives an "*RRCConnectionRelease*" message from the network.

In this tutorial, the C-DRX is beyond the scope of this work; thus, we will focus only on the I-DRX mode since it is closely related to the NPDCCH Type1 common search space. In addition, C-DRX is optional for NB-IoT. Note that more information about the computation of the on/off phases for C-DRX mode can be found in Section 5.7 of [71].

b) Scheduling of Paging in Type1 Common Search Space: For the I-DRX mode, the 3GPP defined the NPDCCH Type1 common search space over which any UE can be reachable during its energy saving phase. As previously explained in Section V-H1, this search space is mainly used by the eNB to send direct indication signaling or scheduling information for paging messages. This allows the eNB to inform the UEs about any change in the configuration of the network (e.g., change in SIB1-NB or in SIBs-NB) or a paging message that is going to be sent from the eNB.

Fig. 30 shows the UE operating in the I-DRX mode. It can be observed that the Idle phase is composed of several I-DRX cycles which are divided into two parts: active and sleep periods. The active period is composed from a NPDCCH occasion in the form of a dedicated subframe called "paging occasion (PO)", and the sleep period covers the rest of the time of the I-DRX cycle. To find these POs of the Type1 common search space and the duration of I-DRX cycle, the UE needs the following parameters transmitted in SIB2-NB:

- *defaultPagingCycle-r13* (T)
- *nB-r13* (nB)
- *npdcch-NumRepetitionPaging-r13* (R),

where T represents the DRX cycle length in frames and nB is a parameter that allows derivation of the "paging frame (PF)" and the PO (a PF is one radio frame which may contain one or multiple PO(s)). The R parameter represents

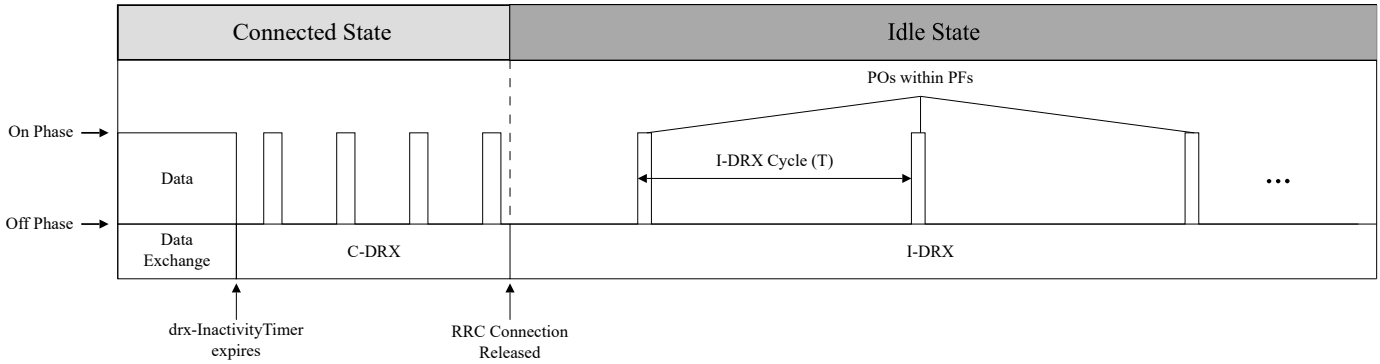

Fig. 30. Illustration of C-DRX and I-DRX modes at UE side.

the number of repetitions to apply for each PO. Note that nB is defined in function of T and can take values such as $\{4T, 2T, T, T/2, T/4, T/8, etc.\}$.

In order to find the PFs and POs at the eNB side (i.e., find all possible POs to join any UE from the eNB point of view) and the UE side (i.e., find the specific POs dedicated to the UE), additional parameters are required that are computed from T and nB. These parameters are listed in Table XI and defined in [72]. The first two parameters are N and N_s, where N is the number of PFs within an I-DRX cycle and N_s is the number of POs within a PF. The last parameter i_s is used with the table of Section 7.2 in [72] to get the PO subframe index that we call here "PO^{sf}_{index}". It is defined as a function of the international mobile subscriber identity (IMSI) of the UE: $i_s = \frac{UE\_ID}{N} \mod Ns$, with $UE\_ID = \text{IMSI} \mod 4096$.

According to all these parameters, the UE follows the following steps to find its PO within an I-DRX cycle:

- Find the PF using the formula defined in [78]: $SFN \mod T = (\frac{T}{N}) \times (UE\_ID \mod N)$.
- Compute i_s parameter.
- Find its PO^{sf}_{index} using i_s and the look-up table of Section 7.2 in [78].

The table in Section 7.2 of [72] (for FDD mode) provides the PO subframe index with possible values $\{0, 1, 2, 4, 5, 9\}$, as a function of the entries i_s and Ns. If the PO^{sf}_{index} corresponds to a downlink subframe that is already used by NPBCH, NPSS, NSSS, SIB1-NB or SIBs-NB, then the UE shall start monitoring the next available downlink subframe.

Fig. 31 illustrates an example of Type1 common search space scheduling. In this example, we show which PF and PO the UE shall monitor considering the following parameters: $T = 256$ (i.e., 2.56 s), $nB = T/4 = 64$, $R = 2$ (i.e., 2 repetitions) and $UE\_ID = 466$. In this configuration, we obtain the following values: $N = 64$, $Ns = 1$ and $i_s = 0$. This means that from the eNB side there is one PF every four frames and one PO in every PF, as illustrated in Fig. 31-(a). Moreover, using the table of Section 7.2 in [72], we get the paging index $PO^{sf}_{index} = 9$. However, since the 10^{th} subframe (i.e., subframe #9) of every even frame is dedicated to NSSS, the eNB postpones all transmissions of the POs to the next available downlink subframe, which here corresponds to subframes #1 and #2 (subframe #2 is used for the repetition).

At the UE side, all the possible PFs are found by using

TABLE XI
COMMON AND SPECIFIC PARAMETERS FOR SCHEDULING AND MONITORING POS.

Parameter	Value	Role
N	$\min(T, nB)$	Number of PFs within DRX cycle
Ns	$\max(1, nB/T)$	Number of POs within PFs
i_s	$\lfloor UE_{ID}/N \rfloor \mod Ns$	Index of PO table

$SFN \mod T = (\frac{T}{N}) \times (UE\_ID \mod N)$. Thus, using the configuration shown in Fig. 31, we obtain $PF = 72 + n \times 256$, with $n \in \mathbb{N}$. In other words, the first paging frame occurs in frame number 72 and the second one is in frame number 328 (which belongs to the next I-DRX cycle). In this respect, the UE monitors all these PFs and, more specifically, the subframes #9 (since $PO^{sf}_{index} = 9$) and the repetitions over subframes #0. However, since subframe #9 and #0 are already used by NSSS and NPBCH, the UE monitors subframes #1 and #2, as illustrated in Fig. 31-(b).

c) Extended DRX (eDRX): In order to further reduce the power consumption of NB-IoT UEs compared to DRX mode, the 3GPP defined the eDRX mode in Section 7.3 of [78]. This mode allows the UEs to extend their sleep phase up to 2.91 hours in one eDRX cycle (compared to 10.24 s in I-DRX). In NB-IoT, the eDRX mode is only supported in the RRC Idle state and thus is not supported for RRC connected state.

In this mode, the concept of H-SFN is used in which the UE determines a "paging hyperframe (PH)" over which it monitors the possible POs defined for a set of PFs. These PFs and POs are located inside what is called "paging time windows (PTWs)". Fig. 32 illustrates the principle of the eDRX cycle over which a PTW window is defined. Each PTW is bounded by PTW_{start} and PTW_{end}, where PTW_{start} and PTW_{end} correspond to frames in which the PTW zone starts and ends, respectively. Note that each PTW is UE-specific where the PH, PTW_{start}, and PTW_{end} are determined through formulas involving the identity of the UE.

To find the PH and the PTW boundaries for a dedicated UE in the eDRX mode, the following parameters are required (See Section 7.3 in [72]):

- eDRX cycle (T_{eDRX}).

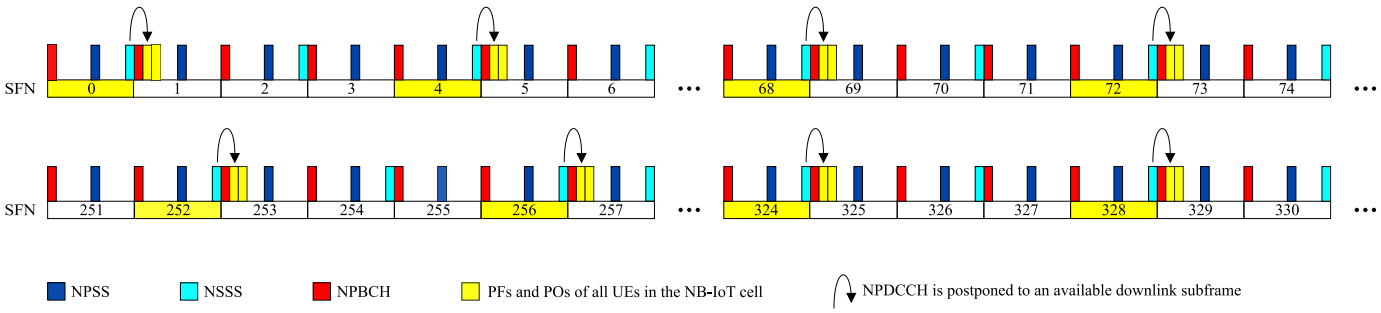

(a) Type1 common search space seen by the eNB.

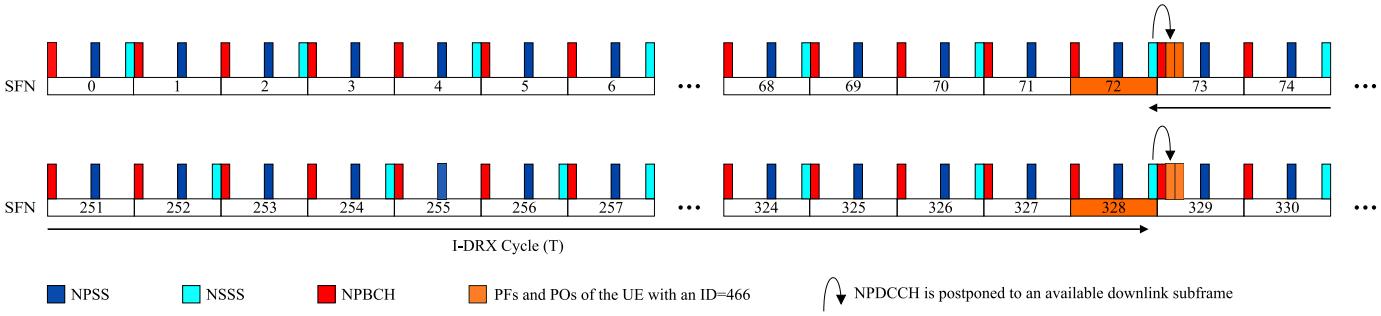

(b) Type1 common search space seen by the UE.

Fig. 31. Example of Type1 common search space scheduling considering $T = 256$ (2.56 s), $nB = T/4 = 64$, $R = 2$, and $UE_{ID} = 466$.

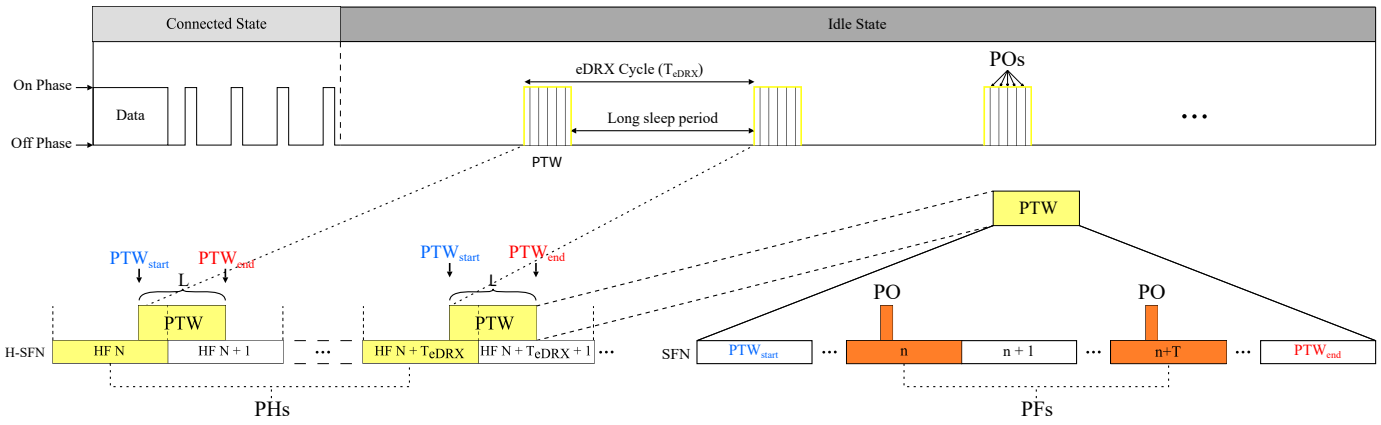

Fig. 32. Illustration of the eDRX principle at the UE side.

- PH that respects: $H\text{-}SFN \mod T_{eDRX} = UE\_ID\_H \mod T_{eDRX}$, where UE_ID_H is computed using the UE "serving temporary mobile subscriber identity (S-TMSI)" [93].
- Starting frame of PTW: $PTW_{start} = 256 \times i_{eDRX}$ with $i_{eDRX} = \left\lfloor \frac{UE\_ID\_H}{T_{eDRX}} \right\rfloor \mod 4$.
- Last frame of PTW: $PTW_{end} = (PTW_{start} + L \times 100 - 1) \mod 1024$, where L represents the PTW length (in seconds).

It can be seen in Fig. 32 that the eDRX principle is similar to the DRX mode except for a difference in terms of sleep period. In fact, over one PTW, the UE can be reached over several PFs and POs. To find these PFs and POs, the UE follows exactly the same procedure as that used for I-DRX, described previously in Section V-H2b.

d) Power Saving Mode (PSM): In Release 13, the "power saving mode (PSM)" was defined for NB-IoT [54]. The goal for PSM is to further increase the life time of UE batteries and achieve the defined target of 10 years of autonomy. This mode allows NB-IoT devices to increase their sleep phase from several hours (as in eDRX) up to more than one year (up to 413 days). In PSM, the UE turns off its radio components completely while it is still registered in the network. This means that the UE cannot monitor any NPDCCH occasions (i.e., there is no transmission or reception for any kind of channel or signal). The duration of the PSM mode is defined by two timers: the tracking area update (TAU) timer, denoted by T3412, and the activity timer (T3324) [73].

As illustrated in Fig. 33, when the UE enters the RRC idle state, it triggers the activity timer T3324 (3 hours) and the TAU timer T3412 (413 days). Once the T3324 expires, the UE switches directly into the PSM mode and does not wake

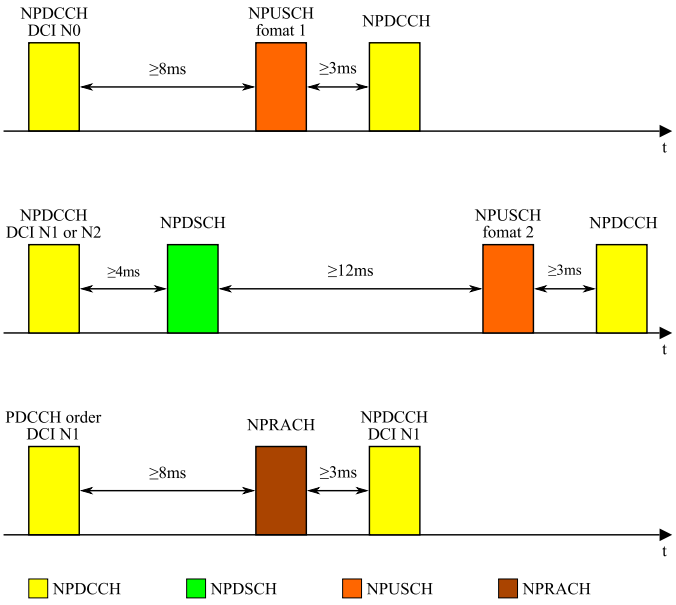

Fig. 34. Illustration of NB-IoT guard times between downlink and uplink transmissions.

up until the expiration of TAU timer T3412. The details of these procedures are beyond the scope of this tutorial.

I. Guard Times Between Uplink and Downlink Transmissions

Due to the low processing capabilities and low-cost components of NB-IoT devices, the 3GPP introduced a set of guard times between the different uplink and downlink transmissions. These guard times ensure sufficient time for the UEs to process any sent/received message. In 3GPP specifications, these guard times are defined in Section 16.6 of [68] and in Section 5.1.4 of [84]. They are summarized here and are illustrated in Fig. 34 in the same order as listed below:

- After the reception of a NPDCCH-carrying DCI N0, the UE shall not transmit a NPUSCH format 1 message before at least 8 ms. Moreover, the UE should not expect any new NPDCCH message before at least 3 ms.
- After the transmission of a NPDCCH-carrying DCI N1 or N2, the eNB should not transmit any NPDSCH message before at least 4 ms (i.e., the UE is not able to receive before at least 4 ms).
- After the reception of a NPDSCH message, the UE shall not transmit a NPUSCH format 2 message-carrying ACK/NACK before at least 12 ms. Moreover, the UE should not expect any NPDCCH message before at least 3 ms after the transmission of the ACK/NACK.
- After the reception of a NPDCCH-carrying DCI N1 for ”PDCCH order” (i.e., ordering the transmission of NPRACH), the UE shall not transmit a NPRACH preamble before at least 8 ms. Moreover, it should not expect a response to its preamble over the NPDCCH before at least 3 ms.

VI. NB-IoT Features in Release 14 & Release 15

In order to improve the performance and capacity of the NB-IoT system, the 3GPP defined and introduced new features in 3GPP Release 14 and Release 15. In the following sections, we present these features to cover all the functionalities of the NB-IoT system. However, to not extend beyond the scope of our tutorial, we detail only the features that are related to the physical layer aspects. Fig. 35 illustrates these newly introduced features in Release 14 and Release 15.

A. Release 14 Features

In Release 14, the following features were added to the NB-IoT system:

- Multi-carrier configuration
- Paging and random access over non-anchor carriers
- Narrowband positioning reference signal (NPRS)
- New TBS size and two-HARQ processes
- Contention free random access procedure
- New NPDCCH search spaces for multicast transmission/group messaging
- Downlink channel quality reporting
- Release assistance indication (RAI)
- Relaxed monitoring for cell reselection, connected mode mobility and new power class
- New scrambling for NPDSCH and NPDCCH
- Unacknowledged mode (UM) for radio link control (RLC)

1) Multi-Carrier Configuration: In Release 13, the 3GPP introduced the ”multi-carrier” feature that allows the NB-IoT eNB to configure one additional non-anchor carrier for downlink and uplink transmissions. These new PRBs allow for an increase in the capacity of the NB-IoT cell. In Release 14, the 3GPP improved this feature by providing extra PRBs. The eNB can configure up to 15 downlink and 15 uplink non-anchor carriers (see Section 6.7.4 and SIB22-NB in [85]). This further improves the capacity of the cell in terms of device density up to approximately 1,000,000 IoT devices per square kilometer [76].

2) Paging and Random Access over Non-Anchor Carriers: As previously described (in Section VI-A1), the eNB can configure non-anchor carriers in order to increase cell capacity. In Release 13, the non-anchor carriers were only used for data transfer (i.e., for NPDCCH, NPDSCH and NPUSCH transmissions) and configured within an RRC procedure during connected mode (e.g., *RRCConnectionReconfiguration*). In Release 14, the non-anchor carriers can be additionally used for paging (see Section 7.1 in [78]) and for random access procedures (i.e., Message 1 to Message 4) (see Section 5.1.1 in [84]).

3) Narrowband Positioning Reference Signal (NPRS): The NPRS is introduced for NB-IoT in Release 14 in Section 10.2.6A of [79]. The goal of NPRS is to provide the positioning service without the need for high-cost GPS-based solutions. The usage of this signal in NB-IoT provides better results for indoor applications where GPS coverage is limited.

This new downlink signal is dedicated to helping NB-IoT UEs compute their positions and send them back to the network. The concept behind the positioning operation is that each UE computes its position using at least three NPRSs from the surrounding eNBs. This computation is based on

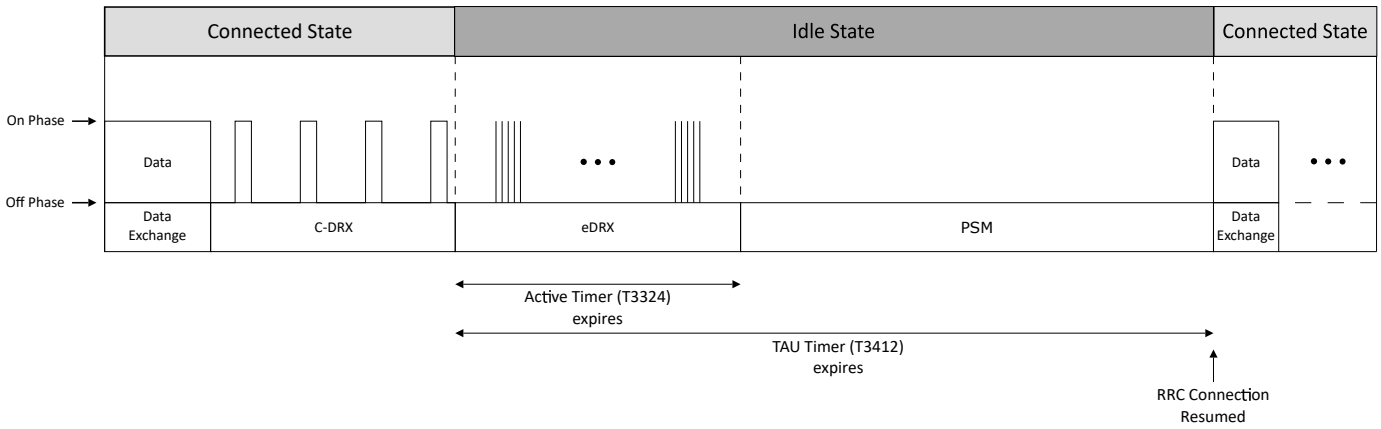

Fig. 33. Illustration of PSM principle at the UE side.

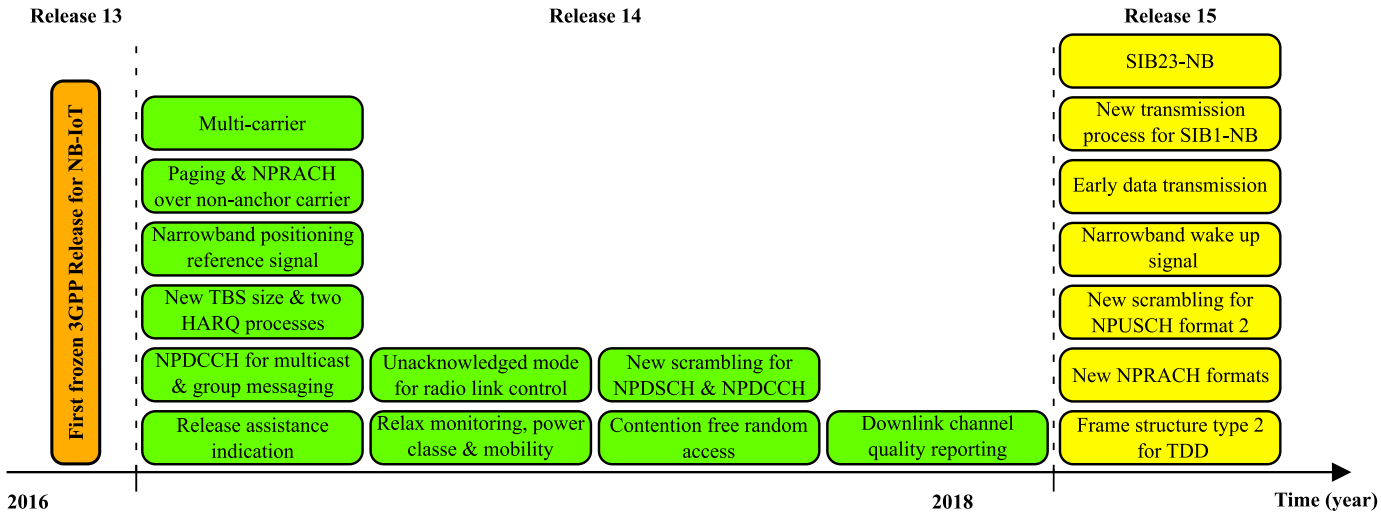

Fig. 35. Illustration in time domain of the new NB-IoT features per order of appearance in Release 14 and Release 15 of 3GPP specifications.

the "observed time difference of arrival (OTDOA)" technique developed for LTE in 3GPP Release 9 [58], [59] that includes the basic operation of computing the "time of arrival (ToA)" of the NPRSs. The UE reports these time differences to the network in order to derive its location.

The NPRS elements are "QPSK-like" complex samples that are generated using the same sequence that was defined for the LTE positioning reference signal. The mapping process of the NPRS REs depends on the operation mode (i.e., in-band, guard-band or stand-alone) [60] and on the N_{ID}^{NPRS} value [79]:

- For in-band mode, two mapping patterns are possible, depending on the number of antenna ports used for PBCH LTE. Fig. 36(a) shows the mapping of NPRS REs when using one or two antenna ports for PBCH LTE with a $N_{ID}^{NPRS} = 0$. In the case of four antenna ports, the NPRS REs mapped over the 8^{th} OFDM symbols in Fig. 36(a) are not used. If N_{ID}^{NPRS} is not configured by higher layers, $N_{ID}^{NPRS} = N_{ID}^{Ncell}$. Otherwise, $N_{ID}^{NPRS} \in \{0, 1, ..., 4095\}$.
- For guard-band and stand-alone modes, a new specific NPRS mapping pattern has been defined in Release 14 [79], such as shown in Fig. 36(b). The mapping is defined for only one antenna port.

The subframes holding NPRS can be configured in two ways: Type 1 or Type 2. The first configuration uses a bitmap defined in higher layers called "*nprsBitmap-r14*" [80]. The length of the bitmap defines the periodicity of the NPRS transmission which can have two possible values: 10 ms and 40 ms. The second configuration is defined through an NPRS periodicity (T_{NPRS}) over which N_{NPRS} consecutive NPRS subframes are transmitted. The NPRS period has an offset of $\alpha_{NPRS}.T_{NPRS}$ with $\alpha_{NPRS} \in \{0, 1/8, 2/8, 3/8, ...\}$ and $T_{NPRS} \in \{160ms, 320ms, 640ms, ...\}$. Therefore, in this configuration, the NPRS transmission starts in the frame and subframe satisfying $(10n_f + n_{sf} - \alpha_{NPRS}T_{NPRS}) \bmod T_{NPRS} = 0$ [79] and lasts N_{NPRS} consecutive subframes. A list of these parameters can be found in Section 6.5.1.2 of [80].

The eNB can be configured to use only Type 1 or Type 2 configurations, or both. If the two configurations are used at the same time, a subframe will carry an NPRS if it was indicated by the two configurations. It is important to note that, if *nprsBitmap-r14* is not configured, the REs in the OFDM

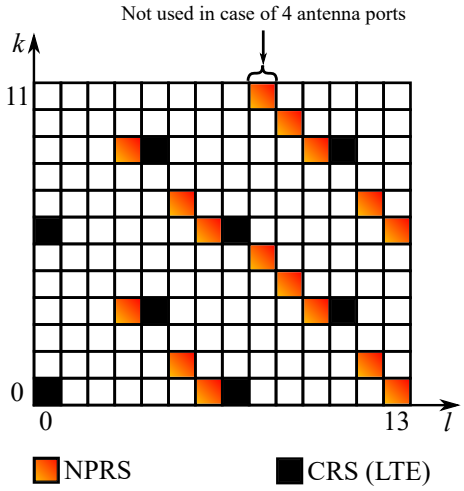

(a) NPRS mapping for in-band mode (one or two antenna ports).

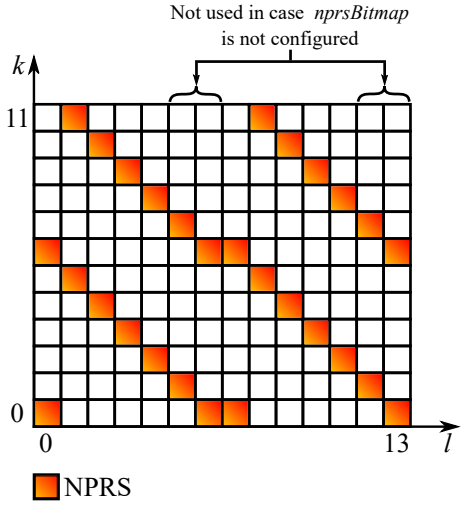

(b) NPRS mapping for guard-band and stand-alone modes (one antenna port).

Fig. 36. NPRS mapping pattern for in-band, guard-band and stand-alone operation modes.

symbols 5, 6, 12 and 13 shall not be used for the transmission of NPRS, as shown in Fig. 36(b) (*nprsBitmap-r14* should always be defined for in-band operation mode). Moreover, the NPRS mapping process should avoid all the subframes that are dedicated to NPSS, NSSS, NPBCH and SIB1-NB.

a) NPRS Muting: As for LTE, muting is also possible for NB-IoT. It consists of improving the detection of the NPRS when two cells are sharing the same frequency shift (i.e., $N_{ID1}^{NPRS} \mod 6 = N_{ID2}^{NPRS} \mod 6$) and one of them has stronger signal power. This muting option can be activated for both NPRS configurations (Type 1 and Type 2). If it is used with Type 1, each bit is used to indicate if a set of 10 consecutive NPRS subframes is muted or not. If it is used with Type 2, each bit indicates if NPRS is muted or not over a positioning period. Finally, if Type 1 and Type 2 are used at the same time, if NPRS is muted for one configuration it applies to the other one as well [60]. The muting option is configured through the element "*nprs-MutingInfoB-r14*" [80].

4) New TBS Size and Two-HARQ Processes: To reduce the transmission time and power consumption required for large data content transfer, the 3GPP defined in Release 14 new TBSs for downlink and uplink shared channels (i.e., NPDSCH and NPUSCH). These TBSs allow for a higher number of bits to be sent per transmission. For the NPDSCH, the maximum TBS size is increased from 680 to 2536 bits, and for the NPUSCH it is increased from 1000 to 2536 bits (see Table 16.4.1.5.1-1 and Table 16.5.1.2-2 in [83]). In addition, two-HARQ processes for downlink and uplink were introduced to further increase the peak rates (compared to one HARQ process in Release 13) (see Sections 16.4 and 16.5 of [83]).

5) Contention Free Random Access Procedure: In Release 14, the NPRACH resources can be configured to perform a contention free random access procedure. This feature consists of providing a dedicated set of subcarriers from the N_{sc}^{NPRACH} defined for each CE level, to be used when a non-contention based random access procedure is triggered (see Section 5.1.2 of [84]). In such a procedure, the eNB indicates to the UE the first subcarrier index to be used for its preamble transmission. The eNB can activate this feature through the parameter "*ra-CFRA-Config*" of the IE "*MAC-MainConfig-NB-r13*" of the "*RRCConnectionSetup-NB*" message [85].

6) New NPDCCH Search Spaces for Multicast Transmission/Group Messaging: In Release 14, the Multicast transmission/group messaging feature was introduced for NB-IoT. This feature allows the network to simultaneously address a group of NB-IoT UEs to perform a specific application (e.g., firmware update, execution of a common task, etc.), saving network radio resources.

This feature is based on the LTE feature called "single cell point to multipoint (SC-PTM)" and was adapted to meet the low complexity requirements of NB-IoT devices. It is based on two logical channels: the single cell multicast control channel (SC-MCCH) and the single cell multicast traffic channel (SC-MTCH). The 3GPP defined new search spaces to ensure the transmission of the content of these new logical channels: Type1A-NPDCCH common search space (for SC-MCCH) and Type2A-NPDCCH common search space (for SC-MTCH). The scheduling of these search spaces is similar to the scheduling of Type2 common and UE-specific search spaces, as described in Section V-H1. However, these new search spaces have their own dedicated values for scheduling parameters (see Section 16.6 of [83]).

7) Downlink Channel Quality Reporting: In LTE, the UE is able to report the received signal quality to the eNB in order to optimize transmissions. In Release 14, the 3GPP introduced a new feature for NB-IoT called "downlink channel quality reporting". This feature allows for NB-IoT devices to report the quality of the received downlink signal. The eNB can benefit from this information to estimate of the quality of the communication channel and thus adapt the transmission parameters effectively (e.g., adapting the TBS or the number of repetitions for NPDCCH/NPDSCH). This information is reported in Message 3 of the random access procedure (see *RRCConnectionRequest-NB* message in [85]). This feature can be activated by the eNB through SIB2-NB.

TABLE XII
INITIALIZATION VALUES FOR SCRAMBLING SEQUENCES OF NB-IOT DOWNLINK CHANNELS IN RELEASE 14 OF 3GPP TS 36.211.

Channel	Initialization value of c_{init}
NPDSCH	$(n_{RNTI}+1)\times((10n_f+\lfloor\frac{n_s}{2}\rfloor) \mod 61+1)2^9 + N_{ID}^{Ncell}$
NPDCCH	$(N_{ID}^{Ncell}+1)\times((10n_f+\lfloor\frac{n_s}{2}\rfloor) \mod 8192+1)2^9 + N_{ID}^{Ncell}$

8) Release Assistance Indication (RAI): As previously described in Section V-H2a, the NB-IoT UE switches from RRC connected state to Idle state upon reception of an *RRCConnectionRelease* message from the eNB. However, if the UE has no more data to transmit and it does not receive the release message from the eNB, the UE has to wait until the expiry of the inactivity timer. Thus, in order to avoid the power consumption until the expiry of inactivity timer, the 3GPP introduced in Release 14 the RAI feature. This new feature allows the UEs to initiate the connection release with the network to quickly switch to the idle state and thus improve the lifetime of their batteries (see Section 5.4.5 in [84]).

9) Relaxed Monitoring for Cell Reselection, Connected Mode Mobility, and New Power Class: In addition to the previously presented features, in Release 14, the 3GPP introduced new features such as: relaxed monitoring for cell reselection and connected mode mobility. The former allows NB-IoT devices to reduce their monitoring time for neighboring cells and thus reduces the power consumption of their batteries. The latter allows the network to maintain the connection with the NB-IoT devices in case of radio link failure. Finally, a low power class of NB-IoT devices was introduced (Class 6 with 14 dBm of output power (Section 6.2.5F in [81])). To handle this low power class, the existing mechanisms and procedures were adapted made in Release 14 (e.g., in terms of coverage level and signaling).

10) New Scrambling for NPDSCH and NPDCCH: In Release 14, an additional scrambling was defined for the complex QPSK elements of the NPDSCH and NPDCCH. Similar to the one defined for the NPBCH in Release 13, the scrambling consists of applying a phase shift ϕ to the complex elements, where the phase shift takes values in the set $\phi \in \{-\frac{\pi}{2}, 0, \frac{\pi}{2}, \pi\}$. The initialization values of the scrambling sequences for downlink channels in Release 14 are summarized in Table XII, where n_s is the slot index within the frame. These initialization formulas can be found for each channel in the subsections entitled "Mapping to resource elements" of Section 10.2 in [79].

11) Unacknowledged Mode (UM) of Radio Link Control (RLC): A new high layer features was also introduced for NB-IoT in Release 14 at the RLC layer, supported by the UM for NB-IoT only for SC-MCCH and SC-MTCH (see Section 4.2.1 in [82]). This feature allows a reduction in the number of signaling messages during the communication with the NB-IoT devices [94], while tolerating latency and data losses.

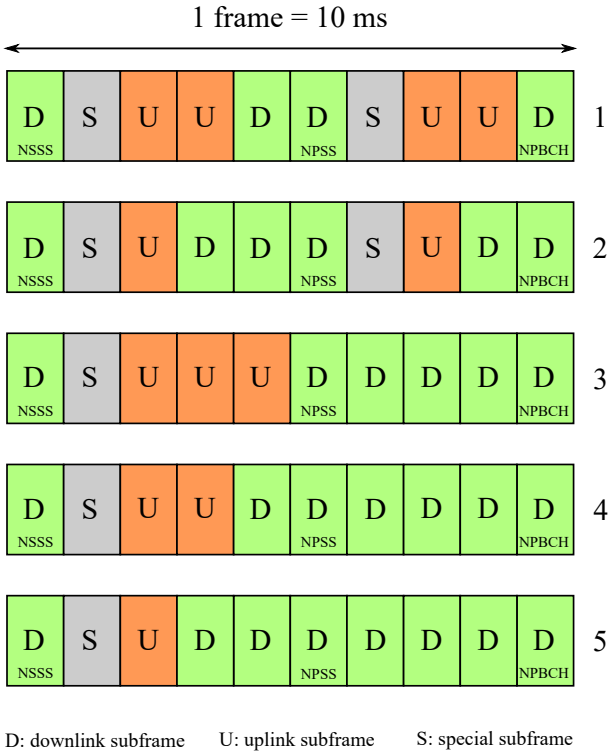

Fig. 37. TDD radio frame configurations in NB-IoT.

B. Release 15 Features

In Release 15, the following features were added to NB-IoT system:

- Frame Structure Type 2 for TDD
- New NPRACH formats
- New Scrambling for NPUSCH Format 2
- Narrowband wake up signal (NWUS)
- Early data transmission (EDT)
- New transmission process for SIB1-NB
- Additional parameters for SIBs-NB and new SIBs-NB

1) Frame Structure Type 2 for TDD: One of the main NB-IoT features introduced in Release 15 is the definition of a new frame structure for TDD transmission mode. This frame structure is called "frame structure type 2". In this mode, both downlink and uplink transmissions are performed in the same frequency band. As for LTE, the NB-IoT TDD frame has several configurations, as shown in Fig. 37. These configurations are numbered from 1 to 5 according to 3GPP notations [86]. The letters D, U, and S refer to downlink, uplink, and special subframes, respectively. However, the special subframe is not used exactly like in LTE, where constraints are added for NB-IoT (e.g., uplink pilot time slot is not used in all formats). The set of LTE TDD bands over which NB-IoT can be configured with frame structure type 2 is indicated in [87].

For all the frame configurations in TDD mode, the NPBCH and the NSSS are transmitted in subframes #9 and #0, respectively (inversely to FDD mode). However, the NPSS keeps the same position over subframe #5 as in FDD mode. At the same time, the uplink transmissions through the NPUSCH are performed in relation to the chosen frame format (see Table

TABLE XIII
PARAMETERS OF NPRACH PREAMBLE FORMATS FOR FRAME STRUCTURE TYPE 1 OF FDD MODE. REPRODUCED FROM TABLE 10.1.6.1-1 IN [86].

Preamble format	G	P	N	T_{CP}	T_{seq}
0	4	4	5	66.7 μs	1333.3 μs
1	4	4	5	266.7 μs	1333.3 μs
2	6	6	3	800 μs	2400 μs

10.1.2.3-2 of [86]). In other words, the 3.75 kHz subcarrier spacing can be used only with frame configurations 1 and 4. However, the 15 kHz spacing can be used with any frame configuration (i.e., 1 to 5). This can be explained since one slot of 2 ms in 3.75 kHz spacing requires two consecutive uplink subframes.

Furthermore, the uplink latency could be significantly higher in TDD than in FDD, particularly for 3.75 kHz subcarrier spacing. In fact, the transmission of one RU of 16 uplink slots using a 3.75 kHz carrier will last 32 ms in FDD mode, whereas it lasts 160 ms in TDD mode. Further details about TDD mode are beyond the scope of this tutorial.

2) New NPRACH Formats: In Release 15, new NPRACH formats are introduced for the FDD and TDD modes. To introduce these new formats, a common definition was proposed in order to encompass all the preambles for both transmission modes. In the new definition, the basic concept is as follows: a preamble is composed of a set of P symbol groups, each with a set of N identical symbols with one CP (with T_{seq} as a length of symbol group). The number of time-contiguous symbol groups constituting the preamble is given by G.

a) Release 15 NPRACH Formats for FDD: To better explain this new definition, we recall the preamble format 0 in FDD mode. The preamble is conceived from four symbol groups (i.e., $P = 4$), each with a set of five identical symbols with one CP (i.e., $N = 5$). The four symbol groups are transmitted in a time contiguous manner to form one preamble transmission (i.e., $G = 4$). Table XIII, lists the set of preamble parameters of FDD modes according to the new common definition.

It can be seen in Table XIII that, a new preamble format is defined for NB-IoT (format 2) in Release 15. This new preamble is composed of six symbol groups with a total duration of 19.2 ms. Each group is composed of one CP and three symbols, where the CP has the same duration of one symbol which equals to 800 μs. This leads to a symbol group duration of $4 \times 0.8 = 3.2$ ms. Consequently, the symbol duration of format 2 is three times longer compared to format 0 and format 1, allowing for a longer communication range.

It is important to note that the preamble format 2 of Table XIII is used with a subcarrier spacing of 1.25 kHz. This means that over one PRB of 180 kHz bandwidth, a set of 144 subcarriers can be used to perform the preamble transmission. In this respect, a new frequency hopping was defined specifically for preamble format 2. The same principle still applies, but with some small changes. The number of contiguous subcarriers over which the frequency hopping is performed was increased to $N_{sc}^{RA} = 36$ subcarriers (rather than 12 for format 0 & 1). Moreover, the subcarrier indexes

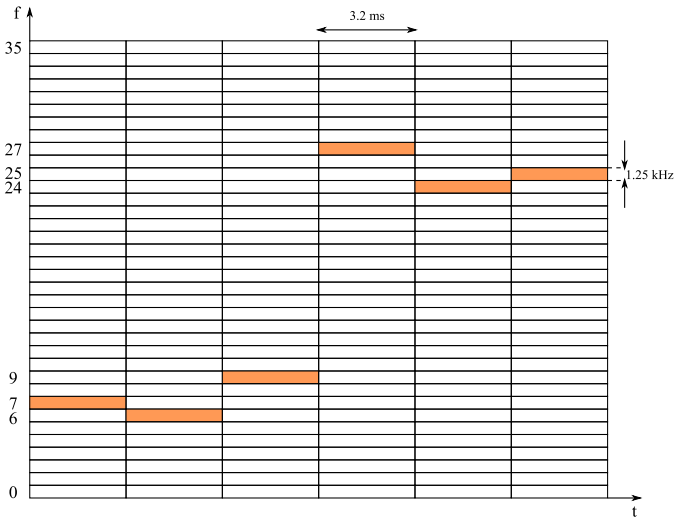

Fig. 38. Example of preamble transmission in FDD mode with NPRACH format 2.

(i.e., $n_{sc}^{RA}(i)$) constituting the preamble are constrained by new rules described below (for clarity, the same notations as in Section III-B1 are used here).

If the first subcarrier index $n_{sc}^{RA}(0)$ was randomly chosen from $\{0, 1, .., 143\}$, then the other indexes can be obtained as follows (see Section 10.1.6.1 in [86]):

$$\tilde{n}_{sc}^{RA}(i) = \begin{cases} \tilde{n}_{sc}^{RA}(i-1) + 1, \text{ if } (i \bmod 6) \in \{1,5\}, \\ \qquad \text{and } \tilde{n}_{sc}^{RA}(i-1) \bmod 2 = 0 \\ \tilde{n}_{sc}^{RA}(i-1) - 1, \text{ if } (i \bmod 6) \in \{1,5\}, \\ \qquad \text{and } \tilde{n}_{sc}^{RA}(i-1) \bmod 2 = 1 \\ \tilde{n}_{sc}^{RA}(i-1) + 3, \text{ if } (i \bmod 6) \in \{2,4\}, \\ \qquad \text{and } [\tilde{n}_{sc}^{RA}(i-1)/3] \bmod 2 = 0 \\ \tilde{n}_{sc}^{RA}(i-1) - 3, \text{ if } (i \bmod 6) \in \{2,4\}, \\ \qquad \text{and } [\tilde{n}_{sc}^{RA}(i-1)/3] \bmod 2 = 1 \\ \tilde{n}_{sc}^{RA}(i-1) + 18, \text{ if } i \bmod 6 = 3, \\ \qquad \text{and } [\tilde{n}_{sc}^{RA}(i-1)/3] < 18, \\ \tilde{n}_{sc}^{RA}(i-1) + 18, \text{ if } i \bmod 6 = 3, \\ \qquad \text{and } [\tilde{n}_{sc}^{RA}(i-1)/3] \geq 18, \\ (\tilde{n}_{sc}^{RA}(0) + f(i/6)) \bmod N_{sc}^{RA}, \\ \qquad \text{if } i \bmod 6 = 0 \text{ and } i > 0 \end{cases}, \tag{13}$$

where f is the same deterministic function presented previously in Section III-B1. This function is used to obtain the first subcarrier index of each further repetition (i.e., if more than one repetition is scheduled, $n_{sc}^{RA}(6)$ is computed using f as indicated in the last line of (13)). The other indexes in each repetition can then be found using the other rules of (13). In Fig. 38, an example of preamble transmission using format 2 is illustrated. In this example, the first subcarrier index is supposed $n_{sc}^{RA}(0) = 7$. Thus, using the frequency hopping rules of (13), we get: $n_{sc}^{RA}(1) = 6$, $n_{sc}^{RA}(2) = 9$, $n_{sc}^{RA}(3) = 27$, $n_{sc}^{RA}(4) = 24$, and $n_{sc}^{RA}(5) = 25$.

b) Release 15 NPRACH Formats for TDD: For NB-IoT TDD mode, five NPRACH preamble formats were designed: 0, 1, 2, 0-a, and 1-a. The design parameters corresponding

TABLE XIV
PARAMETERS OF NPRACH PREAMBLE FORMATS FOR FRAME STRUCTURE TYPE 2 OF TDD MODE. REPRODUCED FROM TABLE 10.1.6.1-2 IN [86].

Preamble format	Supported TDD configuration	G	P	N	T_{CP} in μs	T_{seq} in μs
0	1,2,3,4,5	2	4	1	155.2	266.7
1	1,4	2	4	2	266.7	533.3
2	3	2	4	4	266.7	1066.7
0-a	1,2,3,4,5	3	6	1	52.8	266.7
1-a	1,4	3	6	2	100.1	533.3

to each preamble format are listed in Table 10.1.6.1-2 of [86] and are provided here in Table XIV. Note that all these formats are based on a subcarrier spacing of 3.75 kHz and the frequency hopping is constrained to 12 contiguous subcarriers (i.e., $N_{sc}^{RA} = 12$). In addition, the frequency hopping values between the subcarrier indexes are equal to ± 1 or ± 6 (see Section 10.1.6.1 in [86]).

It can be observed in Table XIV that not all the formats can be used with any TDD frame configuration. In fact, depending on the frame configuration, more or less contiguous uplink subframes can be used for NPRACH. Therefore, each preamble format is associated with a TDD frame if its configuration (i.e., N, P and G) can fit the available uplink subframes. For example, the transmission of preamble format 2 is split into two parts (since $G = 2$, $P = 4$ and $N = 4$), where each part will last $G \times (T_{CP} + T_{seq}) = 2 \times (266.7\mu s + 1066\mu s) = 2.667$ ms. Therefore, the only TDD frame configuration that can support a preamble transmission of 2.667 ms is configuration 3 since it has three uplink subframes (3 ms).

3) New Scrambling for NPUSCH Format 2: For uplink, a new scrambling was also proposed for NPUSCH transporting ACK/NACK (i.e., format 2). This scrambling is proposed in association with a new Release 15 feature called "scheduling request" (details on the scheduling request procedure are provided in [56]). The scrambling procedure consists of multiplying by -1, one out of two of the 16 REs used to transmit the ACK/NACK information (Section 10.1.3.2 in [86]). This will provide better protection for the ACK/NACK message and better decoding at the eNB receiver side. Note that the scheduling request feature is a higher layer procedure and therefore beyond the scope of this tutorial.

4) Narrowband Wake Up Signal (NWUS): To further reduce the power consumption for NB-IoT devices, the 3GPP introduced the NWUS feature in Release 15. The goal of this feature is to reduce the number of monitored paging occasions by NB-IoT devices, especially when there is infrequent need for the paging signaling. Note that this feature is optional and can be enabled or disabled by the eNB.

The NWUS is designed using a ZC sequence of length 132. This provides a highly reliable signal with very good cross-correlation and auto-correlation properties, which minimizes the miss detection rate. The UE uses a low-power recognition technique to identify the signal [55] (e.g., using matched filter or correlation metrics). Upon detection of the NWUS, a time gap (see Fig. 39) is left to the UE to resynchronize with the network and then switch on its receiver chain to further monitor the upcoming POs.

The NWUS sequence is described in Section 10.2.6B of [86]. It is expressed as the multiplication of the ZC sequence $z(n) = e^{-\frac{j\pi un(n+1)}{131}}$ and the same scrambling sequence composed of $\{\pm 1, \pm j\}$ used to scramble the NPBCH elements, as described in Section III-A4. However, the scrambling sequence is initialized by a newly defined parameter c_{init_WUS} (defined in Section 10.2.6B.1 of [86]) that depends on the frame and slot indexes of the PO to which the NWUS is associated. It is noteworthy that the NWUS ZC sequence $z(n)$ is similar to that defined for NSSS, in which the sequence length is 132 (corresponding to 12 subcarriers $\times$ 11 OFDM symbols).

a) Mapping and Repetition Process of NWUS: The mapping of the $z(n)$ sequence over one subframe is performed exactly as for the NSSS, as described in Fig. 9; the only difference is that the REs dedicated to CRS and NRS are avoided. However, in guard-band or stand-alone mode, the first 3 OFDM symbols are used during the mapping process. Therefore, copies of symbols $l = 7$, 8, and 9 are mapped to symbols $l = 0$, 1 and 2, respectively.

The NWUS sequence can be repeated up to 1024 times, as indicated by the parameter L_{NWUS_max} in Table 16.9-1 of [88]. The L_{NWUS_max} parameter indicates the length of NWUS transmission; its value is computed by multiplying *WUS-MaxDurationFactor-NB-r15* parameter (transmitted in SIB2-NB) by *npdcch-NumRepetitionPaging-r13* (also transmitted in SIB2-NB). The downlink subframes within the L_{NWUS_max} duration that are occupied by the SIB1-NB and SIBs-NB are counted as NWUS repetitions but are not used for transmission of the NWUS. The scrambling of the $z(n)$ sequence is triggered once at the beginning of the first transmitted subframe.

b) Example of NWUS Transmission: The repetition process of NWUS is described in Section 16.9 of [88] and in Section 7.4 of [89], and is illustrated here in Fig. 39. It can be seen on the figure that the NWUS starting subframe $w0$ is deduced from the ending subframe $g0$, where $w0 = g0 - L_{NWUS\_max}$. The ending subframe equals $g0 = PO - timeoffset$, where PO is the paging occasion subframe described in Section V-H2b and "$timeoffset$" is the time gap between NWUS and the first PO ($timeoffset$ is transmitted in SIB2-NB). Note that NWUS can be used in both DRX and eDRX modes and the UEs can be configured to monitor up to four POs, as shown in Fig. 39.

5) Early Data Transmission (EDT): In 3GPP Release 13, two optimized data transfer procedures were defined for NB-IoT: control plane cellular Internet of things (CP CIoT) evolved packet system (EPS) optimization and the user plane CIoT (UP CIoT) EPS optimization. The goal of these procedures is to reduce the signaling overhead compared to the default procedure. In Release 15, in order to further improve battery lifetime of the NB-IoT devices and the data exchange latency, the 3GPP introduced the EDT feature (see RRCConnectionResumeRequest-NB message in [90] and Section 8.6.2.1 in [91]).

This new feature allows for an early data exchange during the random access procedure; more precisely, exchanging data using Message 3 and Message 4 (these messages are

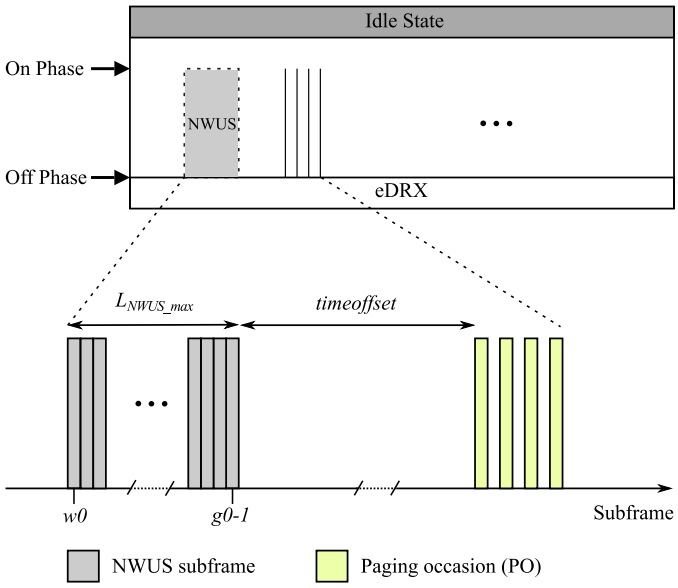

Fig. 39. Illustration of NWUS principle at the UE side: the UE triggers the PO only in the presence of NWUS.

usually used for contention resolution in legacy procedure). This feature allows further reduction of the signaling overhead and message latency while increasing battery lifetime [57]. In contrast, if the UE has more data to send, it switches to the optimized procedure of Release 13 (i.e., CP and UP CIoT data transfer).

6) New Transmission Process for SIB1-NB: In Release 15, additional SIB1-NB transmissions can be performed per repetition to allow for faster decoding and thus power saving during the cell access. Up to 16 SIB1-NB transmissions per repetition can be performed for SIB1-NB compared to eight in Release 13. These new transmissions are performed in SF#3 of the same radio frames where SIB1-NB transmission occurs in SF#4. This feature is only possible for NB-IoT FDD mode and for the configuration using 16 SIB1-NB repetitions per periodicity. Moreover, it can be activated/deactivated by the eNB (see MIB-NB message and Section 5.2.1.2a in [90]).

7) Additional Parameters for SIBs-NB and New SIBs-NB: In Release 13, several SIBs-NB were defined for NB-IoT: SIB1-NB, SIB2-NB, SIB3-NB, SIB4-NB, SIB5-NB, SIB14-NB, and SIB16-NB. In Release 14, additional SIBs-NB were defined for NB-IoT in order to broadcast additional information toward NB-IoT devices. These new SIBs-NB are: SIB15-NB, SIB20-NB and SIB22-NB. In Release 15, the SIB23-NB is introduced. The goal of these SIBs-NB is to incorporate the new parameters of the newly introduced features of Releases 14 and 15 including those previously described in this section (e.g., multicast, multi-carrier, TDD mode, etc.).

In addition, the existing SIBs-NB (e.g., SIB1-NB, SIB2-NB, SIB3-NB and SIB5-NB) were also upgraded with new parameters to support improvements in some existing or new features, such as cell selection or reselection, NWUS, etc. Moreover, some of these new parameters were added to improve the configuration of existing channels like NPRACH. Further information is provided in Section 6.7.3.1 of [90].

VII. Conclusion

The IoT is rapidly gaining prominence due to its nearly limitless potential in terms of applications for individuals and industries. In this respect, many standards, technologies and communication protocols were developed to implement these applications and anticipate future needs. In this work, we addressed the Release 13 of the NB-IoT 3GPP LPWA technology. More specifically, we addressed its physical layer design by considering the transmitter and receiver parts of the eNB and the UE. We presented in detail the characteristics of the physical channels and signals with examples of their encoding/decoding chains and mapping/demapping processes. Moreover, the scheduling and transmission procedures of these channels and signals were addressed to complete the comprehensive review and to show the dependencies with higher layers. Finally, the new features and improvements added to the NB-IoT standard in Release 14 and Release 15 were addressed with a detailed description of the features related to the physical layer.

In this work, we aimed to provide a hands-on tutorial of NB-IoT 3GPP technology in order to aid in the understanding of its 3GPP specification documents that are mixed with those for LTE. The goal was to address one of the most promising IoT standards and provide a reference document to be used by readers to acquire the key concepts quickly. This work will help readers including students, researchers and engineers aiming to understand and/or implement the NB-IoT standard since it includes all the necessary elements to gain a fundamental understanding of the 3GPP standard.

Finally, this tutorial can be considered as a solid basis ground for future research studies on the NB-IoT system. Researchers working in this field can benefit from this work to start specific studies on the PHY or MAC layer (e.g., preamble detection, radio resource allocation algorithms for uplink and downlink channels, etc.). Moreover, as described in this work, the 3GPP standard fully describes the PHY layer from the point of view of the eNB and UE transmitters. Consequently, the reception and demodulation processes on the eNB and UE side can be widely studied and improved in future works as they are open to any innovation. In addition, it should be noted that most of the Release 13 physical layer functionalities of the NB-IoT standard presented in this tutorial were implemented in the open source software OpenAirInterface[4]. In this respect, most of these functionalities can be tested in practice with commercial UEs, and other functionalities could be implemented and updated.

References

[1] James Manyika, Michael Chui, Peter Bisson, Jonathan Woetzel, Richard Dobbs, Jacques Bughin, and Dan Aharon. Unlocking the potential of the Internet of Things | McKinsey, June 2015.

[2] Ericsson. Internet of Things forecast Ericsson Mobility Report, September 2016.

[3] Ala Al-Fuqaha, Mohsen Guizani, Mehdi Mohammadi, Mohammed Aledhari, and Moussa Ayyash. Internet of Things: A Survey on Enabling Technologies, Protocols, and Applications. *IEEE Communications Surveys & Tutorials*, 17(4):2347–2376, Fourthquarter 2015.

[4] https://www.openairinterface.org/

[4] Usman Raza, Parag Kulkarni, and Mahesh Sooriyabandara. Low Power Wide Area Networks: An Overview. *IEEE Communications Surveys & Tutorials*, 19(2):855–873, Secondquarter 2017.

[5] Keyur K Patel and Sunil M Patel. Internet of Things-IOT: Definition, Characteristics, Architecture, Enabling Technologies, Application & Future Challenges. *IJESC*, 6(5):6122 – 6131, May 2016.

[6] Alem Colakovic and Mesud Hadzialic. Internet of Things (IoT): A review of enabling technologies, challenges, and open research issues. *Elsevier Computer Networks*, 144:17–39, October 2018.

[7] K. Mekki, E. Bajic, F. Chaxel, and F. Meyer. A comparative study of LPWAN technologies for large-scale IoT deployment. *ICT Express*, 5(1):1 – 7, March 2019.

[8] B. Vejlgaard, M. Lauridsen, H. Nguyen, I. Z. Kovacs, P. Mogensen, and M. Sorensen. Coverage and Capacity Analysis of Sigfox, LoRa, GPRS, and NB-IoT. In *proc. of VTC'17-Spring*, pages 1 – 5, Sydney, NSW, Australia, June 2017.

[9] A. Ikpehai, B. Adebisi, K. M. Rabie, K. Anoh, R. E. Ande, M. Hammoudeh, H. Gacanin, and U. M. Mbanaso. Low-Power Wide Area Network Technologies for Internet-of-Things: A Comparative Review. *IEEE Internet of Things Journal*, 6(2):2225 – 2240, April 2019.

[10] W. Ayoub, A. E. Samhat, F. Nouvel, M. Mroue, and J. Prvotet. Internet of Mobile Things: Overview of LoRaWAN, DASH7, and NB-IoT in LPWANs Standards and Supported Mobility. *IEEE Communications Surveys Tutorials*, 21(2):1561–1581, 2019.

[11] J. Schlienz and D. Raddino. Narrowband Internet of Things - Whitepaper. Technical report, Rohde & Schwarz, 2016.

[12] Min Chen, Yiming Miao, Yixue Hao, and Kai Hwang. Narrow Band Internet of Things. *IEEE Access*, 5:20557–20577, September 2017.

[13] Y. . E. Wang, X. Lin, A. Adhikary, A. Grovlen, Y. Sui, Y. Blankenship, J. Bergman, and H. S. Razaghi. A primer on 3gpp narrowband internet of things. *IEEE Communications Magazine*, 55(3):117–123, March 2017.

[14] Rohde & Schwarz International. Narrowband Internet of Things.

[15] R. Ratasuk, N. Mangalvedhe, Y. Zhang, and J.-P. Robert, M. Koskinen. Overview of Narrowband IoT in LTE Rel-13. In *proc. of CSCN'16*, pages 1 – 7, Berlin, Germany, November 2016.

[16] E. Rastogi, N. Saxena, A. Roy, and D. R. Shin. Narrowband internet of things: A comprehensive study. *Computer Networks*, 173:1 – 40, May 2020.

[17] B Buurman, J. Kamruzzaman, G. Karmakar, and S. Islam. Low-power wide-area networks: Design goals, architecture, suitability to use cases and research challenges. *IEEE Access*, 8:17179 – 17220, January 2020.

[18] Xingqin Lin, Ansuman Adhikary, and Y.-P. Eric Wang. Random Access Preamble Design and Detection for 3gpp Narrowband IoT Systems. *arXiv:1605.05384 [cs, math]*, May 2016. arXiv: 1605.05384.

[19] Sergio Martiradonna, Giuseppe Piro, and Gennaro Boggia. On the Evaluation of the NB-IoT Random Access Procedure in Monitoring Infrastructures. *Sensors*, 19(14):3237, July 2019.

[20] Sakshi Popli, Rakesh Kumar Jha, and Sanjeev Jain. A Survey on Energy Efficient Narrowband Internet of Things (NBIoT): Architecture, Application and Challenges. *IEEE Access*, 7:16739–16776, November 2019.

[21] Collins Burton Mwakwata, Hassan Malik, Muhammad Mahtab Alam, Yannick Le Moullec, Sven Parand, and Shahid Mumtaz. Narrowband Internet of Things (NB-IoT): From Physical (PHY) and Media Access Control (MAC) Layers Perspectives. *Sensors*, 19(11):2613, June 2019.

[22] Luca Feltrin, Galini Tsoukaneri, Massimo Condoluci, Chiara Buratti, Toktam Mahmoodi, Mischa Dohler, and Roberto Verdone. Narrowband IoT: A Survey on Downlink and Uplink Perspectives. *IEEE Wireless Communications*, 26(1):78–86, February 2019.

[23] G. Berardinelli, L. A. M. Ruiz de Temino, S. Frattasi, M. I. Rahman, and P. Mogensen. OFDMA vs. SC-FDMA: performance comparison in local area imt-a scenario. *IEEE Transactions on Wireless Communications*, 15(5):64 – 72, October 2008.

[24] V. Savaux and Y. Louët. PAPR Analysis as a Ratio of Two Random Variables: Application to Multicarrier Systems With Low Subcarriers Number. *IEEE Transactions on Communications*, 66(11):5732 – 5739, November 2018.

[25] Hassan Malik, Haris Pervaiz, Muhammad Mahtab Alam, Yannick Le Moullec, Alar Kuusik, and Muhammad Ali Imran. Radio Resource Management Scheme in NB-IoT Systems. *IEEE Access*, 6:15051–15064, March 2018.

[26] Jia-Ming Liang, Kun-Ru Wu, Jen-Jee Chen, Pei-Yi Liu, and Yu-Chee Tseng. Energy-Efficient Uplink Resource Units Scheduling for Ultra-Reliable Communications in NB-IoT Networks. *Hindawi Wireless Communications and Mobile Computing*, 2018:1–17, July 2018.

[27] Rubbens Boisguene, Sheng-Chia Tseng, Chih-Wei Huang, and Phone Lin. A survey on NB-IoT downlink scheduling: Issues and potential solutions. In *proc. of IWCMC'17*, pages 547–551, Valencia, Spain, June 2017.

[28] R. Frank. Polyphase codes with good nonperiodic correlation properties. *IEEE Transactions on Information Theory*, 9(1):43 – 45, January 1963.

[29] D. Chu. Polyphase codes with good periodic correlation properties. *IEEE Transactions on Information Theory*, 18(4):531 – 532, July 1972.

[30] H. Kröll, M. Korb, B. Weber, S. Willi, and Q. Huang. Maximum-Likelihood Detection for Energy-Efficient Timing Acquisition in NB-IoT. In *proc. of WCNCW'17*. San Francisco, CA, March 2017.

[31] A. Bhamri, L. Zexian, L. Lindh, and C. Ribeiro. Primary Synchronization Signal Detection Method for Device-to-Device in LTE-Rel 12 and Beyond. In *proc. of VTC'15-Fall*. Noston, MA, USA, September 2015.

[32] Qualcomm. NB-PSS and NB-SSS Design. Technical Report R1-161981, Qualcomm Inc., Sophia-Antipolis, March 2016.

[33] K. Manolakis, D. M. Gutiérrez-Estévez, V. Jungnickel, W. Xu, and C. Drewes. A Closed Concept for Synchronization and Cell Search in 3GPP LTE Systems. In *proc. of WCNC'09*, Budapest, Hungary, April 2009.

[34] Intel Corporation. Synchronization and cell search in NB-IoT: Performance evaluations. Technical Report R1-161898, 3GPP TSG RAN WG1, Sophia-Antipolis, April 2016.

[35] A. Ali and W. Hamouda. On the cell search and initial synchronization for nb-iot lte systems. *IEEE communications Letters*, 21(8):1843 1846, August 2017.

[36] Y. Li, S. Chen, W. Ye, and F. Lin. A Joint Low-Power Cell Search and Frequency Tracking Scheme in NB-IoT Systems for Green Internet of Things. *Sensors*, 18(10):22, September 2018.

[37] V. Savaux. DFT-based low-complexity optimal cell ID estimation in NB-IoT. *EURASIP Journal on Advances in Signal Processing*, 2020(14):1 – 12, April 2020.

[38] A. Chakrapani. NB-IoT Uplink Receiver Design and Performance Study. *submitted to IEEE Internet of Things Journal, arXiv:1906.07096*, 0(0):13, June 2019.

[39] K. S. Pasupuleti. Timing Advance and Time Alignment Timer (online), 2014.

[40] G. Huang, A. Nix, and S. Armour. Decision feedback equalization in SC-FDMA. In *proc. of PIMRC'08*, pages 1 – 5, Cannes, France, September 2008.

[41] B. Karakaya, H. Arslan, and H. A. Cirpan. Channel Estimation for LTE Uplink in High Doppler Spread. In *proc. of WCNC'08*, pages 1 – 5, Las Vegas, NV, USA, March-April 2008.

[42] G. Berardinelli, B. E. Priyanto, T. B. Sorensen, and P. E. Mogensen. Improving SC-FDMA Performance by Turbo Equalization in UTRA LTE Uplink. In *proc. of VTC'08-Spring*, pages 2557 – 2561, Singapore, Singapore, May 2008.

[43] S. Coleri, M. Ergen, A. Puri, and A. Bahai. A study of channel estimation in ofdm systems. In *Vehicular Technology Conference*, volume 2, pages 894–898, Vancouver, BC, Canada, september 2002.

[44] M. K. Ozdemir and H. Arslan. Channel Estimation for Wireless OFDM Systems. *IEEE Communications Surveys and Tutorials*, 9(2):18 – 48, 2nd Quarter 2007.

[45] Y. Liu, Z. Tan, H. Hu, L. J. Cimini, and G. Y. Li. Channel Estimation for OFDM. *IEEE Communication Surveys and Tutorials*, 16(4):1891 – 1908, Fourth quarter 2014.

[46] V. Savaux and Y. Louët. LMMSE channel estimation in OFDM context: a review. *IET Signal Processing*, 11(2):123 – 134, April 2017.

[47] V. Savaux, H. Dembélé, and M. Kanj. Uplink Channel Estimation and Equalization in NB-IoT System. In *proc. of WMNC'19*, page 8, Paris, France, September 2019.

[48] M. M. Rana, J. Kim, and W.-K. Cho. Low Complexity Downlink Channel Estimation for LTE Systems. In *proc. of ICACT'10*, pages 1 – 5, Phoenix Park, South Korea, February 2010.

[49] M. Simko, D. Wu, C. Mehlführer, J. Eilert, and D. Liu. Implementation Aspects of Channel Estimation for 3GPP LTE Terminals. In *proc. of European Wirelees'11*, pages 1 – 5, Vienna, Austria, April 2011.

[50] Xuewu Dai, Wuxiong Zhang, Jing Xu, John E. Mitchell, and Yang Yang. Kalman interpolation filter for channel estimation of LTE downlink in high-mobility environments. *EURASIP Journal on Wireless Communications and Networking*, 2012(1):232 – 245, July 2012.

[51] M. Nasreddine, N. Bechir, W. Hakimiand, and M. Ammar. Channel Estimation for Downlink LTE System Based on Lagrange Polynomial Interpolation. In *proc. of ICWMC'14*, pages 65 – 69, Seville, Spain, June 2014.

[52] P. Hoeher, S. Kaiser, and P. Robertson. Two-Dimensional Pilot-Symbol-Aided Channel Estimation by Wiener Filtering. In *proc of ICASSP'97*, volume 3, pages 1845 – 1848, Munich, Germany, April 1997.
[53] V. Savaux, M. Djoko-Kouam, Y. Louët, and A. Skrzypczak. Effect of polynomial interpolations on the estimation performance of a frequency-selective Rayleigh channel in orthogonal frequency division multiplexing systems. *IET Signal Processing*, 9(1):97 – 109, February 2015.
[54] Borja Martinez, Ferran Adelantado, Andrea Bartoli, and Xavier Vilajosana. Exploring the Performance Boundaries of NB-IoT. *IEEE Internet Things J.*, 6(3):5702–5712, June 2019. arXiv: 1810.00847.
[55] S. Yong. Power saving methods for LTE-M and NB-IoT devices, White paper. Technical report, Rhode & Schwarz, June 2019.
[56] J. Lee and J. Lee. Prediction-Based Energy Saving Mechanism in 3GPP NB-IoT Networks. *Sensors*, 9(17):1 – 22, September 2017.
[57] A. Hoglund, D. P. Van, T. Tirronen, O. Liberg, Y. Sui, and E. A. Yavuz. 3GPP Release 15 Early Data Transmission. *IEEE Communications Standards Magazine*, 2(2):90 – 96, June 2018.
[58] M. Thorpe and E. Zelmer. LTE Location Based Services Technology Introduction. Technical report, Rhode & Schwarz, September 2013.
[59] S. Fischer. Observed Time Difference Of Arrival (OTDOA) Positioning in 33GPP LTE. Technical report, Qualcomm Technologies, Inc., June 2014.
[60] X. Lin and all. Positioning for the internet of things: A 3gpp perspective. *IEEE Communications Magazine*, 55(12):179 – 185, December 2017.
[61] A. Adhikary, X. Lin, and Y. . E. Wang. Performance Evaluation of NB-IoT Coverage. In *2016 IEEE 84th Vehicular Technology Conference (VTC-Fall)*, pages 1–5, September 2016.
[62] J. Xu, J. Yao, L. Wang, Z Ming, K.Wu, and L. Chen. Narrowband internet of things: Evolutions, technologies, and open issues. *IEEE Internet of Things Journal*, 5(3):1449 – 1462, June 2018.
[63] Jiming Chen, Kang Hu, Qi Wang, Yuyi Sun, Zhiguo Shi, and Shibo He. Narrowband Internet of Things: Implementations and Applications. *IEEE Internet of Things Journal*, 4(6):2309–2314, December 2017.
[64] E. M. Migabo, K. D. Djouani, and A. M. Kurien. The Narrowband Internet of Things (NB-IoT) Resources Management Performance State of Art, Challenges, and Opportunities. *IEEE Access*, 8:97658–97675, 2020.
[65] 3GPP. 3GPP TS 36.211, Physical channels and modulation (Release 13, v13.9.0). Technical report, 3GPP, April 2018.
[66] 3GPP. 3GPP TS 36.101, User Equipment (UE) radio transmission and reception (Release 13, v13.9.0). Technical report, 3GPP, November 2017.
[67] 3GPP. 3GPP TS 136.104, LTE; Evolved Universal Terrestrial Radio Access (E-UTRA); Base Station (BS) radio transmission and reception (Release 13, v13.9.0). Technical report, 3GPP, October 2017.
[68] 3GPP. 3GPP TS 36.213, Physical layer procedures (Release 13, v13.9.0). Technical report, 3GPP, April 2018.
[69] 3GPP. 3GPP TS 36.306, User Equipment (UE) radio access capabilities (Release 13, v13.9.0). Technical report, 3GPP, July 2018.
[70] 3GPP. 3GPP TS 36.214, Physical layer Measurements (Release 13, v13.5.0). Technical report, 3GPP, October 2017.
[71] 3GPP. 3GPP TS 36.321, Medium Access Control (MAC) protocol specification (Release 13, v13.9.0). Technical report, 3GPP, July 2018.
[72] 3GPP. 3GPP TS 36.304, User Equipment (UE) procedures in idle mode (Release 13, v13.8.0). Technical report, 3GPP, January 2018.
[73] 3GPP. 3GPP TS 124.008, Mobile radio interface Layer 3 specification; Core network protocols; Stage 3 (Release 13, v13.12.0). Technical report, 3GPP, January 2018.
[74] 3GPP. 3GPP TS 36.331, Radio Resource Control (RRC): Protocol specification (Release 13, v13.9.1). Technical report, 3GPP, April 2018.
[75] 3GPP. 3GPP TS 36.212, Multiplexing and channel coding (Release 13, v13.8.0). Technical report, 3GPP, July 2018.
[76] 3GPP. 3GPP TR 45.820, Cellular system support for ultra-low complexity and low throughput Internet of Things (CIoT) (Release 13, v13.1.0) . Technical report, 3GPP, November 2015.
[77] 3GPP. 3GPP TS 23.401, General Packet Radio Service (GPRS) enhancements for Evolved Universal Terrestrial Radio Access Network (E-UTRAN) access (Release 13, v13.14.0). Technical report, 3GPP, January 2020.
[78] 3GPP. 3GPP TS 36.304, User Equipment (UE) procedures in idle mode (Release 14, v14.7.0). Technical report, 3GPP, October 2018.
[79] 3GPP. 3GPP TS 36.211, Physical channels and modulation (Release 14, v14.9.0). Technical report, 3GPP, May 2019.
[80] 3GPP. 3GPP TS 36.355, LTE Positioning Protocol (LPP) (Release 14, v14.7.0). Technical report, 3GPP, October 2018.
[81] 3GPP. 3GPP TS 36.101, User Equipment (UE) radio transmission and reception (Release 14, v14.9.0). Technical report, 3GPP, January 2019.
[82] 3GPP. 3GPP TS 36.322, Radio Link Control (RLC) protocol specification (Release 14, v14.1.0). Technical report, 3GPP, October 2017.
[83] 3GPP. 3GPP TS 36.213, Physical layer procedures (Release 14, v14.9.0). Technical report, 3GPP, May 2019.
[84] 3GPP. 3GPP TS 36.321, Medium Access Control (MAC) protocol specification (Release 14, v14.9.0). Technical report, 3GPP, January 2019.
[85] 3GPP. 3GPP TS 36.331, Radio Resource Control (RRC), Protocol specification (Release 14, v14.9.0). Technical report, 3GPP, January 2019.
[86] 3GPP. 3GPP TS 36.211, Physical channels and modulation (Release 15, v15.6.0). Technical report, 3GPP, July 2019.
[87] 3GPP. 3GPP TS 36.307, Requirements on User Equipments (UEs) supporting a release-independent frequency band (Release 15, v15.6.0). Technical report, 3GPP, October 2019.
[88] 3GPP. 3GPP TS 36.213, Physical layer procedures (Release 15, v15.6.0). Technical report, 3GPP, July 2019.
[89] 3GPP. 3GPP TS 36.304, User Equipment (UE) procedures in idle mode (Release 15, v15.4.0). Technical report, 3GPP, July 2019.
[90] 3GPP. 3GPP TS 36.331, Radio Resource Control (RRC) Protocol specification (Release 15, v15.9.0). Technical report, 3GPP, March 2020.
[91] 3GPP. 3GPP TS 36.413, S1 Application Protocol (S1AP) (Release 15, v15.8.0). Technical report, 3GPP, December 2019.
[92] 3GPP. 3GPP TS 23.002, LTE Network architecture (Release 15, v15.0.0). Technical report, 3GPP, July 2018.
[93] 3GPP. 3GPP TS 23.003, Numbering, addressing and identification (Release 10, v10.5.0). Technical report, 3GPP, April 2012.
[94] GSM Association. NB-IoT Deployment Guide to Basic Feature set Requirements (online), June 2019.

Matthieu Kanj received his engineering degree from the Superior National School of Computer and Applied Mathematics of Grenoble (ENSIMAG), Grenoble, France, in 2012, and a Ph.D. degree in computer science from Rennes 1 University, Rennes, France, in 2016. He is currently a research engineer at the Institute of Research and Technology b<>com. His research interests include computer science, mobile networks, radio communications/architectures, narrow-band internet of things (NB-IoT), optical networks architecture, Flex-Grid technology, and GMPLS protocol suite for optical networking.

Vincent Savaux (M'16) received his engineering degree from the High School of Engineering, ECAM Rennes, an M.Sc. degree from the University of Rennes 1, France, in 2010, and his Ph.D. degree in telecommunications from École Suprieur dÉlectricité-Supélec in 2013. From 2014 to 2015, he was a post-doctoral researcher with the Signal, Communication, and Embedded Electronics (SCEE) Research Group, CentraleSuplec, Campus de Rennes, France. Since 2016, he has been a research engineer with the Institute of Research and Technology b<>com, Rennes, France. His research activities mainly focus on signal processing for wireless systems, including IoT technologies. He received the Exemplary Reviewer 2014 Appreciation from the IEEE WIRELESS COMMUNICATIONS LETTERS and the IEEE COMMUNICATIONS LETTERS.

Mathieu Le Guen received his engineering degree from the Institut National des Sciences Appliquées (INSA) of Rennes, France, in 2019. He is currently a research engineer at the Institute of Research and Technology b<>com. His research activities mainly focus on scheduling processes, allocation and resource management, narrow-band internet of things (NB-IoT) PHY & MAC layers.